Locality in AdS/CFT

Ricardo Rodrigues
Mestrado em Física
Departamento de Física e Astronomia
2023

Orientador
Miguel Costa, Professor Catedrático, Faculdade de Ciências da Universidade do Porto

Coorientador
Vasco Gonçalves, Doutorado Equiparado a Investigador Auxiliar, Faculdade de Ciências da Universidade do Porto

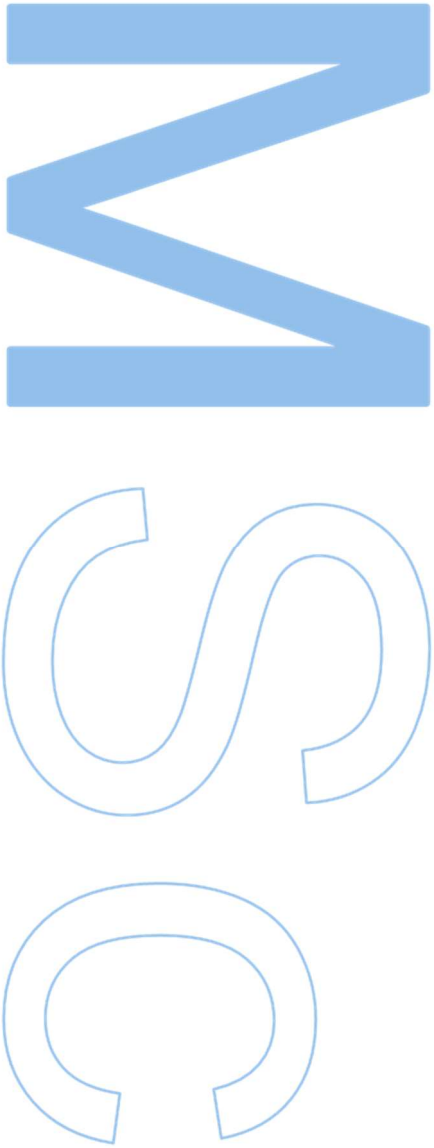


U.PORTO
FACULDADE DE CIÊNCIAS
UNIVERSIDADE DO PORTO

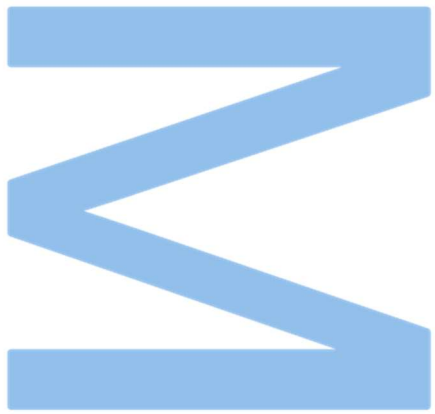

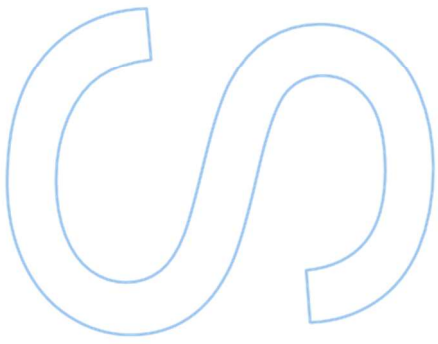

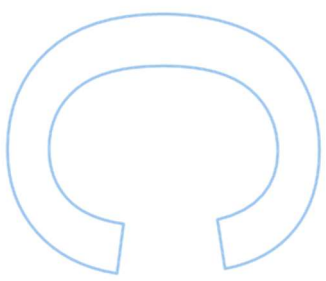

“ We know a lot of things, but what we don’t know is a lot more. ”

Edward Witten

Acknowledgements

This work would not have been possible without the invaluable support and tireless efforts of several people, to whom I am forever grateful for their encouragement and dedication.

First and foremost, I want to express my gratitude to my supervisor, Vasco Gonçalves, for his guidance and for the countless hours of captivating discussions we had in his office. I have no doubt that they were not only crucial to my understanding of this thesis topic, but also to my growth as a physicist and as a person. His good disposition, humor and encouragement certainly made it all easier, and inspired me to do better.

I also want to express my gratitude to my co-supervisor, Miguel Costa, for all the assistance he offered me throughout this journey. Additionally, I want to convey my thanks to him for igniting my passion for physics. His dedication and enthusiasm in all of his classes, from Quantum Mechanics all the way to Quantum Field Theory, have greatly contributed to my desire of working in High-Energy Physics.

I am also grateful to my colleagues from the same year as me for all the help they have provided me throughout these years, as well as the many conversations and laughs we shared in the university's halls. A special thanks is due to Henrique Veiga, who has suffered from my countless questions about the several homework we had and who helped me prepare for the exams during our bachelor's and master's years. I also want to express my gratitude to all the guys from the PhD students' room, João Vilas Boas, Carlos Fernandes, Filipe Serrano, and Aaditya Salgarkar, for our daily physics discussions, as well as all the lunches and afternoon snacks where we have the most diverse of talks.

Because there is more to life than just work, I am also forever grateful to all of my friends and family, who make my life outside of physics filled with joy and laughter.

Last but not least, I want to express my deep gratitude to my parents, who I cherish the most. They always believe in me and support me in everything I do. I cannot thank them enough for all that they have done for me.

Abstract

Within the context of AdS/CFT, our understanding of how bulk locality emerges from the boundary remains incomplete. Moreover, it would be useful to have some kind of tool or criterion which given a boundary CFT, would tell us whether or not it has a bulk dual which is local at scales much smaller than the AdS radius of curvature. A recent paper by Caron-Huot [1] proposed two devices, which he calls 'Holographic Cameras', that help us precisely with these questions. In particular, the signals of these cameras are easily-interpretable images from which we can conclude about the locality of the bulk theory without ambiguity. However, although the construction works for any four point function with a specific operator ordering, the only considered case there is of the scalar correlator. This thesis aims to extend this analysis for spinning correlators by computing the associated conformal blocks in the Regge limit, which in turn are vital to plot the signal of the camera. We start by introducing the basics of Conformal Field Theories and AdS/CFT. Then, we proceed to give a brief overview of the large higher-spin gap and large N conjecture and the construction of the Holographic Cameras, which are both related with the study of locality in the bulk. Finally, after presenting Regge kinematics and going over the methods that will be used here to compute the conformal blocks, we obtain these functions in the Regge limit for two distinct types of spinning correlators: with one spinning operator and three scalars and with two spinning operators and two scalars. We finish this thesis by stating the main results and conclusions of our work and point out the next steps we could take in the future.

Resumo

Dentro do contexto de AdS/CFT, a nossa compreensão sobre como a localidade do 'bulk' emerge a partir da fronteira permanece incompleta. Adicionalmente, seria útil termos alguma espécie de ferramenta ou critério que, dada uma CFT na fronteira, nos dissesse se esta possui ou não uma teoria dual no 'bulk' que fosse local a escalas muito menores do que o raio de curvatura de AdS. Um artigo recente proposto por Caron-Huot [1] propõe dois dispositivos, a que ele chama de 'Câmeras Holográficas', que nos ajudam precisamente a responder a estas questões. Em particular, os sinais destas câmeras são imagens de fácil interpretação, a partir dos quais podemos concluir also sobre a localidade da teoria do 'bulk' sem qualquer ambiguidade. No entanto, embora a construção funcione para qualquer função de quatro pontos com uma certa ordenação específica dos operadores, o único caso considerado nesse artigo é o da função de correlação só com operadores escalares. Esta tese tem como objetivo estender a análise do artigo para funções de correlação que têm operadores com spin não nulo, calculando os blocos conformes associados no limite de Regge, que por sua vez são essenciais para obter o sinal da câmera. Assim, começamos por introduzir os conceitos básicos de Teorias de Campos Conformes e AdS/CFT. Depois, procedemos a dar uma breve introdução sobre a conjetura de 'large higher-spin gap and large N', bem como a construção das Câmeras Holográficas, sendo que estão ambas relacionadas com o estudo de localidade no bulk. Finalmente, após explicar em que consiste o limite de Regge e introduzir os métodos que serão usados neste trabalho para calcular os blocos conformes, obtemos essas mesmas funções no limite de Regge para dois tipos distintos de funções de correlação: com um operador com spin e três escalares e com dois operadores com spin e dois escalares. Finalizaremos esta tese com a apresentação dos resultados principais deste trabalho e respetivas conclusões, e destacamos os passos seguintes que poderíamos tomar no futuro.

Contents

List of Figures

Glossary

QFT	Quantum Field Theory
CFT	Conformal Field Theory
AdS	Anti de-Sitter
GR	General Relativity
SCT	Special Conformal Transformation
OPE	Operator Product Expansion
RG	Renormalization Group
IR	Infra-Red
UV	Ultra-Violet
LHS	Left Hand Side
RHS	Right Hand Side

Chapter 1

Introduction

1.1 Motivation

It is a well known fact that nature is governed by four fundamental forces: gravity, strong and weak interactions and electromagnetism. The last three are well described by quantum field theory, the framework where the famed Standard Model is formulated. An indication of the success of this latter is the extremely precise predictions it has given us over time, such as the anomalous magnetic moment of the electron. However, in spite of its successes, the understanding of QFTs is not yet fully satisfactory as we lack the tools to analyze them in the strongly coupling regime. As for the gravitational force, General Relativity constitutes our most powerful tool in this matter, having been one of the most important triumphs of the 20th-century physics. Nevertheless, despite all of its successes, it still has its own limitations and open questions. Indeed, there are some cases where both gravitational and quantum effects need to be taken into account, such as in the vicinity of a black hole. In light of this, one of the most important remaining tasks of modern physics is then to incorporate the principles of quantum mechanics in General Relativity, thereby constructing a so-called quantum gravity theory.

Throughout the years, several ideas for a theory which would solve both issues were proposed and explored. One such proposal, which is still a target of great debate and research nowadays is the AdS/CFT duality, put forward by Juan Maldacena in 1998 [2]. When it was first introduced, it used sound arguments to relate two apparently distinct theories, namely $\mathcal{N} = 4$ Super Yang-Mills theory, which is a Conformal Field Theory, and a type IIB string theory on an asymptotically $\mathrm{AdS}_5 \times S^5$ spacetime. According to the duality, not only are they related, as they are in fact equivalent to each other. This

equivalence, however, is not restricted to this case. The main notion behind AdS/CFT is that some CFTs in a $d-$dimensional spacetime are equivalent to a corresponding theory of quantum gravity/string theory in an asymptotically AdS $(d+1)$-dimensional spacetime. The CFT is said to inhabit the boundary of AdS while the gravitational theory lives in the bulk. Although no explicit proof has been given, this duality is generally accepted due to the several successful tests which indicate its validity. One such instance, is the agreement of the spectrum of some operators, which was extracted from correlation functions computed from both the gauge theory and the gravitational theory perspective. However, it is important to be aware that AdS/CFT will not provide us with a theory of quantum gravity describing the world we live in. It can, nonetheless, be used to gain intuition about general traits that such a theory would have.

Since its proposal, the AdS/CFT correspondence has proven to be particularly useful in understanding universal features of strongly coupled field theories, by looking at their dual bulk description. However, one has still to understand how to answer long-standing questions about bulk physics from the boundary perspective. For instance, would it be possible to know what happens to an observer that falls inside a blackhole by posing this question in the language of CFTs? In principle, not only should this be possible but it would also be easier for us since we are more acquainted with the formalism of QTFs. However, this is far from being a trivial matter since both theories are constructed in terms of completely different spaces and operators. Therefore, we would need to have a "dictionary" mapping all operators from one theory to the other in order to address this issue. It seems therefore, that there is still a lot of work to be done such that we can answer the plethora of questions about this topic.

Among these, one important topic which is yet to be fully understood, is the locality of the bulk theory. Specifically, we would like to be able to answer questions such as: how do the CFT degrees of freedom organize themselves in order to give rise to bulk locality? What conditions does the CFT have to obey such that its dual is local? Is there any construction that could tells us whether or not the bulk theory is local? Being able to tackle these issues would allow us take a step further in fully understanding how holography encodes bulk locality and consequently the emergence of spacetime.

1.2 Outline

In this thesis we will tackle the topic of locality of the bulk theory. In particular, we will compute certain functions which are deeply related to CFTs correlation functions, and that can be used to provide us information about the locality of the dual theory.

In chapter 2, we review the basics of Conformal Field Theories. We begin by motivating the study of these theories. Then, we present the conformal symmetry group and its generators and argue how it deeply constrains the observables of these theories. In addition, we go over some of the tools which will be used throughout this work such as the Operator Product Expansion, the Conformal Blocks, the Embedding Space formalism, among many others.

In chapter 3, we give a brief overview of this topic's state-of-art. In particular, we present a key conjecture which dictates the necessary conditions for a CFT to have a local bulk dual. We then proceed to introduce the construction of the Holographic Cameras from [1], whose signals allow to unambiguously infer about the locality of the bulk theory. Under certain conditions, which we will explain here, the four point functions defining one of these devices are equivalent to the corresponding correlators given by Conformal Regge theory. Since this paper only considered scalar correlators for plotting the camera's signal in a few cases, we found it compelling to extend the analysis for spinning correlation functions. Doing so would not only validate this formalism further but could also provide us with additional information.

In order to write these correlators according to Conformal Regge theory, it is indispensable to know the corresponding conformal blocks in the Regge limit. Thus, in chapter 4, we start by extending the presentation on conformal blocks, where we explain how to obtain and analytically continue these functions. Afterwards, we compute the conformal blocks in the Regge limit of four point functions with one spinning operator and three scalars as well as with two spinning operators and two scalars.

Finally, in chapter 5, we present our conclusions and address the future directions of this work.

Chapter 2

Conformal Field Theories

Conformal Field Theories are not only relevant in the context of AdS/CFT but also on their own. In particular, they have been studied extensively over the last few decades for numerous reasons, some of which we will briefly point out here. Presently, one of the biggest difficulties of modern physics is trying to understand the strongly coupled behavior of QFTs. This stems from the fact that we only possess perturbative methods, which by definition work strictly in the weak regime. It would thus be useful to find a non-perturbative technique, such that we could overcome this problem. It is in this context that CFTs come up. In particular, because these theories possess a larger symmetry group (conformal symmetry), some of their observables are completely determined. Naturally, this trait suggests that understanding the strongly coupled behavior in these theories might be simpler. Nevertheless, CFTs remain entirely non-trivial. While there has been notable progress in this area, there is still a lot to be comprehended.

One particular reason why CFTs are so compelling to study, is that they are fixed points of the Renormalization Group flow. Within the framework of the Wilson renormalization [3], we start by considering an arbitrary QFT described by a microscopic Lagrangian, $\mathcal{L}$. Necessarily, this theory has a large momentum cutoff Λ, associated with the scale of atomic distances, above which the description of the system by a continuum theory breaks down. Indeed, this is made clear by the UV divergences one finds when taking the integrals to these higher scales. Thus, the partition function of this QFT is given by:

$$Z[J] = \int [\mathcal{D}\phi]_\Lambda \; e^{\int \mathcal{L} + J\,\phi} \;, \tag{2.1}$$

where

$$[\mathcal{D}\phi]_\Lambda \equiv \prod_{|k|<\Lambda} d\phi(k) \ , \tag{2.2}$$

with $\phi(k)$ the Fourier components of the field ϕ. The main idea of this construction is to analyze the influence of the high energy degrees of freedom to the physical predictions of the theory. In order to assess this, we can integrate the Fourier components whose momenta is closer to the cutoff and compare it with the original partition function. The starting point is then to integrate over a small shell in momentum space $b\,\Lambda < |k| < \Lambda$, where $0 < b < 1$, which leads to a new cutoff scale, $b\Lambda$. This integration takes us to a slightly different partition function:

$$Z[J] = \int [\mathcal{D}\phi]_{b\Lambda}\ e^{\int \mathcal{L}_{\text{eff}} + J\phi} \ . \tag{2.3}$$

The effective Lagrangian $\mathcal{L}_{\text{eff}}$ differs from the original one with respect to the couplings. In particular, these have changed in order to account for the integration and for fact that the Lagrangian now concerns a different energy scale. This is the so called "running of coupling constants". Moreover, because the Lagrangian has distinct parameters, it corresponds to a completely different point in the space of all QFTs. By iterating this process while taking the thickness of the momentum shell to be infinitesimally small, $b \approx 1$, we get a continuous flow in this space. This is referred to as an RG flow. This flow continues until it reaches a point where further momentum shell integration does not alter the physical description of the theory anymore. These are known as fixed points and correspond to scale invariant theories. Given that CFTs possess scale invariance, they are necessarily fixed points.

Because completely different microscopic theories can flow asymptotically to the same fixed point, this means that they can all be described by the same CFT at larger scales. We say that these theories belong to the same universality class. Naturally, all of these theories will have the same critical exponents, correlation functions, etc. One such instance of this occurs with the $3d$ Ising model, which consists in a lattice of length a, where each site has a classical spin $s_i \in \{\pm 1\}$, and where we consider nearest-neighbor interactions. Usually, we are interested in obtaining spin correlation functions such as:

$$\langle s(r)s(0)\rangle \sim e^{-\frac{r}{\xi(T)}} \ , \tag{2.4}$$

where $\xi(T)$ is the characteristic length. At the critical temperature $T = T_c$ the system undergoes a phase transition and $\xi(T_c) = \infty$. When this happens, any sense of scale disappears such that we find a scale invariant theory, or more specifically for this case, a

CFT. Interestingly, this CFT is exactly the same as the one appearing in the $\lambda\phi^4$ theory, which corresponds to the Wilson-Fisher fixed point.

In addition to the $3d$ Ising model, other systems such as water or uni-axial magnets, which undergo such a phase transition, flow to the same fixed point. This means that all of these theories belong to the same universality class. Moreover, we say that these theories are IR equivalent at their critical points.

2.1 Conformal symmetry and conformal algebra

The symmetries/conserved charges of a given QFT inhabiting a particular spacetime are determined by the Killing vector fields ($\epsilon = \epsilon^\mu \partial_\mu$). This stems from the fact that conserved currents, which we associate with symmetries, are constructed with the Killing fields. Consequently, the conserved charges, which result from integrating these currents, also depend on them.

In flat space, where we can either have Poincaré or Euclidean symmetry, depending on the considered signature, we have that the stress-energy tensor is conserved:

$$\partial_\mu T^{\mu\nu} = 0 \ . \tag{2.5}$$

Relatedly, the Killing vector fields can be contracted with the stress-energy tensor in order to construct a general conserved current [4]:

$$J^\mu = \epsilon_\nu T^{\mu\nu} \ . \tag{2.6}$$

In addition, by integrating this current over a spatial volume, we obtain a conserved charge associated to each symmetry/Killing field:

$$Q_\epsilon = \int_\Sigma dS_\mu \, \epsilon_\nu \, T^{\mu\nu} \ , \tag{2.7}$$

where Σ is some closed surface. Given that it is a conserved quantity, it obeys:

$$0 = \partial_\mu \left(\epsilon_\nu \, T^{\mu\nu}\right) = \left(\partial_\mu \epsilon_\nu\right) T^{\mu\nu} + \epsilon_\nu \, \partial_\mu \, T^{\mu\nu} = \frac{1}{2}\left(\partial_\mu \epsilon_\nu + \partial_\nu \epsilon_\mu\right) T^{\mu\nu} \ , \tag{2.8}$$

which in due turn implies

$$\partial_\mu \epsilon_\nu + \partial_\nu \epsilon_\mu = 0 \ . \tag{2.9}$$

These are nothing more than the Killing equations.

For Poincaré/Euclidean invariant theories, these equations admit the following solutions:

$$p_\mu = \partial_\mu \quad \text{(translations)} \ , \quad m_{\mu\nu} = x_\nu \partial_\mu - x_\mu \partial_\nu \quad \text{(rotations)} \ . \tag{2.10}$$

Let us now see how CFTs have even more symmetries. To do this, we will start by considering scale invariant theories, which remain unchanged under

$$x^\mu \to \lambda \, x^\mu \ , \tag{2.11}$$

which can also be thought as a rescaling of the metric

$$g_{\mu\nu} \to \lambda^2 \, g_{\mu\nu} \ . \tag{2.12}$$

Let us now take the rescaling factor to be given as $\lambda - 1 = \epsilon$ and consider a negligible rescaling $\epsilon \approx 0$. Consequently, the infinitesimal change in the metric is $\delta g_{\mu\nu} = 2\,\epsilon\, g_{\mu\nu}$. Now, given that the stress-energy tensor measures the response to a change in the metric, we have

$$\delta S \propto \int d^D x \, T_{\mu\nu} \, \delta g^{\mu\nu} = 2\epsilon \int d^D x \, T^\mu_{\ \mu} \ . \tag{2.13}$$

If the theory is to be scale invariant, it must satisfy $\delta S = 0$ for every ϵ. Therefore, the stress-energy tensor must be the total divergence of some vector operator [5, 6] :

$$T^\mu_{\ \mu} = \partial_\mu K^\mu \ . \tag{2.14}$$

Since the stress tensor has dimension d, the vector operator K^μ must have dimension $d-1$ at the fixed point. However, except for conserved currents, most vector operators acquire anomalous dimensions. Hence, K^μ is generally a conserved current, i.e. $\partial_\mu K^\mu = 0$, such that $T^\mu_{\ \mu} = 0$. Note, however, that there are scale invariant theories with $T^\mu_{\ \mu} \neq 0$ (see [7] for such an example).

Interestingly, a scale invariant theory satisfying $T^\mu_{\ \mu} = 0$ becomes a conformal invariant theory. To see why, consider a transformation leading to $\delta g_{\mu\nu} = c(x)\, g_{\mu\nu}$, for some arbitrary position dependent function $c(x)$. Such a theory satisfies:

$$\delta S \propto \int d^D x \, T_{\mu\nu} \, \delta g^{\mu\nu} = \int d^D x \, c(x) \, T^\mu_{\ \mu} = 0 \ , \tag{2.15}$$

thereby making it invariant under such transformations, which are called Weyl transformations. The majority of these Weyl transformations, however, changes the spacetime geometry from flat to curved, which we do not want. Fortunately, there is a subclass

of them which keep the spacetime flat, the so-called conformal transformations. These transformations can be realized infinitesimally as local diffeomorphisms:

$$x^\mu \to x^\mu + \epsilon_\mu(x) \ . \tag{2.16}$$

Moreover, these transformations change the metric in a way that needs to be equivalent to that of a infinitesimal Weyl transformation. Hence, we must have:

$$\partial_\mu \epsilon_\nu + \partial_\nu \epsilon_\nu = c(x)\, g_{\mu\nu} \ . \tag{2.17}$$

In flat space, we either replace $g_{\mu\nu}$ in the above expression by $\delta_{\mu\nu}$ for Euclidean spacetime or by $\eta_{\mu\nu}$ for Minkowski spacetime. The above expression encodes the Killing equations for the case of conformal symmetry, which in addition to translations and rotations, admits two more solutions:

$$d = x^\mu \partial_\mu \qquad \text{(dilatations)}\,, \qquad k_\mu = 2x_\mu (x\cdot\partial) - x^2 \partial_\mu \qquad \text{(SCTs)}\,. \tag{2.18}$$

Dilatations are related to rescaling and therefore scale invariance. On the other hand, special conformal transformations can be shown to be given as a combination of inversions and translations in the following way: $SCT = I \circ P \circ I$. We thus have that the conformal group is constituted by: translations, rotations, dilatations and SCTs. This is summarized in the following table.

Transformation	**Generator**	**Coordinate transformation**	**Number**
Translation	p^μ	$x'^\mu = x^\mu + a^\mu$	d
Rotation	$m_{\mu\nu}$	$x'^\mu = M^\mu_{\ \nu}\, x^\nu$	$\frac{d(d-1)}{2}$
Dilatation	d	$x'^\mu = \lambda\, x^\mu$	1
SCT	k^μ	$x'^\mu = \frac{x^\mu - b^\mu\, x^2}{1-2(b\cdot x)+b^2x^2}$	d

Table 2.1: Conformal transformations, respective generators, finite form and number of degrees of freedom

Summing the degrees of freedom of the different transformations we obtain a total of $\frac{(d+1)(d+2)}{2}$, which is precisely the number of generators of rotations in a $(d+2)-$dimensional space. This hints a relation between the two groups, as will be seen ahead.

Since we know the conformal vector fields, we can construct the conserved charges by using (2.7). These charges are of particular importance because they provide us a

representation of the conformal algebra. In particular, they obey*

$$\left[Q_{\epsilon_1}, Q_{\epsilon_2}\right] = Q_{-[\epsilon_1,\epsilon_2]} \ . \tag{2.19}$$

Using this equality, one finds that the conformal charges satisfy the following commutation relations:

$$\begin{aligned} &[M_{\mu\nu}, M_{\rho\sigma}] = \delta_{\nu\rho}\, M_{\mu\sigma} - \delta_{\mu\rho}\, M_{\nu\sigma} + \delta_{\nu\sigma}\, M_{\rho\mu} - \delta_{\mu\sigma}\, M_{\rho\nu} \ , \\ &[M_{\mu\nu}, P_\rho] = \delta_{\nu\rho} P_\mu - \delta_{\mu\rho} P_\nu \quad , \quad [M_{\mu\nu}, K_\rho] = \delta_{\nu\rho} K_\mu - \delta_{\mu\rho} K_\nu \ , \\ &[D, P_\mu] = P_\mu \ , \ \ [D, K_\mu] = -K_\mu \ , \ \ [K_\mu, P_\nu] = 2\,\delta_{\mu\nu}\, D - 2\, M_{\mu\nu} \ . \end{aligned} \tag{2.20}$$

The above relations define the conformal algebra. It is interesting to see that the first line corresponds exactly to the algebra of $SO(d)$. Accordingly, the second line tells us that P^μ and K^μ transform as vectors under rotations. Even more interesting, however, is the last line, which reveals that P^μ and K^μ act respectively as raising and lowering operators with regard to the dilatation operator D. This is somewhat similar to how in the single quantum harmonic oscillator the ladder operators $a^\dagger$ and a, respectively increase or decrease the energy by one unit, which in turn is the eigenvalue of the operator $a^\dagger a$. As it turns out, the conformal algebra is isomorphic to $SO(d+1,1)$. To see this, one can define a new set of generators L_{AB}, where $A, B \in \{-1, 0, \ldots, d\}$, and identify them with the conformal generators as:

$$L_{\mu\nu} = M_{\mu\nu} \, , \quad L_{-1,0} = D \, , \quad L_{0,\mu} = \frac{1}{2}\left(P_\mu + K_\mu\right) \ , \quad L_{-1,\mu} = \frac{1}{2}\left(P_\mu - K_\mu\right) \ , \tag{2.21}$$

where $\mu, \nu \in \{1, \ldots, d\}$. It is then a simple but tedious task to show that these generators L_{AB} satisfy the algebra of $SO(d+1,1)$. Indeed, this isomorphism was already implied before when we verified that the number of conformal generators and $SO(d+1,1)$ generators agreed with each other. Thus, the action of the conformal group in $\mathbb{R}^d$ can be seen as rotations on $\mathbb{R}^{d+1,1}$. Naturally, this second approach seems easier to work with and in particular to figure out the constraints imposed by conformal invariance on the theory's observables. This relation is the main idea behind the embedding space formalism, which will be presented after the next section.

*For $d = 2$ CFTs this is this commutation relation is slightly different. See [8]

2.2 Primaries and descendants

Given a certain CFT, we may identify the operators by their eigenvalue with respect to the dilatation operator:

$$\big[D, \mathcal{O}(0)\big] = \Delta\, \mathcal{O}(0)\,, \tag{2.22}$$

where Δ is called the conformal dimension of $\mathcal{O}$. For reasons that will be explained later, these dimensions must be positive $\Delta \geq 0$. Additionally, the operators are also characterized by their spin J, which is related with the irreducible representation under which they transforms under rotations:

$$\big[M_{\mu\nu}, \mathcal{O}^{a_1 \ldots a_J}(0)\big] = \big(S_{\mu\nu}\big)_{b_1 \ldots b_J}^{\ a_1 \ldots a_J}\ \mathcal{O}^{b_1 \ldots b_J}(0)\,. \tag{2.23}$$

Here, $S_{\mu\nu}$ are matrices satisfying the same algebra as $M_{\mu\nu}$ while the indices a_i, b_i concern the $SO(d)$ representation of $\mathcal{O}$. We often omit these spin indices for simplicity.

Now, as we had commented before, the conformal generators K_μ and P_μ act as lowering and raising operators with respect to the dilatation operators, respectively. In particular, each time we act with K_μ on a certain operator we lower the conformal dimensions by one unit. As such, if we act multiple times with this generator, we must eventually reach zero, given that conformal dimensions are bounded from below. It is customary to define the primary operators as the ones that are annihilated by K_μ:

$$\big[K_\mu, \mathcal{O}(0)\big] = 0\,. \tag{2.24}$$

Acting with momentum generators on these primaries, we construct operators of higher dimensions, which we refer to as descendants:

$$\mathcal{O}(0) \to P_{\mu_1} \ldots P_{\mu_\ell} \left(P^2\right)^n \mathcal{O}(0)\,, \qquad \Delta \to \Delta + 2\,n + \ell\,. \tag{2.25}$$

Note that we have distinguished between acting with momentum generators with free indices or contracted indices. This is essential since both things have a significant difference. In particular, while in the first case the spin of the operators is also increased, in the second it is not.

To the set of a given primary operator and all of its descendants we call a conformal family. Each of these is characterized by the dimension Δ and spin J of the corresponding primary.

Lastly, it is worth remarking that in a CFT every local operator is a linear combination of primaries and descendants. For a proof of this, see for example [8].

2.3 Embedding Space formalism

When considering a CFT living in d dimensions, we have seen that the conformal group is $SO(d+1,1)$. Thus, while its action in $\mathbb{R}^d$ might be non-trivial, it is simpler in the embedding space $\mathbb{M}^{d+2}$ since it acts linearly through rotations. Figuring out the constraints imposed by conformal symmetries should thus be easier from this second perspective. The idea then is to embed the d dimensional space and the CFT living on it in $\mathbb{M}^{d+2}$.

This lift between both spaces is done through a one-to-one correspondence between points x^μ in $\mathbb{R}^d$ and null-rays in the embedding space $\mathbb{M}^{d+2}$, given by the vectors

$$P_x^A = \lambda \left(1, x^2, x^\mu\right) \ , \quad \lambda \in \mathbb{R} \, . \tag{2.26}$$

Here we are using the coordinates

$$P^A = \left(P^+, P^-, P^a\right) \, , \tag{2.27}$$

and the metric

$$P \cdot P = \eta_{AB} \, P^A \, P^B = -P^+ \, P^- + \delta_{ab} \, P^a \, P^b \ . \tag{2.28}$$

Under the action of $SO(d+1,1)$ the null rays get mapped to other null rays, which translates into a map between points of the physical space $\mathbb{R}^d$. Importantly, these transformations between the x^μ correspond precisely to conformal transformations. This had to be the case in order for this formalism to work.

We can also lift fields to the embedding space. For this, we define a generic field inhabiting the lightcone ($P^2 = 0$) by a tensor $F_{A_1 \ldots A_J}(P)$ of $SO(d+1,1)$ satisfying the following properties:

- Depends homogeneously on P with weight $-\Delta$: $F_{A_1 \ldots A_J}(\lambda \, P) = \lambda^{-\Delta} \, F_{A_1 \ldots A_J}(P)$;
- Is symmetric and traceless;
- Is transverse: $P^{A_1} \, F_{A_1 \ldots A_J}(P) = 0$;

For a certain null ray, characterized by a given direction $(1, x^2, x^\mu)$, we can move along it by varying λ. Moreover, we know how the fields transform under rescalings by λ. Therefore, if we know the value of the field in some point of a light-ray, we necessarily know it for the

entire light-ray. This invariance under $P \to \lambda P$ can be seen as sort of a gauge freedom. Consequently, if the field is known in a particular section of the lightcone it becomes determined in all of it. Generally, we choose the Poincaré section,

$$P_x^A = (1, x^2, x^\mu)\,, \tag{2.29}$$

although other choice would be valid as well. The restriction of the tensor $F_{A_1\ldots A_J}$ to the Poincaré section, which has only d dimensions, can be projected to $\mathbb{R}^d$. This gives a symmetric and traceless field on the physical space,

$$f_{\mu_1\ldots\mu_J}(x) = \frac{\partial P^{A_1}}{\partial x^{\mu_1}} \cdots \frac{\partial P^{A_J}}{\partial x^{\mu_J}} F_{A_1\ldots A_J}(P)\,, \tag{2.30}$$

where

$$\frac{\partial P^{A_1}}{\partial x^{\mu_1}} = \left(0, 2\,x_{\mu_1}, \delta_{\mu_1}^{a_1}\right)\,. \tag{2.31}$$

Due to the transversality of the tensors $F_{A_1\ldots A_J}$, terms proportional to P_{A_i} project to zero in the physical space. We call these tensors pure gauge.

It can then be showed [9, 10] that the tensors $f_{\mu_1\ldots\mu_J}$ behave like symmetric and traceless primary fields of dimension Δ and spin J under conformal transformations. Thus, this formalism allows also to lift the operators of a CFT to the embedding space and consequently correlation functions.

2.4 Null Polarization Vectors

There are times when we want to consider operators with nonzero spin. Working with all the indices of the fields $f_{\mu_1\ldots\mu_J}$, however, is a slightly bothersome matter. In order to obtain neater equations, we contract these tensors with appropriate vectors and get rid of the indices. As an outcome, we obtain a polynomial which encodes the original tensor. A thorough presentation of this construction is given in [11].

The idea is then as follows. We take a symmetric and traceless tensor $f_{\mu_1\ldots\mu_J}$ and contract the indices with vectors z^μ:

$$f(x; z) = f_{\mu_1\ldots\mu_J}(x)\, z^{\mu_1} \ldots z^{\mu_J}\,. \tag{2.32}$$

The z^μ are referred to as polarization vectors. In particular, because the field is traceless we restrict these to be null, $z^2 = 0$. Consequently, two polynomials which differ from each other by $O(z^2)$ terms encode the same tensor. Moreover, because we contract every index

with a polarization vector, the resulting polynomial will be of degree J in z, thus encoding the spin of the field.

Given a polynomial, we can also retrieve the indices and obtain the original tensor with the Todorov differential operator:

$$D_a = \left(h - 1 + z \cdot \frac{\partial}{\partial z}\right) \frac{\partial}{\partial z^a} - \frac{1}{2} z_a \frac{\partial^2}{\partial z \cdot \partial z}\,, \tag{2.33}$$

where $h \equiv d/2$. In particular, the tensor can be retrieved by:

$$f_{\mu_1 \ldots \mu_J}(x) = \frac{1}{J!(h-1)_J} D_{\mu_1} \ldots D_{\mu_J} \tilde{f}(x, z)\,, \tag{2.34}$$

where $(n)_J = \Gamma(n+J)/\Gamma(n)$ is the Pochhammer symbol and $\tilde{f}(x,z)$ represents the polynomial $f(x,z)$ restricted to the submanifold $z^2 = 0$, i.e.:

$$f(x,z) = \tilde{f}(x,z) + O(z^2)\,. \tag{2.35}$$

This construction can be also be used in the embedding space. Given a symmetric, traceless and transverse tensor $F_{A_1 \ldots A_J}$ in $\mathbb{M}^{d+2}$ we can contract it with vectors $Z^A \in \mathbb{M}^{d+2}$:

$$F(P,Z) = F_{A_1 \ldots A_J}(P)\, Z^{A_1} \ldots Z^{A_J}\,. \tag{2.36}$$

Analogously to before, we once again use null vectors ($Z^2 = 0$) due to the tracelessness of the tensors. Moreover, because these are also transverse we further restrict to the subset of Z's satisfying $Z \cdot P = 0$. Hence, polynomials which differ modulo terms proportional to P^2 and $Z \cdot P$ encode the same tensor. Here, the polynomial will also encode the spin J of the field by the degree in Z.

The transversality condition of the tensors imposes that the polynomials obey:

$$P \cdot \frac{\partial}{\partial Z} F(P,Z) = 0 \;\; \Leftrightarrow \;\; F(P,Z) = F(P, Z + \alpha\, P)\;, \;\; \forall\, \alpha \in \mathbb{R}\,, \tag{2.37}$$

which then dictates the transversality of the polynomials.

In order to retrieve the tensors from the polynomials we can proceed in the same way as before (2.34), by acting with the Todorov operator in $d+2$ dimensions,

$$D_A = \left(h - 1 + Z \cdot \frac{\partial}{\partial Z}\right) \frac{\partial}{\partial Z^A} - \frac{1}{2} Z_A \frac{\partial^2}{\partial Z \cdot \partial Z}\,, \tag{2.38}$$

in the polynomials with no $O(P^2)$ and $O(P \cdot Z)$ terms.

We could now wonder about the relation about the polynomials in the physical $f(x,z)$ and embedding space $F(P,Z)$. Indeed, taking into account how we go from the embedding

space to the physical space (2.30) we have that the polynomials in these spaces are related as

$$f(x,z) = F(P_x, Z_{z,x})\,, \tag{2.39}$$

where $Z_{z,x} = (0, 2\,x\cdot z, z)$, which in turn satisfy

$$Z_{z,x}\cdot P_x = 0 \ , \quad Z_{z,x}^2 = z^2 \ . \tag{2.40}$$

In the case of a traceless tensor, the RHS of the right equality is 0.

Lastly, we give the map between certain quantities in both spaces, which are essential for writing correlation functions interchangeably in the embedding and physical space:

$$Z_i\cdot Z_j \longleftrightarrow z_i\cdot z_j \ , \quad P_i\cdot Z_j \longleftrightarrow z_j\cdot x_{ij} \ , \quad P_i\cdot P_j \longleftrightarrow -\frac{1}{2}\,x_{ij}^2 \tag{2.41}$$

2.5 Conformal correlators

Most of the times we are studying a CFT, we are interested in obtaining correlation functions of local operators. As we will see now, conformal symmetry alone is strong enough to completely fix the structure of two and three point functions in such a theory. Although for higher point functions this is not the case anymore, symmetry still help us figuring out the general structure that these functions must have.

2.5.1 Two point correlation functions

2.5.1.1 Scalar operators

Start by considering the correlation function of the two scalar primaries located at different points $\langle \mathcal{O}_1(x_1)\,\mathcal{O}_2(x_2)\rangle$. Translation and rotation invariance immediately impose $\langle \mathcal{O}_1(x_1)\,\mathcal{O}_2(x_2)\rangle = f(|x_1-x_2|)$. Moreover, if this correlator is to be scale invariant, it must vanish under the action of D on both of its operators. Thus, we have:

$$\begin{aligned} 0 &= \langle \big[D, \mathcal{O}_1(x)\mathcal{O}_2(x)\big]\rangle = \langle \big[D,\mathcal{O}_1(x)\big]\ \mathcal{O}_2(x)\rangle + \langle \mathcal{O}_1(x)\ \big[D,\mathcal{O}_2(x)\big]\rangle \\ &= \left(x_1^\mu \partial_{1,\mu} + \Delta_1 + x_2^\mu \partial_{2,\mu} + \Delta_2\right) f(|x_1-x_2|)\,, \end{aligned} \tag{2.42}$$

where we have used the commutation relation between the operator D and a local primary located at an arbitrary position x:

$$\big[D, \mathcal{O}(x)\big] = (x\cdot\partial + \Delta)\ \mathcal{O}(x)\,. \tag{2.43}$$

It is easy to show that the solution of (2.42) is:

$$f(|x_1 - x_2|) = \frac{C}{|x_1 - x_2|^{\Delta_1+\Delta_2}} \,. \tag{2.44}$$

Consider now a general conformal transformation. In particular, given a conserved charge Q_ϵ we can construct the operator $U = e^{Q_\epsilon}$, which implements a finite conformal transformation as:

$$U\,\mathcal{O}^{a_1\ldots a_J}(x)\,U^{-1} = \Omega(x')^\Delta\, D\left(R(x')\right)^{a_1\ldots a_J}_{b_1\ldots b_J} O^{b_1\ldots b_J}(x') \,. \tag{2.45}$$

Here, x' denotes the transformed coordinate, $\Omega(x)$ is a local scale factor and $D\left(R(x')\right)^{a_1\ldots a_J}_{b_1\ldots b_J}$ is a matrix which implements the action of the rotation R in the representation of $\mathcal{O}$. Given that the two point function is a conformal object, it must be invariant under these transformations:

$$\begin{aligned}\langle \mathcal{O}_1(x_1)\,\mathcal{O}_2(x_2)\rangle &= \langle \Big(U\,\mathcal{O}_1(x_1)\,U^{-1}\Big)\,\Big(U\,\mathcal{O}_2(x_2)\,U^{-1}\Big)\rangle \\ &= \Omega(x_1')^{\Delta_1}\,\Omega(x_2')^{\Delta_2}\,\langle \mathcal{O}_1(x_1')\,\mathcal{O}_2(x_2')\rangle \,.\end{aligned} \tag{2.46}$$

In addition, we have that under any conformal transformation, distances transform as:

$$(x-y)^2 = \frac{\left(x'-y'\right)^2}{\Omega(x')\,\Omega(y')} \,. \tag{2.47}$$

The validity of this expression is easy to show for translations, rotations and dilatations. It is also possible to show this holds true for inversions, which implies it is valid for SCTs since these are built up from inversions and translations. Imposing the equality of the two point function under (2.46) and (2.47) we can fix it even further:

$$\Omega(x_1')^{\Delta_1}\,\Omega(x_2')^{\Delta_2}\frac{C}{|x_1 - x_2|^{\Delta_1+\Delta_2}} = \left(\Omega(x_1')\,\Omega(x_2')\right)^{\frac{\Delta_1+\Delta_2}{2}}\,\frac{C}{|x_1 - x_2|^{\Delta_1+\Delta_2}} \,. \tag{2.48}$$

This equality is verified when either $C = 0$ or $\Delta_1 = \Delta_2$. By absorbing the constant C in the definition of the operators, we get that two point functions are completely determined by symmetry and given as:

$$\langle \mathcal{O}_1(x_1)\,\mathcal{O}_2(x_2)\rangle = \frac{\delta_{\Delta_1,\Delta_2}}{\left(x_{12}^2\right)^{\frac{\Delta_1+\Delta_2}{2}}} \,, \tag{2.49}$$

where $x_{ij} \equiv x_i - x_j$. Interestingly, these correlators are nonzero only when the operators have identical dimensions. Moreover, note that (2.49) imposes $\Delta_1 \geq 0$ since otherwise, the correlation function would diverge when the separation between the two operators became very large. This would be completely unphysical.

2.5.1.2 Spinning operators

We can also consider two point functions of spinning operators and show that they are completely fixed by symmetry as well. Similarly to the scalar case, spinning two points functions are also diagonal in the space of operators, meaning that they are only nonzero when both operators have the same dimension Δ and spin J. For these objects, however, we would be better at computing them in the embedding space where the conformal group acts linearly.

Let us denote the two point function of a spin J primary by:

$$G^{A_1\dots A_J\,,\,B_1\dots B_J}(P_1,P_2)=\langle\mathcal{O}^{A_1\dots A_J}(P_1)\,\mathcal{O}^{B_1\dots B_J}(P_2)\rangle\ . \tag{2.50}$$

It is convenient to employ the formalism of the polarization vectors since we are dealing with a tensor with indices:

$$G(P_1,P_2,Z_1,Z_2)=Z_1^{A_1}\dots Z_1^{A_J}\,Z_2^{B_1}\dots Z_2^{B_J}\,G_{A_1\dots A_J\,,\,B_1\dots B_J}(P_1,P_2)\ . \tag{2.51}$$

According to what was said previously, this polynomial must satisfy the following conditions: it must transform homogeneously under scalings, with weight $-\Delta$; it must have degree J in Z_1 and Z_2; it must be transverse, thus obeying (2.37). Taking into account these considerations and dropping terms proportional to P_i^2 and $P_i\cdot Z_i$, which are vanishing for our purposes, we can only have [11]:

$$\tilde{G}(P_1,P_2;Z_1,Z_2)=C_{\mathcal{O}}\,\frac{H_{12}^J}{(P_{12})^{\Delta+J}}\ , \tag{2.52}$$

where $P_{ij}\equiv-2\,P_i\cdot P_j$ and H_{12} is given by:

$$H_{ij}\equiv-2\left[(Z_i\cdot Z_j)(P_i\cdot P_j)-(Z_i\cdot P_j)(Z_j\cdot P_i)\right]\ . \tag{2.53}$$

This structure is referred to as a building block. More of these will be seen for three point functions.

We can now project this result into the physical space by using the relations from (2.41). This gives

$$\langle\mathcal{O}^{\mu_1\dots\mu_J}(x_1)\,\mathcal{O}^{\nu_1\dots\nu_J}(x_2)\rangle=C_{\mathcal{O}}\left(\frac{I^{\,(\mu_1\,\nu_1}(x_{12})\dots I^{\mu_J\,\nu_J)}(x_{12})}{(x_{12}^2)\,\Delta}-\text{traces}\right)\ , \tag{2.54}$$

where

$$I^{\mu\nu}(x)\equiv\delta^{\mu\nu}-2\,\frac{x^\mu\,x^\nu}{x^2}\,. \tag{2.55}$$

The symmetrization over the indices μ_i, ν_i and subtraction of the traces in (2.54) are necessary in order to obtain a symmetric and traceless result, just like the operators. These, however, result directly from how the embedding space and the null polarization vectors formalism are constructed.

Most of the times, we can also normalize the operators so as to have $C_{\mathcal{O}} = 1$ in (2.54). An exception, however, occurs for the stress tensor in which its normalization is already fixed by the Ward identities, thus preventing us from getting rid of C_T. This constant, however, has a physical significance, which will not be explored here.

2.5.2 Three point correlation functions

2.5.2.1 Scalar operators

The case of the scalar three point function $\langle \mathcal{O}_1(x_1)\, \mathcal{O}_2(x_2)\, \mathcal{O}_3(x_3) \rangle$ is similar to the two point. Once again, translation and rotation invariance impose that $\langle \mathcal{O}_1(x_1)\, \mathcal{O}_2(x_2)\, \mathcal{O}_3(x_3) \rangle = f(x_{12}^2, x_{13}^2, x_{23}^2)$. Moreover, given the structure of the two point function, is it resonable to propose the following ansatz for the three point correlator:

$$f(x_{12}^2, x_{13}^2, x_{23}^2) = \lambda_{123} \left(x_{12}^2\right)^{a_1} \left(x_{13}^2\right)^{a_2} \left(x_{23}^2\right)^{a_3} , \tag{2.56}$$

where the coefficients a_i are undetermined by now and λ_{123} is some constant. Because this correlator is also conformally invariant it must satisfy the analogue of eq.(2.46), namely:

$$\langle \mathcal{O}_1(x_1)\, \mathcal{O}_2(x_2)\, \mathcal{O}_3(x_3) \rangle = \Omega(x_1')^{\Delta_1}\, \Omega(x_2')^{\Delta_2}\, \Omega(x_3')^{\Delta_3}\, \langle \mathcal{O}_1(x_1)\, \mathcal{O}_2(x_2)\, \mathcal{O}_3(x_3) \rangle . \tag{2.57}$$

According to our ansatz, the three point function is also made up strictly from products of squared distances. Therefore, under a conformal transformation it must change according to (2.47). Consistency then requires this result to be equivalent to the previous expression:

$$\Omega(x_1')^{\Delta_1}\, \Omega(x_2')^{\Delta_2}\, \Omega(x_3')^{\Delta_3} = \left[\Omega(x_1')\, \Omega(x_2')\right]^{-a_1} \left[\Omega(x_1')\, \Omega(x_3')\right]^{-a_2} \left[\Omega(x_2')\, \Omega(x_3')\right]^{-a_3} , \tag{2.58}$$

which in turn gives us the a_i coefficients. In the end, conformal symmetry fixes the scalar three point function to be given by:

$$\langle \mathcal{O}_1(x_1)\, \mathcal{O}_2(x_2)\, \mathcal{O}_3(x_3) = \frac{\lambda_{123}}{\left(x_{12}^2\right)^{\frac{\Delta_1+\Delta_2-\Delta_3}{2}} \left(x_{13}^2\right)^{\frac{\Delta_1+\Delta_3-\Delta_2}{2}} \left(x_{23}^2\right)^{\frac{\Delta_2+\Delta_3-\Delta_1}{2}}} . \tag{2.59}$$

The constant λ_{123}, however, cannot be determined by conformal invariance but is rather a dynamical quantity. We call this a OPE coefficient for reasons that will become clear later.

2.5.2.2 Spinning operators

More generally, we can consider three point functions of nonzero spin operators in the symmetric and traceless representation of $SO(d)$. Similarly to the two point case, it is simpler to first compute these objects in the embedding space and only after project to the physical space. A detailed presentation of these objects can be found in [11].

Let us denote the generic three point function of operators in the symmetric and traceless representation of $SO(d)$ by:

$$G(P_1,P_2,P_3)^{\{\mu,\nu,\gamma\}} = \langle \mathcal{O}_1^{\{\mu\}}(P_1)\,\mathcal{O}_2^{\{\nu\}}(P_2)\,\mathcal{O}_3^{\{\gamma\}}(P_3)\rangle \ , \tag{2.60}$$

where we are using the notation $\{\mu\} = \mu_1 \dots \mu_J$. Contracting this object with null polarization vectors Z_i, we get:

$$\begin{aligned} &G(P_1,P_2,P_3,Z_1,Z_2,Z_3) = \\ &Z_1^{\mu_1}\dots Z_1^{\mu_J}\, Z_2^{\nu_1}\dots Z_2^{\nu_J}\, Z_3^{\gamma_1}\dots Z_3^{\gamma_J}\, \langle \mathcal{O}_{1,\{\mu\}}(P_1)\,\mathcal{O}_{2,\{\nu\}}(P_2)\,\mathcal{O}_{3,\{\gamma\}}(P_3)\rangle \ . \end{aligned} \tag{2.61}$$

Taking into account all the same conditions mentioned in the two points case, namely homogeneity under scaling, degree J_i in each Z_i and transversality, this correlation function needs to be given as:

$$\tilde{G}(P_1,P_2,P_3,Z_1,Z_2,Z_3) = \sum_{\{\ell_i\}} \frac{\lambda_{J_1J_2J_3}^{\ell_1\ell_2\ell_3} V_{1,23}^{J_1-\ell_2-\ell_3} V_{2,31}^{J_2-\ell_1-\ell_3} V_{3,12}^{J_3-\ell_1-\ell_2} H_{12}^{\ell_3} H_{13}^{\ell_2} H_{23}^{\ell_1}}{(P_{12})^{\frac{\bar{\tau}_1+\bar{\tau}_2-\bar{\tau}_3}{2}}\,(P_{13})^{\frac{\bar{\tau}_1+\bar{\tau}_3-\bar{\tau}_2}{2}}\,(P_{23})^{\frac{\bar{\tau}_2+\bar{\tau}_3-\bar{\tau}_1}{2}}} \ , \tag{2.62}$$

where $\bar{\tau}_i = \Delta_i + J_i$ and the tilde above G means we have restricted to $P_i^2 = 0$ and $P_i \cdot Z_i = 0$. Here, in addition to the structures H_{ij} we have another kind of building blocks given by:

$$V_{i,jk} \equiv \frac{(Z_i\cdot P_j)(P_i\cdot P_k) - (Z_i\cdot P_k)(P_i\cdot P_j)}{(P_j\cdot P_k)} \ . \tag{2.63}$$

The basic building blocks H_{ij} and $V_{i,jk}$ are transverse polynomials which satisfy $H_{ij} = H_{ji}$ and $V_{i,jk} = -V_{i,kj}$. Consequently, not all of these are linearly independent. It is then a matter of choice to choose the three independent H_{ij} and the three independent $V_{i,jk}$ with which to express the correlators.

In addition, because each term of $\tilde{G}(P_1, P_2, P_3, Z_1, Z_2, Z_3)$ must have the appropriate degrees on the Z_i's, the ℓ_i's must satisfy:

$$\ell_2 + \ell_3 \leq J_1 \ , \quad \ell_1 + \ell_3 \leq J_2 \ , \quad \ell_1 + \ell_2 \leq J_3 \ . \tag{2.64}$$

This translates into a sum over $\ell_i \in \{0, \ldots, \min(J_k)\}$, which labels the different possible structures.

Projecting (2.62) according to (2.30), we obtain the generic spinning three point function in the physical space. In particular, this is is given by (2.62) with $P_{ij} \to x_{ij}^2$ and the building blocks expressed in the physical space:

$$V_{i,j\,k} = \frac{(z_i \cdot x_{ik})\, x_{ij}^2 - (z_i \cdot x_{ij})\, x_{ik}^2}{x_{jk}^2} \quad , \quad H_{ij} = x_{ij}^2 (z_i \cdot z_j) - 2(z_i \cdot x_{ij})(z_j \cdot x_{ij}) \, . \tag{2.65}$$

The three point can thus be written as:

$$\begin{aligned} &\langle \mathcal{O}_1(x_1, z_1) \ldots \mathcal{O}_3(x_3, z_3) \rangle = \\ &\frac{\sum_{\{\ell_i\}} \lambda_{J_1 J_2 J_3}^{\ell_1 \ell_2 \ell_3} \; t^{(\ell_1, \ell_2, \ell_3)}(\tilde{x}_{12}, \tilde{z}_1, \tilde{z}_2, z_3)}{\left(x_{12}^2\right)^{\frac{1}{2}(\Delta_1 + \Delta_2 - \Delta_3 + \sum_i J_i)} \left(x_{13}^2\right)^{\frac{1}{2}(\Delta_1 + \Delta_3 - \Delta_2 + \sum_i J_i)} \left(x_{23}^2\right)^{\frac{1}{2}(\Delta_2 + \Delta_3 - \Delta_1 + \sum_i J_i)}} \, , \end{aligned} \tag{2.66}$$

where

$$\tilde{x}_{12} \equiv x_{13} x_{23}^2 - x_{23} x_{13}^2 \, , \; \tilde{z}_1 \equiv I(x_{13})\, z_1 \, , \; \tilde{z}_2 \equiv I(x_{23})\, z_2 \ , \tag{2.67}$$

and the structures $t^{(\ell_1, \ell_2, \ell_3)}(x, z_1, z_2, z_3)$ are given by:

$$(x^2 z_2 \cdot z_3)^{\ell_1} (x^2 z_1 \cdot z_3)^{\ell_2} (x^2 z_1 \cdot z_2 - 2x \cdot z_1 \, x \cdot z_2)^{\ell_3} (-x \cdot z_1)^{m_1} (-x \cdot z_2)^{m_2} (x \cdot z_3)^{m_3} \, , \tag{2.68}$$

with

$$m_i = J_i - \sum_{k \neq i} \ell_k \ . \tag{2.69}$$

The reason why we have decided to express the spinning three point functions this way, in terms of these t structures, is because these objects appear in the OPE (which is to be introduced later) between spinning operators (see [12]). Indeed, notice how this choice of polynomials t treats $\mathcal{O}_3$ differently from $\mathcal{O}_1$ and $\mathcal{O}_2$. This happens because these structures concern the OPE $\mathcal{O}_1 \times \mathcal{O}_2$ where $\mathcal{O}_3$ is the exchanged operator. Equivalently, we could have chosen a different OPE between these three operators, although we would have to use different but intimately related tensor structures t' (see for [11] this). Moreover, these structures will be relevant farther ahead, such that identifying them like this will prove helpful.

2.5.3 Higher point correlation functions

It seems that following the reasoning of the previous two sections, we would be able to completely fix higher point functions with conformal symmetry alone. Unfortunately, this is not the case, as when we consider more than three points we begin to have nontrivial combinations of the positions, which are conformally invariant, called cross-ratios. In the case of a four point function we have two distinct cross-ratios:

$$u = \frac{x_{12}^2 x_{13}^2}{x_{13}^2 x_{24}^2}\,, \quad v = \frac{x_{14}^2 x_{23}^2}{x_{13}^2 x_{24}^2}\,. \tag{2.70}$$

In order to understand why there are only two independent cross ratios in this case consider the following steps:

- Start with four points at arbitrary positions x_i, with $i = 1, \ldots, 4$.
- Use special conformal transformations to send x_4 to infinity.
- Using translations, move x_1 to the origin, $x_1 = (0, \ldots, 0)$.
- Use rotations and dilatations to move x_3 to $(1, 0, \ldots, 0)$.
- Using rotations that leave x_3 unchanged, move x_2 to $(x, y, 0, \ldots, 0)$.

The final configuration is illlustrated in figure 2.1.

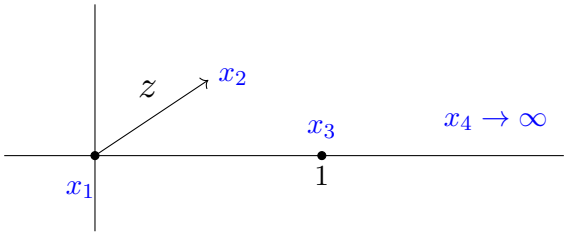

Figure 2.1: Configuration of the four points after we have used conformal transformations to put them in the same plane

In this procedure we have used all possible conformal symmetry transformations to fix everything except for two undetermined quantities x and y, which give two independent conformal invariants. Hence, up to conformal transformations, any set of four points can be described by two quantities. These are usually expressed in terms of complex quantities $z \equiv x + i\,y$ and $\bar{z} \equiv x - i\,y$. It is then a trivial matter to compute u and v in this configuration, which gives:

$$u = z\,\bar{z}\,, \quad v = (1 - z)(1 - \bar{z})\,. \tag{2.71}$$

Thus, the four point function must depend non-trivially in these two cross-ratios. For four scalars with conformal dimensions Δ_i, this correlator can be expressed as:

$$\langle \mathcal{O}_1(x_1)\,\mathcal{O}_2(x_2)\,\mathcal{O}_3(x_3)\,\mathcal{O}_4(x_4)\rangle = \frac{\left(\frac{x_{24}^2}{x_{14}^2}\right)^{\frac{\Delta_{12}}{2}}\left(\frac{x_{14}^2}{x_{13}^2}\right)^{\frac{\Delta_{34}}{2}}}{\left(x_{12}^2\right)^{\frac{\Delta_1+\Delta_2}{2}}\left(x_{34}^2\right)^{\frac{\Delta_3+\Delta_4}{2}}}\,G(u,v)\,. \tag{2.72}$$

The position dependence, which we refer to as the pre-factor, is easily found in the same manner as for the two and three point functions. In particular, it is responsible for the correct scaling properties of the correlator:

$$\langle \mathcal{O}_1(\lambda\,x_1)\ldots\mathcal{O}_4(\lambda\,x_4)\rangle = \lambda^{-(\Delta_1+\Delta_2+\Delta_3+\Delta_4)}\,\langle \mathcal{O}_1(x_1)\ldots\mathcal{O}_4(x_4)\rangle\,. \tag{2.73}$$

It is also possible to consider four point functions of spinning operators. However, if written with the null polarization vectors, the basic building blocks $V_{i,jk}$ and H_{ij} must appear in order to correctly encode the spin of the external operators. As such, the structure of these correlators will be similar to (2.72), but with several cross ratios functions $G_i(u,v)$, each associated with a different four point function tensor structure. These structures, in turn, can be generated using the building blocks.

We could now add one more point x_5 to the correlator and consider a similar analysis. Indeed, by once again making use of conformal transformations we could obtain the configuration of figure 2.1 for the first four points. At first sight this seems to make use of all conformal transformations such that it is not clear how we can handle x_5. However, this is not completely true since the previous procedure did not exploit all of the rotations symmetries. In particular, we can use the set of rotations orthogonal to the plane defined by the other four points, to move x_5 to $(\tilde{x},\tilde{y},\tilde{z},0,\ldots,0)$. This leaves us with three more undetermined quantities, thereby leading to a total of five independent cross ratios. A convenient choice for these is [13]:

$$u_1 = \frac{x_{12}^2\,x_{35}^2}{x_{13}^2\,x_{25}^2}\,, \qquad u_{i+1} = u_i\,|_{x_i\to x_{i+1}}\,, \tag{2.74}$$

where the subscript in x_j is taken modulo 6. Analogously, the five point function of different scalars should be given by a pre-factor which takes care of the scaling properties and a nontrivial function of these cross-ratios:

$$\langle \mathcal{O}_1(x_1)\ldots\mathcal{O}_5(x_5)\rangle = \frac{\left(\frac{x_{23}^2}{x_{13}^2}\right)^{\Delta_{12}}\left(\frac{x_{14}^2}{x_{13}^2}\right)^{\frac{\Delta_{34}}{2}}}{\left(x_{12}^2\right)^{\frac{\Delta_1+\Delta_2}{2}}\left(x_{34}^2\right)^{\frac{\Delta_3+\Delta_4}{2}}}\left(\frac{x_{13}^2}{x_{15}^2\,x_{35}^2}\right)^{\frac{\Delta_5}{2}}\,G\left(u_1,\ldots,u_5\right)\,. \tag{2.75}$$

Analogously, we could consider spinning five point functions, which would also require the presence of tensor structures generated with the basic building blocks. This could go on as we continue to consider more points in the correlation function. However, a time will come when there will not be enough conformal transformations to fix the components of the new points. Indeed, in d dimensions the conformal group is $SO(d+1,1)$ and has $\frac{(d+1)(d+2)}{2}$ transformations. Hence, while the number of points n is less than $d+2$, we can keep using conformal transformations to fix the points. When $n \geq d+2$, however, the totality of these transformations will be used. Since each point has d components, a n point function will have a total of $n\,d$ degrees of freedom, of which only $\frac{(d+1)(d+2)}{2}$ can be constrained. The number of independent cross ratios for a given n point function is then given by

$$\begin{cases} \frac{n(n-3)}{2} & \text{if } n \leq d+2 \\ n\,d - \frac{(d+1)(d+2)}{2} & \text{if } n > d+2 \end{cases} \tag{2.76}$$

Similarly, all of the scalar higher point functions will depend on a non trivial function of these cross ratios and on a prefactor which absorbs the weight of the external operators. When the external operators have nonzero spin, the correlators will also depend on several tensor structures, each associated with a cross ratios function.

2.6 Radial Quantization

Up to now we have seen numerous commutation relations and correlation functions without having explicitly specified the quantization of the theory. In general, we choose to quantize the theory in a way that respects its symmetries. For instance, when we are dealing with Poincaré invariant theories we always choose a certain spacetime direction $x^0 = t$, which we call time. We then opt to foliate spacetime by surfaces of equal t (figure 2.2), each of these endowed with its own Hilbert space. This procedure is advantageous since the temporal component of the momentum operator P^0, which is identified with the Hamiltonian H, move us from surface to surface. In particular, this achieved by an operator, which we call evolution operator U, and which we define as:

$$U = e^{i\,H\,t}\,. \tag{2.77}$$

Since all surfaces are related by this operator, the Hilbert space is the same in all of them. What is more, every state in one of these surfaces is characterized by their energy and

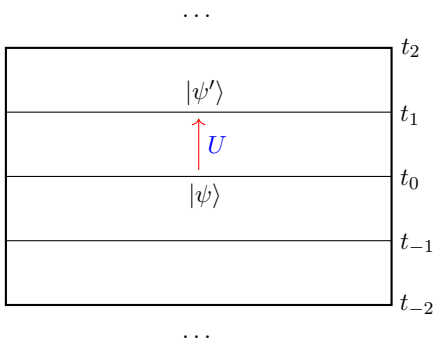

FIGURE 2.2: Spacetime foliation through surfaces of equal time and corresponding time evolution between states living in different surfaces

momentum:

$$P^\mu |k\rangle = k^\mu |k\rangle \,. \tag{2.78}$$

In CFTs, however, this choice of quantization is not the most convenient. Indeed, because these theories are scale invariant it is more natural to foliate spacetime with spheres S^{d-1} of different radii around the origin, associating an Hilbert space to each of them (figure 2.3). We then propagate states between different spheres with the dilatation operator D,

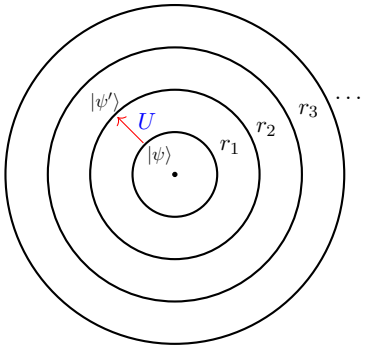

FIGURE 2.3: Spacetime foliation with spheres S^{d-1} of different radii around the origin

by defining the following evolution operator:

$$U = e^{\tau D} \,, \tag{2.79}$$

where $\tau = \ln r$. The states living in these spheres are characterized by their dimensions Δ,

$$D|\Delta\rangle = \Delta|\Delta\rangle \,, \tag{2.80}$$

and their $SO(d)$ spins J,

$$M_{\mu\nu} |\Delta, J\rangle_{\mu_1 \ldots \mu_J} = \left(S_{\mu\nu}\right)_{\mu_1 \ldots \mu_J}^{\nu_1 \ldots \nu_J} |\Delta, J\rangle_{\nu_1 \ldots \nu_J} \,, \tag{2.81}$$

since $M_{\mu\nu}$ are the only commuting generators with D. Here, the matrices $S_{\mu\nu}$ are the same as before. Note, lastly, that we are free to choose the point around which we perform this quantization, similarly to how we can change to different reference frames in Lorentz invariant theories.

2.7 State-Operator Correspondence

An important property of CFTs which is most easily perceptible in the radial quantization picture is the so-called state-operator correspondence. The main idea behind this, is that given a CFT it is possible to define a state from an operator and vice-versa. A detailed presentation of this topic can be found for example in [8, 6].

Indeed, given an operator $\mathcal{O}$ which is inserted inside a sphere B of unitary radius at x, we can define a state at its boundary ∂B by the following path integral:

$$|\mathcal{O}(x)\rangle = \int D\phi_b \, |\phi_b\rangle\langle\phi_b|\mathcal{O}(x)|0\rangle \, . \tag{2.82}$$

Here, $|\phi_b\rangle$ are a basis of states defined only at ∂B, which span the entire Hilbert space of the sphere. Moreover, the vacuum state $|0\rangle$, defined at ∂B as well, results from performing the path integral over the interior of the sphere without any operator insertions. The coefficients of this expansion are given by the path integral over B:

$$\langle\phi_b|\mathcal{O}(x)|0\rangle = \int_{\phi(r,\mathbf{n})=\phi_b(\mathbf{n})}^{r<1} D\phi(r,\mathbf{n})\, \mathcal{O}(x)\, e^{-S[\phi]} \, , \tag{2.83}$$

where we must impose the appropriate boundary conditions, ϕ_b.

This relation can also be constructed in the opposite direction. Let us denote by $|\mathcal{O}_i\rangle$ the eigenstates of the dilatation operator, which we had previously defined by $|\Delta\rangle$ in (2.80), satisfying:

$$D\,|\mathcal{O}_i\rangle = \Delta_i \, |\mathcal{O}_i\rangle \, . \tag{2.84}$$

For each of these states, we can define the corresponding operators $\mathcal{O}_i$ by constructing correlation functions with these. To see this, suppose that we cut holes B_i located at positions x_i in the path integral. Then, we glue in the boundary of these spheres ∂B_i the states $|\mathcal{O}_i\rangle$, as in figure 2.4. This leads to an object that behaves very similarly to a correlation function of local operators and that is given by:

$$\langle\mathcal{O}_1(x_1)\dots\mathcal{O}_n(x_n)\rangle = \int \prod_i D\phi_{b_i} \, \langle\phi_{b_i}|\mathcal{O}_i(x_i)\rangle \int_{\substack{\phi_{\partial B_i}=\phi_{b_i} \\ x\notin B_i}} D\phi(x)\, e^{-S[\phi]} \, . \tag{2.85}$$

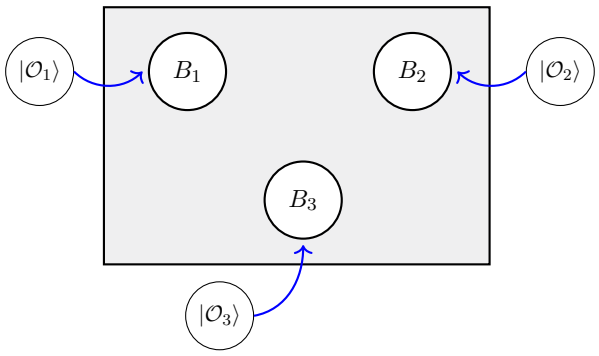

FIGURE 2.4: Cutting holes B_i in the path integral and gluing states on the boundaries ∂B_i to define a correlation function

Here, the second integral is taken outside the spheres B_i and ϕ_{b_i} denotes the field defined at ∂B_i.

It is important that the positions x_i are sufficiently far from each other such that the B_i's do not overlap. In case they do, we can always rescale so as to prevent this. Then, since these positions are arbitrary, we can take them to be infinitesimally close, thereby defining local operators.

The RHS of (2.85) only depends on the states $|\mathcal{O}_i\rangle$ and is able to define a correlation function of local operators $\mathcal{O}_i$. Bearing in mind that local operators are realized in QFTs through their correlation functions, this then suffices to prove the claim.

Since we define local operators as being the ones that satisfy (2.22) (eigenstates of the dilatation operator), the above paragraphs prove the validity of the two directions of the equivalence between states and operators.

A more natural way to think about local operators, is to consider an arbitrary state which gets evolved to the origin by using D. The resulting state will then be defined in the neighborhood of $x = 0$. Due to the state-operator correspondence we just presented, this state is associated unequivocally with an operator defined in the exact same infinitesimal region. This is precisely what we have in mind when we say an operator is local.

2.8 Operator Product Expansion (OPE)

2.8.1 Euclidean OPE

There is a nice property of CFTs which comes about due to the state-operator correspondence. The idea, however, is not a novelty but rather something we are already familiarized for general QFTs. In particular, it consists on being able to replace the product of two

local operators by a linear combination of other operators inserted somewhere in between, in the limit they become very close to each other. This argument is also valid for CFTs, but because these theories have additional symmetries such that we can radially quantize them, the OPE gains additional properties as we will see. In particular, its structure is almost completely fixed by the conformal symmetries.

We start by quantizing the theory around x_2. We then insert two local operators $\mathcal{O}_1(x_1)$ and $\mathcal{O}_2(x_2)$ inside a ball centered around this point. Performing the path integral inside the interior of the ball, the operators define a state $\mathcal{O}_1(x_1)\,\mathcal{O}_2(x_2)|0\rangle \equiv |\psi\rangle$ on its boundary, which in turn can be written as a linear combination of the dilatation operator eigenstates $|\Delta, J\rangle$:

$$|\psi\rangle = \sum_{\Delta,J} c_{\Delta,J}\,|\Delta, J\rangle\ , \qquad c_{\Delta,J} = c_{\Delta,J}(x_{12})\,. \tag{2.86}$$

Due to the state-operator correspondence, each of these states $|\Delta, J\rangle$ is uniquely identified with a local operator which can be either primary or a descendant. Hence, we can write:

$$\mathcal{O}_1(x_1)\,\mathcal{O}_2(x_2)|0\rangle = \sum_{\Delta,J} c_{\Delta,J}(x_{12})\,\mathcal{O}_{\Delta,J}(x_2)\,|0\rangle\,, \tag{2.87}$$

where we are denoting both the primaries and descendants schematically by $\mathcal{O}_{\Delta,J}$, omitting possible spin indices. Recall now that descendants are defined as derivatives of primaries. Taking this into account and once again using the state-operator correspondence, we can translate the above equality into the following statement about operators:

$$\mathcal{O}_1(x_1)\,\mathcal{O}_2(x_2) = \sum_{\mathcal{O}} C(x_{12}, \partial_{x_2})^{\mu_1\ldots\mu_J}\,\mathcal{O}_{\mu_1\ldots\mu_J}(x_2)\,, \tag{2.88}$$

where the sum runs only over all primary operators of the spectrum. Moreover, the $C(x_{12}, \partial_{x_2})$ are known as coefficient functions. As they are a power series of derivatives, they generate the descendants upon acting on the primaries, thus encoding the contribution of these operators as in (2.87). Interestingly, conformal symmetry allows us to fix the OPE even further, such that the above expression becomes:

$$\mathcal{O}_1(x_1)\,\mathcal{O}_2(x_2) = \sum_{\mathcal{O}} \frac{\lambda_{12\mathcal{O}}}{\left(x_{12}^2\right)^{\frac{\Delta_1+\Delta_2-\tau}{2}}}\,F(x_{12}, \partial_{x_2})^{\mu_1\ldots\mu_J}\,\mathcal{O}_{\mu_1\ldots\mu_J}(x_2)\,. \tag{2.89}$$

where $\tau = \Delta - J$ is the twist of the exchanged operator $\mathcal{O}_{\mu_1\ldots\mu_J}$. The above expression is the generally found expression for the OPE in the case of two scalars. Note that the exchanged operator must transform in the symmetric and traceless representation of $SO(d)$ since the OPE is between scalar operators.

To go from (2.88) to (2.89) we have imposed that the three point function computed by means of the OPE agrees with the three point function expression (2.59) in the same limit:

$$\lim_{x_2\to x_1}\langle\mathcal{O}_1(x_1)\mathcal{O}_2(x_2)\mathcal{O}_3(x_3)\rangle = C\left(x_{12},\partial_{x_2}\right)\,\langle\mathcal{O}_3(x_2)\,\mathcal{O}_3(x_3)\rangle\,, \tag{2.90}$$

where we have chosen to perform the OPE $\mathcal{O}_1\times\mathcal{O}_2$. Moreover, because two point functions are diagonal, the only non-vanishing term in the OPE sum is for the exchanged operator $\mathcal{O}=\mathcal{O}_3$.

This equality tells us that the $C(x_{12},\partial_{x_2})$ are proportional to $F(x_{12},\partial_{x_2})$, where the proportionality constants are the three point function coefficients $\lambda_{12\mathcal{O}}$. The latter cannot be fixed by symmetry and in fact depend on the theory. On the other hand, the functions $F(x_{12},\partial_{x_2})$ get completely fixed by this procedure [8]. In particular, it is found that the leading term of the Euclidean OPE is given by:

$$\mathcal{O}_1(x_1)\mathcal{O}_2(x_2) = \sum_{\mathcal{O}}\frac{\lambda_{12\mathcal{O}}}{\left(x_{12}^2\right)^{\frac{\Delta_1+\Delta_2-\tau}{2}}}\frac{\left(x_{12}\cdot D_z\right)^J}{J!\left(\frac{d}{2}-1\right)_J}\mathcal{O}(x_1,z)+\dots\,, \tag{2.91}$$

where the $\dots$ denote subleading contributions. Note also that we could equally as well have quantized the theory around x_1 or any other point. Expression (2.89) would still be valid, but with the exchanged primary inserted around the new origin.

In contrast to the OPE for general QFTs, the sum in (2.89) is valid and converges for a finite separation between the operators. In particular, it converges within a ball enclosing the two operators where no other operator are inserted. Naturally, this defines a radius of convergence for the OPE.

The OPE is a very powerful tool since it can be used to reduce any n point function to an $n-1$ point function:

$$\langle\mathcal{O}_1(x_1)\,\mathcal{O}_2(x_2)\dots\mathcal{O}_n(x_n)\rangle = \sum_k\frac{\lambda_{12k}}{\left(x_{12}^2\right)^{\frac{\Delta_1+\Delta_2-\tau}{2}}}F(x_{12},\partial_{x_2})\,\langle\mathcal{O}_k(x_2)\dots\mathcal{O}_n(x_n)\rangle\,, \tag{2.92}$$

where we have suppressed spinning indices for simplicity and are labeling the primaries by k. Iterating this procedure, we are able to write every conformal correlator as a sum over one-point functions, which in flat space are given by

$$\langle\mathcal{O}(x)\rangle = \delta_{\mathcal{O},I}\,, \tag{2.93}$$

with I the unit operator.

2.8.2 Lorentzian OPE

The OPE we just described makes sense when we take the near coincidence limit $x_{12} \to 0$. However, in Lorentzian signature there is another useful limit which we can take, where we take one operator to approach the lightcone of another. In this limit, $x_{12}^2 \to 0$, we have a different OPE, which is given by [13, 14]:

$$\begin{aligned}\mathcal{O}_1(x_1)\,\mathcal{O}_2(x_2) &= \sum_{\mathcal{O}} \lambda_{12\mathcal{O}}\ (x_{12}\cdot D_z)^J \int_0^1 [dt]\, \frac{e^{t x_{21}\cdot\partial_{x_1}}\,\mathcal{O}(x_1,z)}{(x_{12}^2)^{\frac{\Delta_1+\Delta_2-\tau}{2}}} + \dots \\ &= \sum_{\mathcal{O}} \lambda_{12\mathcal{O}} \int_0^1 [dt]\, \frac{\mathcal{O}(x_1+t x_{21}, x_{12})}{(x_{12}^2)^{\frac{\Delta_1+\Delta_2-\tau}{2}}} + \dots\,. \end{aligned} \tag{2.94}$$

where $\dots$ represents subleading terms and the integration measure is given by:

$$[dt] = \frac{\Gamma(\bar\tau)}{\Gamma(\frac{\bar\tau+\Delta_{12}}{2})\Gamma(\frac{\bar\tau-\Delta_{12}}{2})}\ t^{\frac{\bar\tau-\Delta_{12}}{2}-1}\,(1-t)^{\frac{\bar\tau+\Delta_{12}}{2}-1} dt\,. \tag{2.95}$$

Mostly often, we will refer to the near coincidence limit OPE as the Euclidean OPE while the lightcone limit OPE will be called the Lorentzian OPE. This is because the former is usually taken when we are in the Euclidean signature or the operators are space-like separated, whereas the latter is only valid in Lorentzian signature.

There is a crucial difference between both OPEs, which can be seen by comparing (2.91) with (2.94) in the respective limits. In particular, we find that while in the Euclidean limit ($x_{12} \to 0$) the lowest dimension operators dominate, in the Lorentzian limit ($x_{12}^2 \to 0$), it is those with the lowest twist that give the biggest contribution.

2.9 Conformal Blocks

A nice consequence of the OPE is that it allows us to expand correlators in terms of a certain basis of functions. To see this, start by considering a four point function of scalar operators $\mathcal{O}_i(x_i)$, each with conformal dimension Δ_i, $i = 1, \dots, 4$. As stated before, conformal symmetry imposes the structure of this correlator to be as in (2.72). On the other hand, we can perform the Euclidean OPE twice, for instance between the pairs $\mathcal{O}_1 \times \mathcal{O}_2$ and $\mathcal{O}_3 \times \mathcal{O}_4$. Using formula (2.88), this yields:

$$\begin{aligned}&\langle \mathcal{O}_1(x_1)\,\mathcal{O}_2(x_2)\,\mathcal{O}_3(x_3)\,\mathcal{O}_4(x_4)\rangle = \\ &= \sum_{\mathcal{O}} \lambda_{12\mathcal{O}}\lambda_{34\mathcal{O}}\, C(x_{12},\partial_{x_1})^{\mu_1\dots\mu_J} C(x_{34},\partial_{x_3})^{f_1\dots f_J} \langle \mathcal{O}_{\nu_1\dots\nu_J}(x_1)\mathcal{O}_{f_1\dots f_J}(x_3)\rangle \\ &= \sum_{\mathcal{O}} \lambda_{12\mathcal{O}}\,\lambda_{34\mathcal{O}}\, W_{\mathcal{O}}(x_1,x_2,x_3,x_4)\quad . \end{aligned} \tag{2.96}$$

where we have taken the OPE constants out of the coefficient functions. Here, the functions $W_{\mathcal{O}}(x_1, x_2, x_3, x_4)$ are called conformal partial waves. Analogously to correlators, their structure is fixed by conformal symmetry to be like:

$$W_{\mathcal{O}}(x_1, x_2, x_3, x_4) = \left(\frac{x_{24}^2}{x_{14}^2}\right)^{\frac{\Delta_{12}}{2}} \left(\frac{x_{14}^2}{x_{13}^2}\right)^{\frac{\Delta_{34}}{2}} \frac{G_{\mathcal{O}}(u,v)}{\left(x_{12}^2\right)^{\frac{\Delta_1+\Delta_2}{2}} \left(x_{34}^2\right)^{\frac{\Delta_3+\Delta_4}{2}}}\,, \tag{2.97}$$

where the cross-ratios function $G_{\mathcal{O}}(u, v)$ is referred to as a conformal block. By how they are defined, each of these functions encodes the contribution of a full conformal family to the four point function.

Comparing (2.72) with (2.96) and (2.97) combined, we can make the following identification:

$$G(u,v) = \sum_{\mathcal{O}} \lambda_{12\mathcal{O}}\, \lambda_{34\mathcal{O}}\, G_{\mathcal{O}}(u,v)\ . \tag{2.98}$$

Thus, the four point function can be expanded as sum over conformal blocks. Consequently, knowledge of these functions translates into information about the correlator.

Although these conformal blocks were obtained by taking the Euclidean OPE, we could have equally as well performed the Lorentzian OPE. This, in turn, would have lead to different conformal blocks and therefore an alternative expansion of the same correlator. This will be seen more ahead when we present the results in chapter 4.

2.10 Conformal Bootstrap

Thus far, we have seen that we could use the OPE to reduce any n point function to an $n-1$ point function (2.92). Consequently, any correlator can be written as a sum over one point functions, which are known. Moreover, the OPE is completely fixed by symmetry in terms of the spectrum $\{\Delta_i, J_i\}$ and the OPE coefficients λ_{ijk}. We call this two sets of numbers the CFT data. This then means that we can compute any correlator of the CFT given this set. We could now wonder, whether given some arbitrary CFT data, it always defines a consistent* CFT? The answer would be no. Indeed, there are certain constraints these numbers must obey such that the CFT they define is consistent. For a more detailed presentation on the conformal boostrap see for example [8, 6].

Consider then a four point function of identical scalars $\langle\phi(x_1)\phi(x_2)\phi(x_3)\phi(x_4)\rangle$. This correlator is crossing symmetric, which means that even if any two positions get swapped

*By consistent we mean that the CFT satisfies certain properties such as crossing symmetry in four point functions of identical operators.

$x_i \leftrightarrow x_j$ it remains the same*. Moreover, when we presented the OPE before, we chose to perform it in the $\phi(x_1) \times \phi(x_2)$, $\phi(x_3) \times \phi(x_4)$ channel:

$$\langle \phi(\overbrace{x_1)\phi(x_2)}\phi(\overbrace{x_3)\phi(x_4)}\rangle = \frac{1}{x_{12}^{2\Delta_\phi} x_{34}^{2\Delta_\phi}} \sum_{\mathcal{O}} \lambda^2_{\phi\phi\mathcal{O}} G_{\mathcal{O}}(u,v) \ , \tag{2.99}$$

where we have used the Wick contraction symbol to denote the OPE. However, if the OPE is to be consistent with the crossing symmetry, choosing any other channel, say $\phi(x_1) \times \phi(x_4)$, $\phi(x_2) \times \phi(x_3)$ for example, should give the same result. In other words, the OPE should be associative:

$$\langle \phi(\overbrace{x_1)\phi(x_2)}\phi(\overbrace{x_3)\phi(x_4)}\rangle = \langle \phi(\overbrace{x_1)\phi(\overbrace{x_2)\phi(x_3)}\phi(x_4)}\rangle \ . \tag{2.100}$$

This other choice of OPE results from swapping $1 \leftrightarrow 3$ (or equivalently $2 \leftrightarrow 4$), which in terms of cross ratios corresponds to $u \leftrightarrow v$. Accordingly, each term of the sum (2.99) becomes:

$$\frac{G_{\mathcal{O}}(u,v)}{x_{12}^{2\Delta_\phi} x_{34}^{2\Delta_\phi}} \to \frac{G_{\mathcal{O}}(v,u)}{x_{12}^{2\Delta_\phi} x_{34}^{2\Delta_\phi}} \frac{x_{12}^{2\Delta_\phi} x_{34}^{2\Delta_\phi}}{x_{14}^{2\Delta_\phi} x_{23}^{2\Delta_\phi}} = \frac{G_{\mathcal{O}}(v,u)}{x_{12}^{2\Delta_\phi} x_{34}^{2\Delta_\phi}} \left(\frac{u}{v}\right)^{\Delta_\phi} \ , \tag{2.101}$$

for the OPEs of the RHS of (2.100). Thus, if we replace the appropriate conformal block expansions in (2.100) we get:

$$\sum_{\mathcal{O}} \lambda^2_{\phi\phi\mathcal{O}} \left(v^{\Delta_\phi} G_{\mathcal{O}}(u,v) - u^{\Delta_\phi} G_{\mathcal{O}}(v,u) \right) = 0 \ . \tag{2.102}$$

This is the bootstrap equation for the case of a four point function of identical scalars. As stated before, it constrains the spectrum and the $\lambda_{\phi\phi\mathcal{O}}$ by demanding that the above equality is satisfied for any u and v. Thus, any CFT data that satisfies this, defines a consistent CFT. We stress out that this equation is only satisfied by the whole sum and not each of its individual terms. Otherwise, the conformal blocks of each conformal family would satisfy $v^{\Delta_\phi} G_{\mathcal{O}}(u,v) = u^{\Delta_\phi} G_{\mathcal{O}}(v,u)$, which is not what is observed in the explicit expressions of these functions (see for example (4.63)). Finally, while this equation can be solved numerically (see [8] for example), an analytical analysis of the boostrap equation around the lightcone limit is also possible for example in the large spin regime [15, 16].

*We can think about this from a path integral perspective. This correlator is given by a path integral whose integrand consists on the product of these fields. The result will be the same independently of the order by which we set the operators.

2.11 AdS/CFT

To conclude this chapter, we will now say a few words about how CFTs arise in the AdS/CFT duality. For a detailed presentation of this topic, see for example [17, 18].

Let us begin by presenting the Anti-deSitter spacetime in the Euclidean signature, which is given by:

$$-\left(X^{-1}\right)^2 + \sum_{i=0}^{d} (X^i)^2 = -R^2 \ , \qquad X^{-1} > 0 \ , \tag{2.103}$$

where R denotes its radius of curvature. This equation defines an hyperboloid embedded in $\mathbb{R}^{d+1,1}$, which approaches the light-cone of the embedding space we presented in section 2.3. For this reason, we say that the boundary of AdS is the space of light-rays which go through the origin of $\mathbb{R}^{d+1,1}$.

Moreover, this spacetime has a few interesting properties, which make it relevant to study. One of these traits, is that it is maximally symmetric, which means that has the maximal number of spacetime symmetries. In particular, for $d+1$ dimensions, AdS_{d+1} has $\frac{(d+1)(d+2)}{2}$ symmetries, which as previously remarked, is the same number of rotation generators in a $(d+2)$-dimensional flat space. In addition, it is a homogeneous and locally isotropic spacetime. Consequently, it does not have a center since all points are equivalent. One of the most fascinating properties, however, is that it acts as a confining box for massive particles. Indeed, an analysis of this spacetime timelike geodesics, tells us that massive particles either stay at rest at the origin* or oscillate around it, with a period of 2π. Quantum mechanically, this last property implies that the energy spectrum of a massive particle is discrete.

Now that we have presented AdS, although rather briefly, we are prepared to understand how the AdS/CFT comes by. Indeed, we mentioned below (2.103) that the boundary of this spacetime is the null cone of the embedding space. But this is exactly the same place where the CFT lives, according to the embedding space formalism. As such, it would be natural to be expect that for certain bulk theories, their observables would satisfy the same properties as those of CFTs, as we approach the boundary of this space-time. Interestingly, this is precisely the case. Given a certain bulk theory in AdS, with a corresponding field ϕ of mass m, we can define correlation functions in the bulk. Moreover, we are free to send

*As we stated previously, all points in AdS are equivalent. Hence, we cannot define one single origin for the whole space. It is possible, however, to choose some point as the origin, and parameterize the spacetime with that choice in mind.

those operators to infinity, which is the same of saying to the boundary, such that we have:

$$\lim_{\lambda\to\infty}\left(\lambda^{\Delta}\right)^{n}\left\langle\phi(X_1=\lambda P_1+\dots)\dots\phi(X_n=\lambda P_n+\dots)\right\rangle=\langle\mathcal{O}(P_1)\dots\mathcal{O}(P_n)\rangle\ , \quad (2.104)$$

where each P_i is a point in the null cone in $\mathbb{R}^{d+1,1}$, satisfying $P_i^2=0$, and the $\dots$ inside the position argument, denote terms that do not grow with λ, and which are necessary to have $X^2=-R^2$. As it turns out, when we do this, the resulting correlators at the boundary fulfill the homogeneity and conformal invariance conditions and satisfy an associative OPE, similarly to CFT correlators. It is also important to point out that the above equality naturally defines a quantum operator which is "dual" to ϕ. In fact, we may even relate the mass of the bulk field ϕ with the conformal dimension of the dual operator $\mathcal{O}$:

$$m^2\,R^2=\Delta(\Delta-d)\ . \quad (2.105)$$

This is an instance of the AdS/CFT dictionary we mentioned before, which relates bulk quantities with boundary ones.

At this point, we would like to stress out that simply having a QFT in the bulk is not enough to have the duality. Indeed, one also needs to have gravitational dynamics as well, in order for the dual theory on the boundary to have a stress-tensor and be a full-fledged CFT. That is why when we stated the AdS/CFT duality before, we mentioned gravitational theories in the bulk and not simply QFTs.

There is another relation of the AdS/CFT map worth introducing, which is related with this last fact. Indeed, because we have a QFT with gravity, we can construct the associated partition function as a path integral over the metric and field, with appropriate boundary conditions. However, we presently do not know how to make computations with it (compute correlators that is), which would seem to render it useless. The best we can do, is a semiclassical expansion of it in the regime where the AdS radius of curvature is much bigger than the Planck length, $R\gg\ell_P$. When this happens, the partition function leads to connected correlators of the stress-tensor which scale as:

$$\langle T_{\mu_1\nu_1}(x_1)\dots T_{\mu_n\nu_n}(x_n)\rangle_c\sim\left(\frac{R}{\ell_P}\right)^{d-1}\ , \quad (2.106)$$

where x^μ are some of the coordinates parameterizing the Poincaré patch of AdS (see [17]). Interestingly, when examining CFTs in the regime of large N, where the parameter N is a measure of the degrees of freedom of the theory, one finds that the same correlators scale

as N^2. Thus, not only does this allow to identify:

$$N^2 \sim \left(\frac{R}{\ell_P}\right)^{d-1} , \tag{2.107}$$

but it also suggests that CFTs related with semiclassical gravitational theories in AdS should have large N. This is something that we will return to more ahead, in chapter 3.

Chapter 3

Locality of the bulk theory

In the last few years, there has been a considerable amount of papers addressing the topic of locality in AdS/CFT. While some of them tackle specific different problems within this broader subject, others resort to distinct approaches for the same questions. For instance, the two papers [19, 20] analyze the singular structure of Lorentzian correlators of the boundary CFT, albeit from distinct viewpoints. Nevertheless, they both assert that a specific kind of singularity in these objects signals bulk physics at scales much smaller than the AdS radius of curvature, R.

In this chapter, we will summarize the main ideas of two other papers which are intimately related to the ones mentioned above. In particular, we start by presenting the conjecture from [21], which puts forward the properties that a boundary CFT must have in order for the dual to be local at sub-Ads scales*. Then, we proceed to introduce the construction of the holographic cameras [1], from whose signal we can infer the locality of the dual theory at these scales. It is mostly from the ideas of this second paper, that the main goal of this thesis comes from.

3.1 Large higher-spin gap large N conjecture

Only when the AdS radius of curvature R is much bigger than the Planck length ℓ_P and the strings length ℓ_s, can we have local bulk physics at sub-AdS scales. Otherwise, the notion of locality at these smaller scales (called "sharp locality" in [21]) would not make sense. In due turn, this translates into a large N expansion and a large higher spin gap $\Delta_{\text{gap}}^{\text{higher-spin}}$ of the dual CFT, following from relations (2.105) and (2.107) of the AdS/CFT

*By sub-AdS scales we mean distances much smaller than the AdS radius of curvature R.

map. Therefore, it would be natural to think that this implication also runs in the opposite direction. Such reasoning, lead to the proposal of the following conjecture [21]:

Any large N CFT in which all single-trace operators with spin higher than two have very large dimensions (large gap $\Delta_{gap}^{higher\text{-}spin}$ in the spectrum), has a bulk dual which is local at sub-AdS scales.

Each of these two conditions is essential for their own specific reasons. In particular, the large N criterion needs to be satisfied such that it is possible to distinguish between single-particle and multi-particle states, which can be respectively associated with single-trace operators, $\mathcal{O} = c_J \operatorname{Tr}(\phi^J)$ where c_J is some normalization constant, and multi-trace operators $\tilde{\mathcal{O}} = \mathcal{O}_1 \dots \mathcal{O}_k$, where each $\mathcal{O}_i$ is a single-trace operator. On the other hand, a large higher-spin gap means we can neglect the operators with parametrically large dimensions. This yields a low-energy effective theory, where only operators with spin lesser than two are present. If this was not the case, the theory would have an infinite tower of higher spin fields and an unbounded number of derivatives in the interactions. As a result, the dual theory in bulk AdS would undoubtedly be a non-local theory.

Although the validity of this conjecture is yet to be proven for all cases, it is generally accepted due to the well-founded arguments which support it. Indeed, [21] showed that it holds for a rather general set of CFTs through a counting argument. For starters, the paper considered a model with only one low dimension single-trace operator $\mathcal{O}$ of dimension Δ, and with $\mathbb{Z}_2$ symmetry ($\mathcal{O} \to -\mathcal{O}$). Moreover, it restricted the analysis to account for a maximal spin of the local interactions, or equivalently a maximal spin for which the corrections are nonzero. Considering the four point function of this scalar in the configuration of figure 2.1:

$$\langle \mathcal{O}(0)\mathcal{O}(z,\bar{z})\mathcal{O}(1)\mathcal{O}(\infty)\rangle \equiv \mathcal{A}(z,\bar{z}) = \frac{1}{(z\bar{z})^{\Delta}} + \sum_{n=0}^{\infty}\sum_{J=0}^{\infty} p(n,J)\frac{G_{\Delta(n,J)}(z,\bar{z})}{(z\bar{z})^{\Delta}}\,, \tag{3.1}$$

where $p(n,J)$ denotes the squared OPE coefficients, one then tries to solve the crossing condition for this correlator:

$$\mathcal{A}(z,\bar{z}) = \mathcal{A}(1-z,1-\bar{z})\ . \tag{3.2}$$

Assuming that this model admits a large N expansion, these solutions amount to corrections to the conformal dimensions γ_i (also known as anomalous dimensions) and corrections

to the squared OPE coefficients p_i in the $1/N$ expansion:

$$\Delta(n,J) = 2\Delta + 2n + J + \frac{1}{N^2}\,\gamma_1(n,J) + \dots \ , \quad p(n,J) = p_0(n,J) + \frac{1}{N^2}\,p_1(n,J) + \dots \ , \tag{3.3}$$

resulting from interactions. Note that the conformal dimensions correspond to double-trace operators, due to the symmetry of the model and because higher-trace operators do not contribute at order $1/N^2$.

In case the conjecture holds, the interactions giving rise to these corrections must be dual to local interactions in the bulk. In due turn, this implies that each of these bulk interactions is in a one-to-one correspondence with a pair (γ_1, p_1).

In fact, this turned out to be the case, as it was verified that the number of solutions to the crossing condition (3.2) up to a certain maximal spin, matched with the number of quartic interactions up to the same maximal spin, which are of the type:

$$\phi^4 \ , \quad \phi^2\,\phi_{;\mu\nu}\,\phi^{;\mu\nu} \ , \quad \phi^2\,\phi_{;\mu\nu\sigma}\,\phi^{;\mu\nu\sigma} \ . \quad \dots \tag{3.4}$$

The reason why quartic interactions are the only ones that need to considered, stems once again from the $\mathbb{Z}_2$ symmetry, plus the fact that these are the only ones contributing to the $1/N^2$ order. Recall that we are dealing with a four point function, such that these interactions correspond to contact diagrams.

It was then argued that general solutions could be taken as limits of the bounded-spin ones, which demonstrated the conjecture for this model. Finally, it was briefly explained why the conjecture would still hold after the $\mathbb{Z}_2$ symmetry was dropped and the stress-tensor was added to the system, thereby making it valid for a general set of CFTs. Although this was not explicitly demonstrated in [21], a proof can be found in [22].

3.2 Holographic Cameras

Although the large N large gap criterion helps us understand which CFTs admit local duals, it does not address the question of how locality emerges in the bulk. This topic is investigated in [1] by means of two tools which the paper names as Holographic Cameras. The main idea behind these devices is to send something into the bulk, where it can interact with local excitations following bulk null geodesics. This interaction leads to a point-like signal, which is a diagnostic of local bulk dynamics. However, in case the theory dual is not local, the interpretation of localized excitations propagating in the bulk fails, and the

cameras should provide us with blurred images. Therefore, these quantities produce simple images from which we can very straightforwardly conclude whether or not the dual is local.

This formalism has several upsides. First, not only it allows us to conclude something about the locality of the bulk dual, but it also provides us with information about the bulk, such as its geometry. Moreover, it only requires the analysis of four point functions independently of the spacetime dimension the CFT lives in. This is in contrast with previous approaches, such as [20], which assesses the locality of the bulk theory by the singular behavior of $d+2$ point functions. The reason why one uses this many points, is because we need to have exactly the same number of points as the dimensions of the embedding space, in order to satisfy the necessary conditions for the specific singularity which signals bulk locality. Thus, this construction would requires us to deal with higher-point functions as we increased the spacetime dimensions. Furthermore, the cameras have the advantage that one can look at their data and immediately conclude if the dual theory is well-defined, in the sense that it is a well-constructed theory by itself or if it is defined in terms of the boundary theory. This differs from some of the approaches of bulk reconstruction [23, 24, 25], which always give us a bulk dual, and associated quantities like its metric, even if this theory is not well-defined as explained before.

3.2.1 Cannon

We begin by introducing half of what constitutes the devices, known as the "cannon", whose role is to shoot the particles into the bulk. The process of the cannon starts by considering an arbitrary state $|\psi\rangle$ of the boundary CFT. Then, we create an excitation by acting on this state with an operator $\mathcal{O}$, which for simplicity will be taken to be a scalar, and proceed to integrate it against a wavepacket, which amounts to a Fourier transform:

$$|\Psi\rangle \to |\Psi'\rangle \equiv \int d^d x\, \psi^*_{p,L}(x)\, \mathcal{O}(x)\, |\Psi\rangle \ , \quad \text{with} \ \ \psi_{p,L} \sim e^{i\, p_\mu x^\mu - |\delta x|^2/\left(2L^2\right)} \ . \tag{3.5}$$

In this case, these wavepackets are plane waves with a Gaussian envelope, which are responsible for creating localized high-energy excitations. In particular, these have a fairly well-defined energy and momentum $\left(p^0 L >> 1\right)$ and a relatively small position uncertainty L compared to intrinsic timescales and lengthscales of the state.

Moreover, the momenta p^μ will be taken to be time-like and large, such that we can interpret this whole procedure as creating local excitations being fired into the bulk. Indeed, according to [26], any particle following a null geodesic in the AdS bulk carries a Noether

charge P^A, whose projection in the boundary is necessarily a time-like vector p^μ (see figure 3.1). Thus, opting for a time-like boundary momentum is simply a matter of choice which

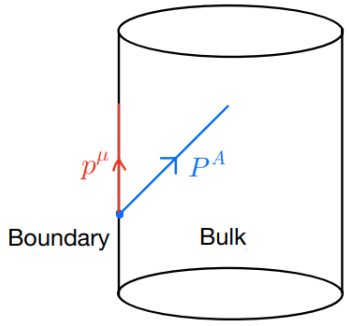

Figure 3.1: Relation between the Noether charge of a particle following a bulk null geodesic with its time-like momentum vector in the boundary.

allows us to interpret (3.5) from the opposite direction of this relation.

In order to confirm if a projectile has indeed been fired into the bulk, we can measure one point functions in the state (3.5), such as the energy-momentum density. This can achieved by computing the one-point function of the stress-energy tensor $T^{\mu\nu}$ in the state (3.5):

$$\begin{aligned}\langle T^{\mu\nu}(y)\rangle_{|\Psi'\rangle} &= \int d^dx\, d^dx'\, \psi_{p,L}(x')\, \psi^*_{p,L}(x)\, \langle\Psi|\mathcal{O}(x')T^{\mu\nu}(y)\mathcal{O}(x)|\Psi\rangle \\ &\sim \int d^d\delta x\, \psi_{p,L}(\delta x)\, \langle\Psi|\mathcal{O}(x+\delta x)T^{\mu\nu}(y)\mathcal{O}(x)|\Psi\rangle\ .\end{aligned} \tag{3.6}$$

Here, x is the point from where we are firing the excitation and y is a point in the future of x in which we measure $T^{\mu\nu}$. Moreover, note that from the first to the second line we have dropped an inessential integration, keeping only the one over the separation of the positions where the excitation is created and absorbed.

Interestingly, we see that the three point function in the second line has an unusual ordering of operators. In the path integral formalism, this could be computed by an integration over the time contour of figure 3.2, which is called Schwinger-Keldysh contour.

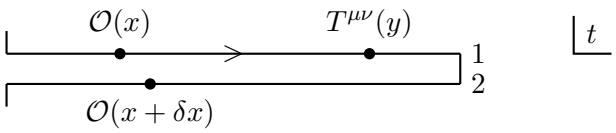

Figure 3.2: Schwinger Keldysh contour and operator insertions for measurement of energy-momentum density

Although this formalism will not be presented here, a nice introduction to it can be found for instance in [27, 28, 29]. The important point here, is that the excitation cannot go

directly from x to $x+\delta x$ but must go along the whole contour. From the AdS perspective, we can see this as an excitation which is evolved forward in time, interacts with $T^{\mu\nu}$ and is then evolved backward in time. Such interpretation is depicted in figure 3.3.

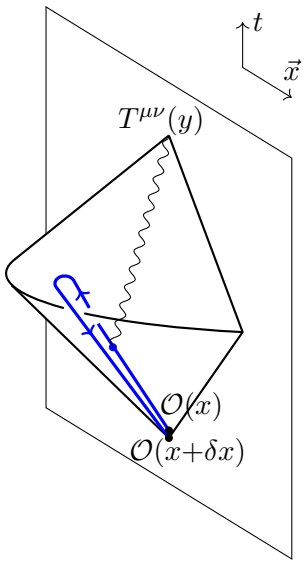

FIGURE 3.3: Schematic representation of the energy-momentum measurement in the bulk of AdS. (Modified figure from [1])

These kinds of correlators have already been studied before in [30], namely for holographic theories in the vacuum state, where it was found that they displayed an expanding shell of energy. Unfortunately, although these are compatible with the idea of local excitations moving in the bulk, they do not constitute irrefutable proof of this as they are not something point-like. The problem then, is that even though the cannon is creating high-quality point-like excitations, the "camera" we are using to see them is not good enough. Hence, in order to have a better image of the bulk we need to complement the cannon with something else.

3.2.2 Radar

The first tool which will be presented is the "holographic radar". In this device, in addition to the point-like excitation fired from x we also send a pulse from z, which is space-like separated from x. The pulse then intersects the projectile's trajectory at a some point P, which belongs to the intersection of the future lightcones of both points. Later, we record the reflection of the pulse from P at a point y. This construction is formulated in terms of the quantity:

$$\int d^d\delta x \, \langle\Psi|\mathcal{O}(x+\delta x)\mathcal{O}'(y)\mathcal{O}'(z)\mathcal{O}(x)|\Psi\rangle \ . \tag{3.7}$$

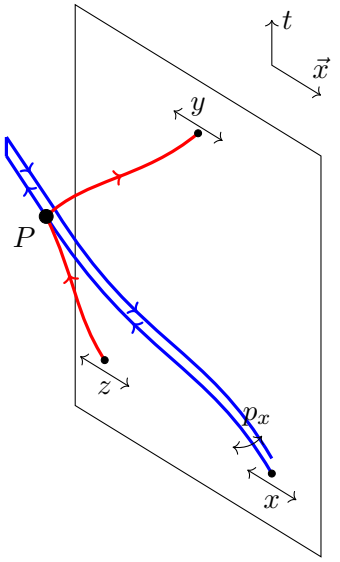

Figure 3.4: Schematic representation of the holographic radar. (Modified figure from [1])

As y approaches the intersection of the future lightcone of P with the boundary, (3.7) diverges. Such a sharp peak signals the existence of a point-like excitation.

Figure (3.4) illustrates this device. Once again, due to the operator ordering, we find that the particle follows the same "folded temporal path" as we have seen in the cannon.

In the ideal regime for the operation of this device, we work with high-energy pulses which follow a null geodesic and are governed by bulk geometrical optics. Therefore, this construction only requires us to work with three null geodesics.

3.2.3 Active Camera

The other device is called the "holographic active camera". It combines the holographic cannon with its time-reversed analogue. As such, it involves two pairs of near-coincident points from which the excitations are created and then absorbed. The signal of this camera is described by the following correlator:

$$\begin{aligned} G(x,p_x,L_x;y,p_y,L_y) \equiv & \int d^d\delta x\, d^d\delta y\, \psi_{p_x,L_x}(\delta x)\, \psi_{p_y,L_y}(\delta y) \\ & \times \langle\Psi|\mathcal{O}'(y+\delta y)\mathcal{O}(x+\delta x)\mathcal{O}'(y)\mathcal{O}(x)|\Psi\rangle \ , \end{aligned} \tag{3.8}$$

where we take y to be in the future of x. In this case, we only have two null geodesics in the bulk, which the excitations follow (see figure 3.5). Naturally, when the trajectories intersect each other ($b_{\text{bulk}} \to 0$) the quantity (3.8) diverges. Therefore, when plotting the signal of the camera for different shooting angles p_y, with fixed p_x, finding a sharp peak

around the shooting angle in which this happens, is the smoking gun that there are point-like excitations moving in the bulk. In addition, we can also keep track of this peak while varying y and p_y so as to obtain a movie of the particles trajectory on the bulk. This movie can in turn be used to extract the bulk geometry, similarly to how the gravity field of the Sun is inferred by studying the trajectories of the orbiting planets. Although we have not commented about this in the holographic radar, it is also possible to build the same kind of movie by varying the time of z.

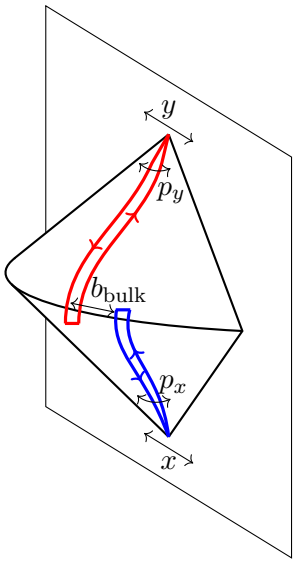

FIGURE 3.5: Schematic representation of the holographic active camera. (Modified figure from [1])

Furthermore, note that it is the Fourier transforms which allow the camera to discern the bulk angles. In particular, the angular resolution will be roughly given by $\delta\theta_i = 1/(p_i\, L_i)$ where $i = x, y$. Since ideally, this camera operates with high-energy excitations, this resolution is small, which means it can give a finely-detailed image of the bulk. In other words, it is able to identify structures with short characteristic wavelengths.

Lastly, we stress out the fact that this device involves an out-of-time order correlator (OTOC). In fact, this is an essential trait of this construction, since it is what allows us to examine the locality of the bulk theory without having to work with more than four points when increasing the spacetime dimensions. Furthermore, it is the reason why active cameras can give us images for an arbitrary state of the CFT and not just the vacuum.

3.2.4 Folded OPE and Eikonal approximation

From now on we will focus on the active camera. As seen above, the signal of this device is given by an OTOC. This, in turn, can be associated with the folded time contour in figure 3.6.

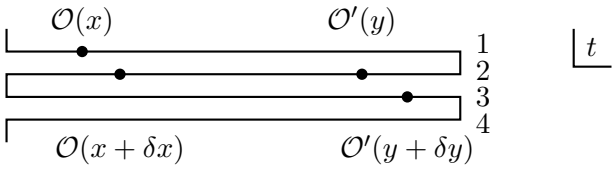

Figure 3.6: Schwinger Keldysh contour and operator insertions for the active camera out-of-time order correlator.

As mentioned before, the excitations must evolve along this contour and cannot jump between different branches. Therefore, we cannot go directly from x to $x+\delta x$ or from y to $y+\delta y$. This means that the operators are not actually "close" to each other and as such we cannot perform the usual OPE (2.89) in the near coincidence limit $\delta x \to 0$, in terms of local operators. There is, nonetheless, a natural extension of the OPE for this case, which instead makes use of non-local operators. This was dubbed as the folded OPE in [1].

It is this folded OPE which explains the dominant contribution of the OTOC, in the limit $\delta x \to 0$, which from now on we call folded OPE limit. Here, we will simply present the expression of this OPE for a gravitational theory, but is derivation and analysis can be found in [1]. In particular, for a scalar in AdS coupled to gravity, the folded OPE and its time-reversed version are given by:

$$\begin{aligned}
\mathcal{O}_2(\delta x)\,\mathcal{O}_1(0) &\sim \langle \mathcal{O}_2(\delta x)\,\mathcal{O}_1(0)\rangle + \frac{\tilde{C}_\Delta}{2}\int_{H_{d-1}} \frac{d^{d-1}\theta}{\left(-\theta\cdot\delta x_-\right)^{2\Delta+1}} L_{0,\theta}[h_{uu}] + \dots\ , \\
\mathcal{O}'_3(\delta y)\,\mathcal{O}'_2(0) &\sim \langle \mathcal{O}'_3(\delta y)\,\mathcal{O}'_2(0)\rangle + \frac{\tilde{C}_{\Delta'}}{2}\int_{H_{d-1}} \frac{d^{d-1}\theta'}{\left(-\theta'\cdot\delta y_-\right)^{2\Delta'+1}} L'_{y,\theta}[h_{vv}] + \dots\ ,
\end{aligned} \tag{3.9}$$

where the subscripts in the operators denote the branch of the Schwinger-Keldysh contour (figure 3.6) in which the operators are inserted, H_{d-1} is the $d-1$ dimensional hyperbolic space, θ^μ is a time-like vector parameterizing this space, u and v are affine times along the lightcone, $\tilde{C}_\Delta$ and $\tilde{C}_{\Delta'}$ are constants, the minus sign in δx_- and δy_- denotes a negative imaginary small part and L, L' represent the "light transforms" defined as:

$$L_{x,p}\left[h_{uu}\right] \equiv \int_{-\infty}^{u_0} du(h_{uu,1} - h_{uu,2})\ , \quad L'_{y,p}\left[h_{vv}\right] \equiv \int_{v_0}^{\infty} dv(-h_{vv,2} + h_{vv,3})\ , \tag{3.10}$$

where u_0 and v_0 are such that all regions with nonvanishing integrand are covered. These light transforms are usually referred to as non-local operators since they are defined through an integration over the lightcone. We point out, however, that they are not operators in the conventional way as they only make sense when inserted in the Schwinger-Keldysh path integral. The first term in (3.9) denotes the contribution of the identity operator whereas the ... designates the contributions of other operators to this OPE.

When in flat space, in the regime of high energies and small scattering angles, scattering amplitudes of the type $\mathcal{A} \sim \langle \mathcal{O}'\mathcal{O}\mathcal{O}'\mathcal{O}\rangle$ are dominated by the exchange of massless particles with maximal spin J [31]. For gravitational theories, these particles are the gravitons, with $J = 2$. Therefore, when we have a theory and state $|\Psi\rangle$ which are holographic, such that they have a dual description in terms of a gravitational theory, we also expect the correlator in (3.8) to be dominated by tree level graviton exchange. In fact, it can be shown by using (3.9) (see [1] for this) that the OTOC is approximately given by:

$$G\left(x, p_x; y, p_y\right) \approx 1 - 8\pi i\, G_N^{(d+1)} \int_{-\infty}^{u_0} du \int_{v_0}^{+\infty} dv \langle h_{uu}(X)\, h_{vv}(Y)\rangle_{\Psi,\text{ret}} \ . \tag{3.11}$$

Here, $X(u)$, $Y(v)$ are coordinates parameterizing null lines in the lightcone with initial conditions (x, p_x) and (y, p_y), and the integrand is the retarded bulk-to-bulk propagator for metric perturbations, which depends only on the bulk geometry dual to the state Ψ. Note also that in contrast with the folded OPE (3.9) in which the integral is over the base of the lightcone H_{d-1}, the camera correlator integral runs only in a single null line. This stems from the integration with wavepackets (Fourier transform), which focus the OPE on a single null geodesic. This how they resolve bulk angles, as was stated before.

It is worth remarking that the above expression for the active camera correlator is valid for any arbitrary state Ψ of the CFT. However, in the vacuum state we can use the results from Conformal Regge theory to numerically compute this observable and plot it for different receiving angles.

3.2.5 Vacuum state and the Conformal Regge theory

3.2.5.1 Regge limit and Folded OPE limit

In order the understand why in the vacuum state Ω of the CFT the folded OPE limit and the Regge limit are physically the same, let us consider the following scalar four point function where all the points are space-like separated. As we have seen before (2.72), such

objects are given by:

$$\langle\Omega|\mathcal{O}'(x_4)\mathcal{O}'(x_3)\mathcal{O}(x_2)\mathcal{O}(x_1)|\Omega\rangle = \frac{1}{x_{12}^{2\Delta_\mathcal{O}}\, x_{34}^{2\Delta_{\mathcal{O}'}}}\,\mathcal{G}(z,\bar{z})\ , \tag{3.12}$$

where the cross-ratios z and $\bar{z}$ are the exactly the ones we defined back in (2.71).

Moreover, we can specify the positions of these operators such as to have the same kinematics of the camera correlator (3.8). In particular, we fix $x = 0$ and $y = e$, with $e^2 = -1$, and choose:

$$x_1 = 0\ , \quad x_2 = \delta x\ , \quad x_3 = e + \delta y\ , \quad x_4 = e\ . \tag{3.13}$$

With this choice, the cross-ratios are given by:

$$z\bar{z} \approx (\delta x_-)^2(\delta y_-)^2\ , \qquad \frac{1}{2}(z+\bar{z}) = -\delta x\cdot\delta y - 2(e\cdot\delta x)(e\cdot\delta y) \equiv -\delta x\cdot\mathcal{I}_e\cdot\delta y\ . \tag{3.14}$$

Thus, in the folded OPE limit ($\delta x \to 0$, $\delta y \to 0$), z and $\bar{z}$ are small. This is in similarity with what happens in the Regge limit, characterized by $z, \bar{z} \to 0$.

However, specifying the kinematics is not enough to obtain the active camera OTOC. In order to achieve the operator ordering of (3.8), we must analytically continue $\mathcal{G}(z,\bar{z})$. The case of $\delta x \succ 0$ and $\delta y \prec 0$ is explained with much detail in appendix C.1 of [1]. The main point is that this analytic continuation requires taking z clockwise around 1 while holding $\bar{z} > 0$ fixed. The outcome of this procedure is then the analytically continued correlator, corresponding to the one in (3.8), and which is given by:

$$G_{3241} \equiv \langle\Omega|\mathcal{O}'(x_3)\mathcal{O}(x_2)\mathcal{O}'(x_4)\mathcal{O}(x_1)|\Omega\rangle = \frac{e^{-i\pi(\Delta_\mathcal{O}-\Delta_{\mathcal{O}'})}}{(-x_{12}^2)^{\Delta_\mathcal{O}}\,(-x_{34}^2)^{\Delta_{\mathcal{O}'}}}\,\mathcal{G}^{\circlearrowleft}(z,\bar{z})\ . \tag{3.15}$$

Here, $\mathcal{G}^{\circlearrowleft}$ denotes the analytically continued cross ratios function, where the arrow indicates the direction traversed in the $z,\bar{z}$ space (or equivalently the u,v space) needed for this procedure. In general, the analytic continuation leads to the gain of an overall phase factor or even an additional term due to crossing of branch cuts, relatively to the original function.

The camera correlator could also be obtained for different cases of δx and δy, for instance $\delta x \succ 0$ and $\delta y \succ 0$, or both space-like, by analytically continuing this expression. What matters is that z and $\bar{z}$ remain infinitesimally small.

The crucial point of this argument is that the analytically continued function $\mathcal{G}^{\circlearrowleft}(z,\bar{z})$ is exactly the same one describing the Regge limit, where a large boost between two pairs of points is applied (see for example [32, 33, 34]). Consequently, when in the CFT vacuum,

we can use the results from Conformal Regge Theory to describe the behavior of the camera correlator in the folded OPE limit, given their equivalence.

There is in fact a more intuitive way to think about this equivalence, as can be seen in figure 3.7. Indeed, in the vacuum state, the dynamics of all the limits depicted in this

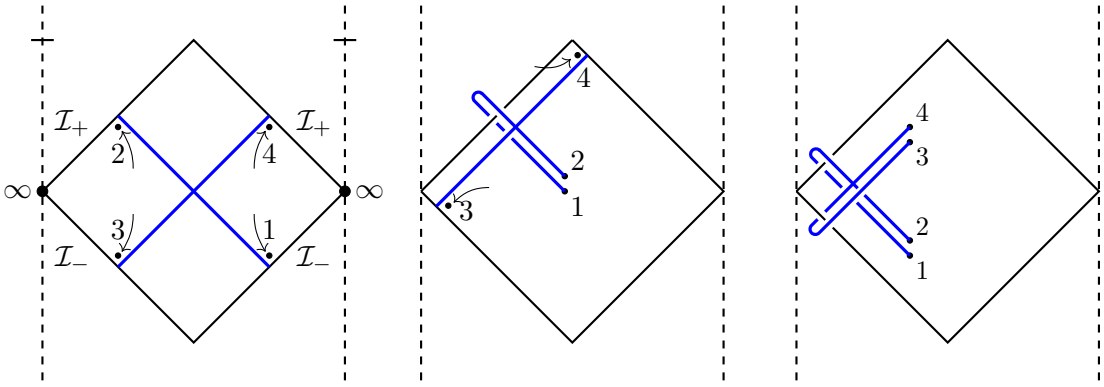

(A) Regge correlator (B) Detectors (C) OTOC

FIGURE 3.7: Geometric interpretation of the equivalence of distinct limits of correlators in the CFT vacuum. (Figure from [1])

picture are equivalent [1]. We are simply picking different choices to place the four points inside the Poincaré patch*, but the correlator remains the same (up to some overall phase). In other words, we are interpreting the same correlator in different physical situations. In fact, this relation has already been explored before in several contexts, such as in [30, 35, 36].

Note, however, that these equivalence relations hold only in the vacuum state. To understand why, consider the following argument supported by figure 3.8. For pure AdS

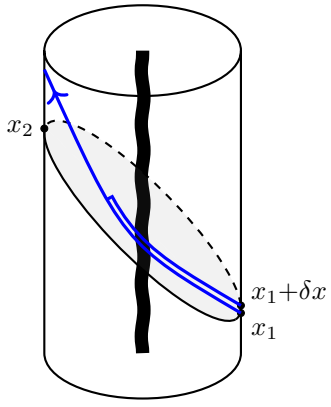

FIGURE 3.8: Schematic representation of scrambling and the inequivalence between the Regge limit and the folded OPE limit for an excited state. (Figure from [1])

spacetime, all lightrays leaving x_1 will arrive at x_2 whether they propagate through the bulk or the boundary. This, in turn, would give rise to the Regge singularity as $x_{12}^2 \to 0$.

*The Poincaré patch is the set of all points which are space-like separated from a reference point at ∞.

However, if we consider an excited state such that the bulk dual has matter or even a blackhole, the bulk null geodesics will suffer a Shapiro time delay. As a result, the Regge limit singularity fades. This occurrence is known as saturation in high-energy scattering or scrambling.

On the other hand, in the folded OPE limit, the null geodesics will traverse the exact same path in different Schwinger-Keldysh time branches, independently of whether the bulk geometry is or not pure AdS. This is so because, even if the lightray in the first branch, which propagates forward in time, suffers a time delay, the one propagating backwards will have the opposite time delay, thus canceling it. We must, nonetheless, restrict the center of mass energy to be below the Planck energy, in order to prevent the probes from backreacting. Accordingly, the $\delta x \to 0$ singularity does not disappear even if the background is far from AdS. This is the reason why the active camera works for an arbitrary excited state and not just the vacuum. For all these other states, however, we cannot expect Conformal Regge Theory to provide us with the expression for the camera correlator.

3.2.5.2 Conformal Regge theory

Taking into account what was said above, let us focus on the case of the CFT vacuum. As such, we can use Conformal Regge theory, which describes the correlator in the Regge limit in terms of the exchange of the so-called Regge trajectories* $J_i(\nu)$. Assuming for simplicity that a single trajectory dominates, the cross-ratios function in (3.15) is given by [33]:

$$\mathcal{G}^{\circlearrowleft}(z,\bar{z}) \approx 1 + 2\pi i \int_0^\infty \frac{d\nu}{2\pi}\, \rho(\nu)\, \alpha(\nu)\, (z\bar{z})^{\frac{1-J(\nu)}{2}}\, \mathcal{P}_{\frac{2-d}{2}+i\nu}\left(\frac{z+\bar{z}}{2\sqrt{z\bar{z}}}\right) , \quad (z,\bar{z}\to 0) \ , \tag{3.16}$$

where the quantum number ν is related to the conformal dimension of the exchanged operator as $\Delta = \frac{d}{2} + i\,\nu$, and $\alpha(\nu)$ are coefficient functions† which are related to the OPE coefficients and are characteristic of the considered boundary theory. Moreover, $\rho(\nu)$ and $\mathcal{P}$ are respectively defined as:

$$\rho(\nu) = \frac{2^{d-2}}{\Omega_{d-1}}\, q_{\frac{2-d}{2}+i\,\nu}\, q_{\frac{2-d}{2}-i\,\nu} \ , \ \text{with} \ q_J \equiv \frac{(d-2)_J}{(\frac{d-2}{2})_J} \ , \ \Omega_d \equiv \frac{2\pi^{\frac{d}{2}}}{\Gamma(\frac{d}{2})} \ , \tag{3.17}$$

and

$$\mathcal{P}_J(\eta) = {}_2F_1\left(-J, d-2+J, \frac{d-1}{2}, \frac{1-\eta}{2}\right) \ . \tag{3.18}$$

*Regge trajectories define a path in the space of the conformal dimension and spin where the analytic continued cross-ratios function describing the correlator in the Regge limit has poles.

†Not to confuse with the coefficient functions in the OPE (2.88)

By specifying (3.16) to the kinematics of the active camera correlator (3.13) and integrating against the wavepackets, one obtains an explicit formula for the contribution of a Regge trajectory to (3.8):

$$G(0,p,L;e,p',L')\big|_{\text{CRT}} \approx$$
$$1 - i\int_0^\infty \frac{d\nu}{2\pi}\rho(\nu)\tilde{\alpha}(\nu)\left(|p||p'|\right)^{J(\nu)-1}\mathcal{P}_{\frac{2-d}{2}+i\,\nu}(\cosh^{-1}\left(\hat{p}\cdot\mathcal{I}_e\cdot\hat{p}'\right))\,e^{-\frac{\nu^2}{2}\sigma_0^2}\,, \tag{3.19}$$

where

$$\sigma_0^2 = \frac{1}{L^2\,|p|^2} + \frac{1}{L'^2\,|p'|^2}\ , \tag{3.20}$$

and where $\tilde{\alpha}(\nu)$ differs from the previous $\alpha(\nu)$ from a choice of normalization which proves useful. In addition, the standard notation $\hat{p} = p/\sqrt{-p^2}$ is being used.

It is worth noticing the Gaussian factor at the end of this integral, which tells us that the intensity peak of the camera's image, in case it exists, follows a normal distribution. On top of that, its variance (3.20) is determined by the angular resolution of the cannons. Hence, whether or not we obtain a high-quality image depends on the properties of the wavepackets we use.

The integral in (3.19) can be computed analytically in some cases. In particular, defining the center of mass energy and bulk impact parameter as:

$$s_{\text{bulk}} = \frac{|p||p'|}{R^2}\quad,\qquad \frac{b_{\text{bulk}}}{R} = \cosh^{-1}\left(\hat{p}\cdot\mathcal{I}_e\cdot\hat{p}'\right)\ , \tag{3.21}$$

this integral can be computed by the saddle point approximation, in the regime of large s_{bulk}, where we expect to find a peak when $b_{\text{bulk}} \to 0$. This was done in appendix A. Moreover, for a gravitational theory this expression corresponds exactly to the graviton propagator on H_{d-1} (see appendix A of [1]).

3.2.6 Image for $\mathcal{N} = 4$ SYM at strong and weak coupling

Given the equation (3.19), we are fully equipped to obtain the signal of the active camera, for any theory and operators we wish to consider. For this, we simply have to know the expressions for the corresponding coefficient functions $\tilde{\alpha}(\nu)$ and leading Regge trajectory $J(\nu)$, and replace them inside the integral.

The choice of [1] was to consider $\mathcal{N} = 4$ SYM and two different operators of its spectrum. Afterwards, the integral (3.19) was computed numerically for fixed $p_x = p$ and different

$p_y = p'$. For simplicity, the choice $|p_x|L_x = |p_y|L_y = |p|L$ was taken. The obtained signals of the holographic camera are then the ones illustrated in figure 3.9.

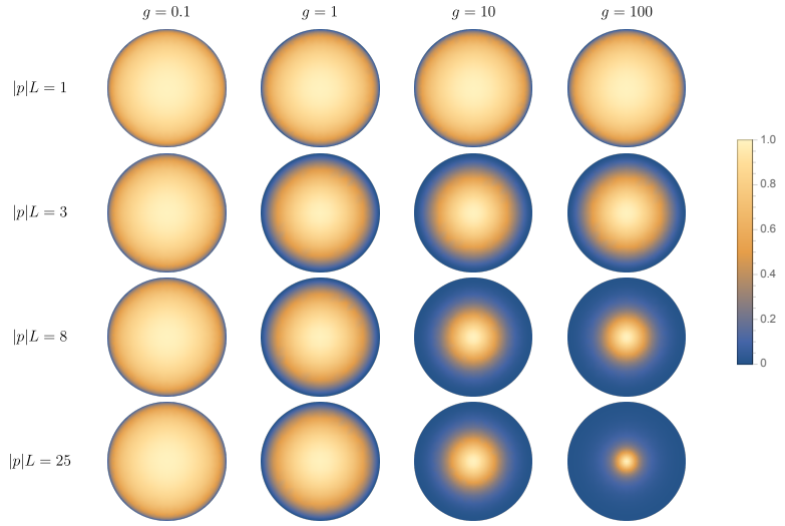

Figure 3.9: Plots of holographic camera signal for the $\mathcal{N} = 4$ SYM theory at different couplings. (Figure from [1])

For the analysis of these images, first recall that a sharp peak signals locality of the bulk dual theory. What is more, the two most important parameters here are the optical quality of the camera $|p|L$ and the coupling of the theory, $g^2 \equiv \lambda/(16\pi^2)$.

Within the strongly coupled regime, we see that a smaller optical quality translates into a blurred image. This is not surprising, since a smaller value of $|p|L$ implies a bigger angular resolution, which prevents us from imaging point-like structures. By increasing this parameter, we are able to find a sharp peak located at the center, which indicates that the strongly coupled regime of $\mathcal{N} = 4$ SYM has a local bulk dual. As we decrease the value of the coupling, we see that the singular behavior starts spreading out until it reaches a point in which we cannot find the sharp peak, no matter how much we "focus" the camera. This leads us to conclude that for weak coupling, this theory does not have a local bulk dual. A possible interpretation of what might be hapenning, is that because the dual is not local, the camera cannot shoot the projectile in a well-defined direction. Additionally, as the point-like excitations propagate through the bulk, they suffer non-local interactions and become delocalized. Consequently, the integral (3.19) no longer decreases rapidly as we move away from the configuration with $b_{bulk} \sim 0$, but instead has a reasonable value for other angles. Naturally, this results in a spreading of the peak.

By looking at these plots, we can also argue that the profile of the holographic camera signal can be roughly approximated by a Gaussian distribution, which has a characteristic variance. This quantity, in due turn, quantifies the spread of the signal peak. From the above observations, we can infer that there are two contributions to the effective variance of the signal, one optical and one dynamical:

$$\sigma^2_{\text{eff}} = \sigma^2_0 + \sigma^2_{\text{dyn}} \ . \tag{3.22}$$

The first one is related with the properties of the probes we use, and is given by (3.20). Indeed, if we do not use excitations which are of the same size of the structures or phenomena we wish to image, we will not obtain focused images of them. This can be fixed by either increasing their energy or the position uncertainty of the wavepackets. Note that this is simply a consequence of the position-momentum uncertainty.

The dynamical contribution, on the other hand, can be explained by the behavior of Regge trajectories. Consider the plot of the leading Regge trajectory for this case, in both the strong and weak coupling regime, depicted in figure 3.10. As it turns out, the dynamical contribution to the effective variance we referred before is essentially the curvature of these trajectories. For weak coupling the curvature is high, which implies a bigger variance and a blurrier image, which does not improve no matter by how much we increase the camera's optical quality. Contrarily, the strongly coupled leading trajectory is nearly flat, which is why we could see that sharp peak in (3.9) for good angular resolution. Interestingly, this curvature is proportional to the inverse of the higher-spin gap of the theory. In fact,

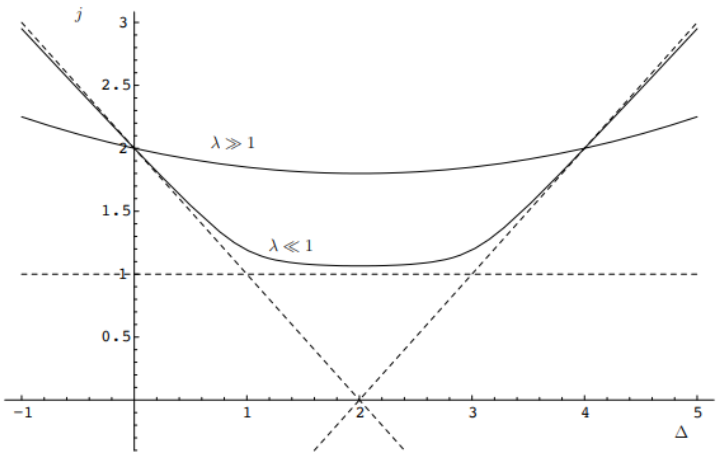

FIGURE 3.10: Leading Regge trajectories in the strong and weak coupling regime of a planar gauge theory. (Figure from [37])

$\Delta_{\text{gap}}^{\text{higher-spin}}$ gives a lower bound to the effective variance as $\sigma_{\text{eff}} \gtrsim 1/\Delta_{\text{gap}}^{\text{higher-spin}}$. Hence, having a local dual implies having a large $\Delta_{\text{gap}}^{\text{higher-spin}}$ such that the leading Regge trajectory is nearly flat. But this is precisely one of the characteristics of the CFT that the conjecture from section 3.1 asserted as necessary, such that the bulk dual would be local at sub-AdS scales.

Interestingly, the other requirement stated in this conjecture is also necessary to have a sharp image. In particular, the coefficient functions for this theory in both regimes depend inversely on the central charge N_c, which is proportionally related with N. Thus, N must be large such that the overall coefficient in the integral of (3.19) is small. This, in turn, allow us to go to higher energies, without surpassing the Planck energy*, such that we can image smaller scale dynamics.

Thus, we have seen for this particular case, that the holographic camera corroborated the large N large $\Delta_{\text{gap}}^{\text{higher-spin}}$ conjecture, which is believed to always hold.

We have seen here the simplicity of the holographic cameras formalism for one case. Indeed, the images from the active camera leave no room for doubt regarding the locality of the bulk dual. However, the only correlators considered here were constituted by scalars. In order for the formalism to be consistent, performing the same analysis with spinning four points functions should lead us to the same conclusions. Furthermore, because the bulk theory is gravitational, it makes sense to consider four point functions with the stress-tensor, since this corresponds to the propagation of gravitons. This would not only further consolidate the construction but it could also provide us with new insights, depending on the sharpness and shape of the peaks.

In order to plot the signal of the active camera, one has to be able to write the corresponding correlators according to Conformal Regge theory. For this, we first need to know the conformal blocks in the Regge limit. Therefore, in the next chapter we will compute the spinning blocks in this kinematical limit. In due turn, these could then be used to write the four point functions analogously to (3.19) and later obtain similar images as in figure 3.9.

*The energy must be kept below the Planck energy as we stated previously in order for the probes to not react with each other

Chapter 4

Conformal Blocks in the Regge Limit

As we mentioned above, knowing the conformal blocks in the Regge limit is vital if we wish to express the spinning four point functions according to Conformal Regge theory, and later obtain the signal of the holographic camera. Therefore, here we will compute the blocks in the Regge limit for correlators with one spinning operator and three scalars, and with two spinning operators and two scalars. Note, however, that only the second kind of correlator could later be used to plot the camera's image. Before the computation of the blocks, we will introduce the methods with which we can compute these functions and exemplify for the case of scalar operators. Additionally, we will also describe how to analytically continue the correlators.

Although the discussion of this chapter focuses on four point functions, given their importance for active cameras in the study of locality, the methods and ideas presented here can also be employed for higher-point functions. In particular, outside the context of bulk locality and as such of this thesis, we are currently trying to compute the conformal blocks of scalar five-point functions with the Casimir differential equation (in the Euclidean limit), using a different choice of cross ratios with respect to the standard ones (see for example [13, 38, 39]). What makes this choice so compelling, is that it turns the Casimir equation into a separable differential equation, such that it is easier to obtain the blocks. In particular, we find that the five point conformal blocks can be written in a factorized form, which was first noticed in [14].

4.1 Regge Kinematics

Prior to the discussion of conformal blocks, we will first give a clear presentation on the Regge limit. In spite of having being mentioned and briefly explained several times before, we found appropriate to dedicate a section to it, given the role it plays in this thesis.

The starting point of this presentation will be to consider a scalar four point function $\langle\phi(x_1)\,\phi(x_2)\,\phi(x_3)\,\phi(x_4)\rangle = G(z,\bar{z})/\left(x_{12}^{2\Delta}x_{34}^{2\Delta}\right)$, which for simplicity we assume to have operators of equal dimension Δ. Because CFTs are better understood in the Euclidean signature, we generally compute correlators in this regime. Equivalently, we can also consider correlators in the Lorentzian signature, with the points all spacelike separated. We say these correlators are in the Euclidean region, since all operators commute and there are no timelike relations. Hence, for all purposes, it is as if we were in the Euclidean signature. However, the Regge limit is intrinsically Lorentzian due the specific causal relations that define it. As such, we must analytically continue the Euclidean region correlators if we wish to analyze the Regge limit.

In this case, we begin by considering a certain configuration of spacelike separated points, which commute with each other. In this initial configuration where all points are spacelike separated, the cross ratios satisfy $0 < z, \bar{z} < 1$. However, because the Regge kinematics is defined by having $x_{14}^2, x_{23}^2 < 0$ (timelike separated) and all others $x_{ij}^2 > 0$ (spacelike separated), we move x_4 to the future of x_1 and x_3 to the past of x_2, as depicted in figure 4.1. In this picture, u and v are not the cross ratios, but rather the lightcone

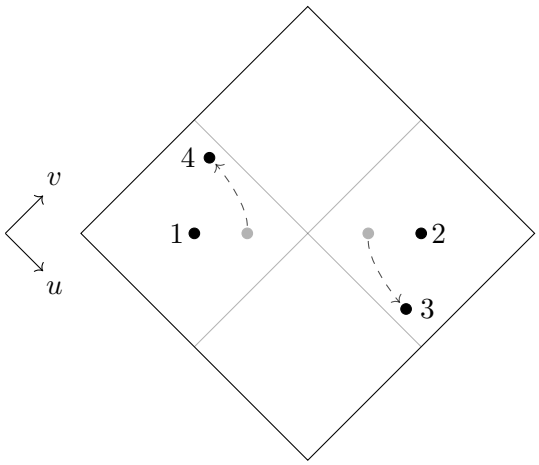

FIGURE 4.1: Analytic continuation from spacelike separated points to the causal relations of the Regge limit. (Figure from [40]

coordinates defined by $u = x - t$ and $v = t + x$. As we do this, the points x_4 and x_3 cross the lightcones of x_1 and x_2, respectively, which leads to branch cut singularities. The way

how we deal with these branch cuts, namely how we move around them, depends on the $i\epsilon$ prescription we use. For this case, in order to achieve the causal relations mentioned before, or equivalently the ordering $\langle\phi(x_4)\,\phi(x_1)\,\phi(x_2)\,\phi(x_3)\rangle$ (or any other ordering without commuting $\phi(x_1)$ with $\phi(x_4)$ and $\phi(x_2)$ with $\phi(x_3)$, since these are timelike separated), we must take:

$$t_{23} \to t_{23} - i\epsilon \ , \qquad t_{41} \to t_{41} - i\epsilon \ , \tag{4.1}$$

with $\epsilon > 0$. This choice of the $i\epsilon$ prescription, is such that in Euclidean time ($\tau = it$), x_3 comes before x_2 ($\tau_{23} > 0$) and x_4 comes after x_1 ($\tau_{41} > 0$). In due turn, this is necessary such that the corresponding Euclidean correlators are not divergent (see [40] for more about Euclidean correlators). Moreover, note that we do not have to specify the $i\epsilon$ prescription for any other pairs, since all other points are spacelike separated and thus commute. In terms of the lightcone coordinates, the $i\epsilon$ transcription translates into:

$$u_{23} \to u_{23} + i\epsilon \ , \quad u_{41} \to u_{41} + i\epsilon \ , \tag{4.2}$$

while v can be kept fixed during the continuation in figure 4.1. To see what this continuation implies for the cross ratios $z, \bar{z}$, we begin by giving their definition:

$$z = \frac{u_{12}u_{34}}{u_{13}u_{24}} \ , \qquad \bar{z} = \frac{v_{12}v_{34}}{v_{13}v_{24}} \ . \tag{4.3}$$

As the v's are kept fixed, $\bar{z}$ remains unchanged. On the other hand, z does not. In order to figure out whether z goes around 0 or 1, which are branch points of the correlator, one has to analyze z and $1 - z$, and figure out which of the two change sign as we analytically continue. However, we can already see from the definition of z and looking at figure 4.1 that this will not happen for z alone, which means it will not go around 0. On the other hand, $1 - z$ is given by:

$$1 - z = \frac{u_{23}\,u_{41}}{u_{31}\,u_{24}} \ . \tag{4.4}$$

As we analytically continue, u_{23} changes sign from positive to negative. Moreover, taking into account the $i\epsilon$ prescription, the term u_{23} gains a phase of π ($u_{23} \to e^{i\pi}\,u_{23}$), as depicted in figure 4.2. A similar analysis for u_{41} shows it also gains the same phase ($u_{41} \to e^{i\pi}\,u_{41}$).

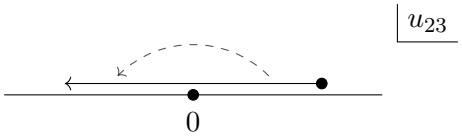

Figure 4.2: Gain of a phase in u_{23} during analytic continuation.

This leads to an overall phase of 2π in $(1-z)$, that is $(1-z) \to e^{2\pi i}(1-z)$, which tells us that z winds counter-clockwise around 1 in this analytic continuation. This path of analytic continuation in the space of cross ratios $z, \bar{z}$, is depicted in figure 4.3. According

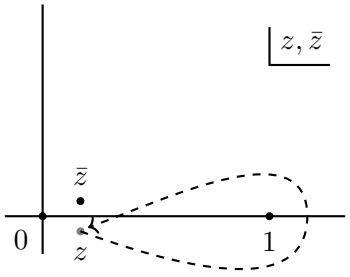

FIGURE 4.3: Path traversed in the space of $z, \bar{z}$ in order to analytic continue the correlators. (Figure from [1])

to our previous definition of $\mathcal{G}^{\circlearrowleft}(z, \bar{z})$ below (3.16), after following the path of the above figure, the analytically continued cross ratios function of this scalar correlator is denoted by $G^{\circlearrowleft}(z, \bar{z})$, where the arrow indicates the direction of the path.

Now that we have the correct causal relations between the points, we can consider the Regge limit, which results from taking a large relative boost between the two pairs of points, 1 and 4, 2 and 3:

$$\begin{aligned} &x_1 = (e^{-\eta}u_1, -e^{\eta}v_1) \ , \ x_2 = (-e^{-\eta}u_2, e^{\eta}v_2) \ , \\ &x_3 = (e^{\eta}u_3, -e^{-\eta}v_3) \ , \ x_4 = (-e^{\eta}u_4, e^{-\eta}v_4) \ , \quad (\eta \to \infty) \, . \end{aligned} \tag{4.5}$$

This is depicted in figure 4.4. Ergo, the Regge limit is characterized by $z, \bar{z} \to 0$, or

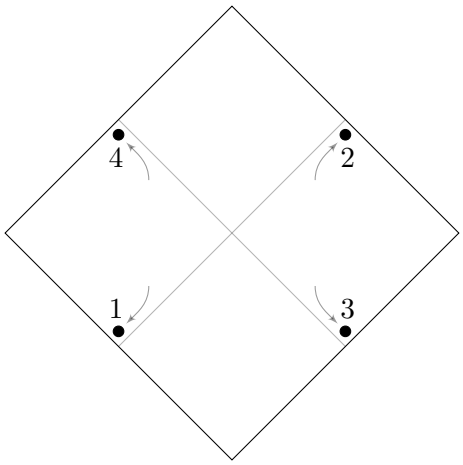

FIGURE 4.4: Schematic representation of the Regge limit.

equivalently in the u, v cross ratios, by $u \to 0$ and $v \to 1$.

After this discussion, we have a clearer understanding of what the Regge limit is, and the path of analytic continuation that needs to be followed, in order to go from the spacelike separated configuration to the one with the causal relations of Regge kinematics. Thus, we are now better prepared to proceed to the conformal blocks, where these concepts will play a central role.

4.2 More on Conformal Blocks

4.2.1 Casimir differential equation

By now, we have already realized that conformal symmetry plays a big role in this discussion. In particular, it completely fixes two and three point functions and imposes the structure of higher-point correlators up to cross-ratios functions. What is more, the conformal algebra is isomorphic to $SO(d+1,1)$ such that its generators, $P_\mu, K_\mu, D, M_{\mu\nu}$, can be identified with the Lorentz group generators L_{AB} in $d+2$ dimensions. In the embedding space formalism these latter are expressed as:

$$L^{AB} = P^A \partial_P^B - P^B \partial_P^A \,. \tag{4.6}$$

Let us now consider once again the scalar four point function. We are free to introduce a complete basis of states labeled by $|n\rangle$ and insert it the correlation function as:

$$\langle \phi_1(x_1)\, \phi_2(x_2)\, \phi_3(x_3)\, \phi_4(x_4)\rangle = \sum_{n,m} \frac{1}{\langle m|n\rangle} \langle 0|\phi_4(x_4)\phi_3(x_3)|m\rangle\langle n|\phi_2(x_2)\phi_1(x_1)|0\rangle \,, \tag{4.7}$$

where the sum runs over both primaries and descendants. Let L_i^{AB} designate the action of the Lorentz group generators on the field $\phi_i(x_i)$. Since all correlation functions in a CFT are conformally invariant we have that:

$$\begin{aligned} &(L_1^{AB} + L_2^{AB} + L_n^{AB})\langle n|\phi_2(x_2)\phi_1(x_1)|0\rangle = 0 \\ &\Leftrightarrow (L_1^{AB} + L_2^{AB})\langle n|\phi_2(x_2)\phi_1(x_1)|0\rangle = -L_n^{AB}\langle n|\phi_2(x_2)\phi_1(x_1)|0\rangle \,. \end{aligned} \tag{4.8}$$

Thus,

$$\begin{aligned} &-\frac{1}{2}\,(L_1^{AB} + L_2^{AB})^2\,\langle n|\phi_2(x_2)\phi_1(x_1)|0\rangle = -\frac{1}{2}\left(L_n^{AB}\right)^2\,\langle n|\phi_2(x_2)\phi_1(x_1)|0\rangle \\ &\Leftrightarrow \mathcal{D}_{1,2}\,\langle n|\phi_2(x_2)\phi_1(x_1)|0\rangle = \mathcal{D}_n\,\langle n|\phi_2(x_2)\phi_1(x_1)|0\rangle \,. \end{aligned} \tag{4.9}$$

Moreover, it can be shown that every primary operator $\mathcal{O}$ satisfies:

$$\mathcal{C}\,|\mathcal{O}\rangle = C_{\Delta,J}|\mathcal{O}\rangle\,, \tag{4.10}$$

where $\mathcal{C} \equiv -\frac{1}{2}L_{AB}L^{AB}$ is the Casimir operator, and the Casimir eigenvalue $C_{\Delta,J}$ of $\mathcal{O}$ is given by:

$$C_{\Delta,J} = \Delta(\Delta - d) + J(J + d - 2)\,. \tag{4.11}$$

Importantly, any descendant of $\mathcal{O}$ will also satisfy the same equation as the primary, i.e. (4.10), with exactly the same eigenvalue. Therefore, each of these $C_{\Delta,J}$ defines a conformal family where Δ and J are the conformal dimension and spin of the primary, respectively.

It will be more useful for us to rewrite the sum (4.7) as:

$$\langle\phi_1(x_1)\,\phi_2(x_2)\,\phi_3(x_3)\,\phi_4(x_4)\rangle = \sum_{\mathcal{O}}\langle 0|\phi_4(x_4)\phi_3(x_3)|\mathcal{O}|\phi_2(x_2)\phi_1(x_1)|0\rangle\,, \tag{4.12}$$

where now the sum runs over only the primary operators of the theory. Moreover, the operator $|\mathcal{O}|$, which projects into the conformal family of $\mathcal{O}$, is given by:

$$|\mathcal{O}| = \sum_{\alpha,\beta=\mathcal{O},P\mathcal{O},\ldots} |\alpha\rangle\,\mathcal{N}^{-1}_{\alpha\beta}\,\langle\beta|\,,\ \text{ with }\ \mathcal{N}_{\alpha\beta} = \langle\alpha|\beta\rangle\,. \tag{4.13}$$

Naturally, the sum of these projectors over all primaries must give the identity:

$$\sum_{\mathcal{O}}|\mathcal{O}| = \mathbf{1}\,. \tag{4.14}$$

Comparing (4.12) with (2.96), we find that each term of the first expression can be identified with a conformal partial wave, up to the OPE coefficients:

$$\langle 0|\phi_4(x_4)\phi_3(x_3)|\mathcal{O}|\phi_2(x_2)\phi_1(x_1)|0\rangle = \lambda_{12\mathcal{O}}\lambda_{34\mathcal{O}}\,\frac{\left(\frac{x_{24}^2}{x_{14}^2}\right)^{\frac{\Delta_{12}}{2}}\left(\frac{x_{14}^2}{x_{13}^2}\right)^{\frac{\Delta_{34}}{2}}}{(x_{12}^2)^{\frac{\Delta_1+\Delta_2}{2}}\,(x_{34}^2)^{\frac{\Delta_3+\Delta_4}{2}}}\,G_{\mathcal{O}}(u,v)\,. \tag{4.15}$$

If we now act with $\mathcal{D}_{1,2}$ on (4.12) and make use of (4.9), we find the following equality:

$$\begin{aligned}
&\mathcal{D}_{1,2}\langle\phi_1(x_1)\,\phi_2(x_2)\,\phi_3(x_3)\,\phi_4(x_4)\rangle = \\
&= \sum_{\mathcal{O}}\sum_{\alpha,\beta=\mathcal{O},P\mathcal{O},\ldots}\langle 0|\phi_4(x_4)\phi_3(x_3)|\alpha\rangle\,\mathcal{N}^{-1}_{\alpha\beta}\,\mathcal{D}_{1,2}\,\langle\beta|\phi_2(x_2)\phi_1(x_1)|0\rangle \\
&= \sum_{\mathcal{O}} C_{\Delta,J}\,\langle 0|\phi_4(x_4)\phi_3(x_3)|\mathcal{O}|\phi_2(x_2)\phi_1(x_1)|0\rangle\,.
\end{aligned}$$

In order to express the first line of this expression as a sum over the same kind of terms as in the last line, we make use (2.96) and (2.97). Doing this, we find that each term of the

sums satisfy:

$$\mathcal{D}_{1,2}\langle 0|\phi_4(x_4)\phi_3(x_3)|\mathcal{O}|\phi_2(x_2)\phi_1(x_1)|0\rangle = C_{\Delta,J}\langle 0|\phi_4(x_4)\phi_3(x_3)|\mathcal{O}|\phi_2(x_2)\phi_1(x_1)|0\rangle\,. \quad (4.16)$$

Finally, by using relation (4.15) we find that the conformal blocks obey what we call the Casimir differential equation:

$$\mathcal{D}\,G_{\mathcal{O}}(u,v) = C_{\Delta,J}\,G_{\mathcal{O}}(u,v)\,, \quad (4.17)$$

where $\mathcal{D}$ is a second-order differential operator given by:

$$\begin{aligned}\mathcal{D} =& \tfrac{1}{2}(1+u-v)\Delta_{12}\Delta_{34} + \Big(u(v+1)-(1-v)^2\Big)\Big[(\Delta_{12}-\Delta_{34}-2)\;\partial_v - 2v\,\partial_v^2\Big] \\ &+ u\left[-2(d+u-v-1) + (1-v+u)\left\{(\Delta_{12}-\Delta_{34})\,\partial_u - 4v\partial_v\,\partial_u + 2u\partial_u^2\right\}\right]. \quad (4.18)\end{aligned}$$

Equation (4.17) would in theory be able to provide us with the conformal blocks expression in the most general cases. Unfortunately, this is a completely non-trivial differential equation from which we can only obtain closed form solutions for even dimensions. For $d = 4$ for example, the conformal blocks are given by [41, 42]:

$$G_{\mathcal{O}}(u,v) = \frac{(-1)^J}{2^J}\frac{z\bar{z}}{z-\bar{z}}\left[k_{\Delta+J}(z)\,k_{\Delta-J-2}(\bar{z}) - (z\leftrightarrow\bar{z})\right]\,, \quad (4.19)$$

with

$$k_\beta(x) \equiv x^{\frac{\beta}{2}}\,{}_2F_1\left(\frac{\beta-\Delta_{12}}{2}, \frac{\beta+\Delta_{34}}{2}, \beta; x\right)\,, \quad (4.20)$$

where ${}_2F_1(a,b,c;z)$ is the Hypergeometric function.

Nevertheless, there are some kinematical limits we can consider in order to simplify the Casimir differential equation and obtain an approximated expression of the conformal blocks in generic dimensions. Alternatively, these functions can also be obtained via different methods, such as through a series expansion on radial coordinates [43, 44] or recursion relations [12].

There is an important property of the Casimir differential equation which deserves to be commented. Indeed, a simple analysis of eq.(4.17) reveals that this equation is invariant under $\Delta \to d-\Delta$. This can be easily seen from the Casimir eigenvalue $C_{\Delta,J}$ expression (4.11) and the lack of dependence in Δ by $\mathcal{D}$. Consequently, the conformal blocks with $\Delta \to d-\Delta$, which go by the name of shadow conformal blocks, are also solutions of the Casimir differential equation. Naturally, a linear combination of the conformal blocks and respective shadow blocks also satisfies (4.17), such that we may equally as well express

the correlation functions in terms of this alternative basis. These linear combinations are sometimes also denoted by conformal partial waves, which is not to be confused with the previous definition of conformal partial waves that will be used throughout this work.

In practice, when expressing the correlation functions in an integral representation, as we will see next, it is convenient to express the correlation functions in terms of these linear combinations of conformal blocks and respective shadows, denoted by:

$$F_{\Delta,J}(z,\bar{z}) = K_{\Delta,J}\, G_{\Delta,J}(z,\bar{z}) + K_{d-\Delta,J}\, G_{d-\Delta,J}(z,\bar{z}) \ , \tag{4.21}$$

where $K_{\Delta,J}$ are coefficients consisting on Gamma functions. The reason why this basis is preferable to work with, is because in contrast with the individual conformal blocks, these are Euclidean single-valued functions, meaning they do not have branch cuts in the Euclidean kinematics $\bar{z} = z^*$. In addition, the functions $F_{\Delta,J}(z,\bar{z})$ form a complete basis of functions. Therefore, it is preferable to expand the Euclidean correlators $G(z,\bar{z}=z^*)$, which are also single-valued, in terms of this basis.

4.2.2 Lightning Review on Conformal Regge Theory

Supposing we knew the conformal blocks, such that we could express the correlator as in (2.99), we would then like to analytically continue it so as to later analyze it in the Regge limit. Our first instinct, would then be to analytically continue each conformal block inside the sum. However, because the analytically continued conformal blocks behave like $G^{\circlearrowleft}_{\Delta,J}(z,\bar{z}) \sim (z\bar{z})^{\frac{1-J}{2}}$, the sum over J diverges in the Regge limit $(z,\bar{z}\to 0)$, which means it is ill-defined. The issue with this line of thought, is that we cannot analytically continue the correlator by analytically continuing each term of the sum, since analytic continuation does not commute with the infinite sum. Therefore, to properly analytically continue this correlator, so as to later analyze it in the Regge limit, we must write it in some other representation, namely in terms of an integral over complex dimensions and spins. This procedure is a key idea of Conformal Regge Theory. We will now present an extremely brief overview of it, although several steps and details will be omitted, given that it is not the main focus of this thesis. A more thorough presentation on the subject can be found for example in [33, 34, 45].

To begin with, we point out that the correlators will be expressed in terms of the functions $F_{\Delta,J}(z,\bar{z})$ introduced before in (4.21), by the reasons explained below the same equation. The first step of the procedure is then to turn the sum over discrete dimensions

to an integral over continuous dimensions [33]:

$$G(z,\bar{z}) = \sum_{J=0}^{\infty} \int_{-\infty}^{\infty} \frac{d\nu}{2\pi i}\, c(\nu, J) F_{\nu,J}(z,\bar{z}) \ , \tag{4.22}$$

where ν is defined by:

$$\nu^2 + \left(\Delta - \frac{d}{2}\right)^2 = 0 \ , \tag{4.23}$$

and with $c\,(\nu, J)$ being analytic functions of ν and J [34, 45], which have poles. The summation and integral representations are equivalent, since some of the poles of the integrand correspond exactly to the dimensions that are being summed over. An adequate deformation of the contour that would englobe all these poles, would give us the sum over the physical conformal dimensions by the residue theorem. Crucially, the contour of this integral must be such that all poles are found on the same side of it.

The next step is to transform the sum over spins into an integral, in order to overcome the aforementioned issue. This is achieved by performing the Sommerfeld-Watson transform (see [33]). The outcome of this step is an integral that runs along a contour that can be deformed to encircle the poles of $c(\nu, J)$.

After these two steps, we obtain an expression for the correlator in terms of two integrals over the dimensions and spins. At this point, we can safely analytic continue this function. Taking into account the aforementioned $(z\bar{z})^{1-J}$ dependence on the integrand, it is straightforward to infer that the pole with the biggest real part will dominate in the Regge limit. Denoting such pole by $j(\nu)$, which depends on the conformal dimension by construction, we finally find that the analytic continued correlator in the Regge limit is approximately given by:

$$G^{\circlearrowleft}(z,\bar{z}) \approx \int_{-\infty}^{\infty} \frac{d\nu}{2\pi i}\, (z\bar{z})^{\frac{1-j(\nu)}{2}}\, \Omega_\nu\left(\frac{\bar{z}}{z}\right) \beta(\nu) \ , \quad (z,\bar{z} \to 0)\,. \tag{4.24}$$

This expression is of the same form of (3.16) if one takes into account that the ν dependent functions are even. Moreover, Ω_ν is an arbitrary function of the ratio of the cross ratios and $\beta(\Delta)$ are the residues of the aforementioned poles, which are related with the coefficient functions $\alpha(\nu)$ in (3.16).

4.2.3 Series expansion of Conformal blocks

Let us now present the first method with which we can compute the blocks. In particular, when we are trying to find the conformal blocks by means of the casimir differential equation, it is helpful to consider either the Euclidean OPE limit ($u \to 0$, $v \to 1$) or the

Lorentzian lightcone limit ($u \to 0$ with fixed v). Doing so is advisable since it simplifies the analysis. Moreover, the OPE provides us with boundary conditions, which we can use to propose an ansatz for the conformal blocks. In turn, we can plug this in the differential equation and solve it order by order, so that in the end we have a series expansion of the blocks. However, because these limits are different in nature, each deserves an unique analysis. In particular, the aforementioned fact regarding which operators give the dominant contribution in each limit, needs to be taken into account when we expand the conformal blocks as a power series.

4.2.3.1 Euclidean OPE limit

Let us then start by considering the Euclidean OPE limit. To begin, it will prove more useful to use the cross ratios σ and ξ of [43]*, which are related to the original u and v by:

$$u = \sigma^2 \ , \quad \xi = \frac{1 - v + u}{2\sqrt{u}} \, . \tag{4.25}$$

In these new variables, the near coincidence limit translates into $\sigma \to 0$ while holding ξ fixed. Moreover, r can be thought of as a radial coordinate whereas ξ is related to an angle.

By taking the Euclidean OPE between any two operators in the scalar four point function, we obtain the leading order behavior of the conformal blocks as $\sigma \to 0$, namely $G_{\Delta,J} \underset{\sigma \to 0}{\sim} \sigma^{\Delta}$ (where we are omitting the dependence on ξ). Alternatively, we could analyze the solution of the Casimir differential at leading order for small σ. Both procedures would suggest that we propose the following ansatz for a single scalar conformal block:

$$G_{\Delta,J} = \sum_{m=0}^{\infty} \sum_{j} a_{m,j} \, g_{\Delta+m,j}(\sigma,\xi) \ , \qquad g_{E,j}(\sigma,\xi) = \sigma^E \, C_j^{h-1}(\xi) \ , \tag{4.26}$$

where $C_n^{\lambda}(z)$ denotes the Gegenbauer polynomial. In order to understand the above equation, recall that given a primary operator $\mathcal{O}^{\mu_1 \cdots \mu_J}$, we may act with the translations generator of the conformal group P_μ to obtain descendants. For instance, at level† two we can have:

$$P^2 \, \mathcal{O}^{\mu_1 \cdots \mu_J} \ , \quad P_{\mu_1} P_{\mu_2} \, \mathcal{O}^{\mu_1 \cdots \mu_J} \ , \quad P^{\nu_1} P^{\nu_2} \, \mathcal{O}^{\mu_1 \cdots \mu_J} \ , \ \ldots \tag{4.27}$$

Note that while both descendants have the same dimension, they have different spins. Nonetheless, they contribute equally to the four-point function, given that in this limit,

*The cross-ratio σ in here corresponds to s in this paper.

†By "level" we mean the number of P's we are acting with on the primary. Here, we use the letter m to label this.

the operators contribution depends purely on their dimension. Thus, they must be encoded at the same order in σ in (4.26). This implies that the Gegenbauer polynomial encodes the contributions of operators with different spins but same conformal dimensions to the block. This analysis also tells us that at each level, where the conformal dimension is $\Delta + m$, the sum over j must be in the interval:

$$j \in \left\{ J + m, J + m - 2, \ldots, \max\left(J - m, J + m \bmod 2\right) \right\} . \tag{4.28}$$

In order to obtain the expansion coefficients $a_{m,j}$, it is more useful to separate the Casimir differential operator into two components, $\mathcal{D} = \mathcal{D}_0 + \mathcal{D}_1$, which are given by:

$$\mathcal{D}_0 = \sigma^2 \partial_\sigma^2 + (d-1)\left[\xi\,\partial_\xi - \sigma\,\partial_\sigma\right] + (\xi^2 - 1)\,\partial_\xi^2 , \tag{4.29}$$

$$\begin{aligned}\mathcal{D}_1 = \sigma \Big[&\Delta_{12}\Delta_{34}\xi - (d - 2 + \xi^2 + (1-\xi^2)(\Delta_{12} - \Delta_{34}))\,\partial_\xi + \xi(1-\xi^2)\,\partial_\xi^2 \\ &+ (\Delta_{12} - \Delta_{34} - 1)\,\xi\,\sigma\,\partial_\sigma + 2\,(1-\xi^2)\,\sigma\,\partial_\sigma\,\partial_\xi - \xi\,\sigma^2\,\partial_\sigma^2 \Big] .\end{aligned} \tag{4.30}$$

Notice that, whereas $\mathcal{D}_0$ keeps the degree in σ fixed, $\mathcal{D}_1$ increases it by one unit. Relatedly, it is possible to show that $g_{E,j}(\sigma,\xi)$ satisfies an eigenvalue equation under the action of $\mathcal{D}_0$:

$$\mathcal{D}_0\, g_{E,j}(\sigma,\xi) = C_{E,j}\, g_{E,j}(\sigma,\xi) , \tag{4.31}$$

where $C_{E,j}$ is the same as the Casimir eigenvalue. By making use of the above equality while imposing its asymptotics as boundary conditions, one finds the explicit expression for the functions $g_{E,j}(\sigma,\xi)$, which is indicated in (4.26). In particular, we use the behavior of the conformal block in the Euclidean OPE limit, which was mentioned above, as the boundary condition. Note also that this differential equation coincides with what would be obtained after expanding the Casimir differential operator up to leading order in σ. Crucially, after imposing the same asymptotics behavior, the solution we obtain is none other than the $m = 0$ term of (4.26).

What is more, the differential operator $\mathcal{D}_1$ is vital to obtain the coefficients $a_{m,j}$. In particular, a simple analysis shows that acting with this differential operator on $g_{E,j}(\sigma,\xi)$ gives a linear combination of the same functions with shifted dimensions and spins [6, 46]. Using this fact in the Casimir equation, we can solve it order by order in σ, ultimately obtaining recurrence relations for $c_{E,j}$. Providing an initial condition then fixes all other coefficients. This will be seen explicitly more ahead, when we compute the blocks of some correlators.

4.2.3.2 Lorentzian OPE limit

We can also conduct a similar analysis for the Lorentzian lightcone limit. Nonetheless, in contrast with the Euclidean limit, we can keep using the u, v cross-ratios. We start by performing the Lorentzian OPE (2.94), which tells us that at leading order in u, the behavior of the blocks goes as $G_{\mathcal{O}} \underset{u\to 0}{\sim} u^{\frac{\tau}{2}}$ (where we are omitting dependence on v). Taking into account this and the fact that equal twist operators contribute equally to the four-point function in this limit, it is reasonable to suggest the following ansatz:

$$G_{\mathcal{O}}(u,v) = \sum_{m=0}^{\infty}\sum_{k=0}^{m} c_{m,k}\, g_{\tau+2m,J-k}(u,v) \ , \quad g_{T,j}(u,v) = u^{T/2}\, \tilde{g}_{T,j}(v) \ , \tag{4.32}$$

where the function $\tilde{g}_{T,j}(v)$ will be made explicit more ahead. The above expression has some resemblances with (4.26). However, it organizes the operators not by its conformal dimension but rather by its twist. This means that for every order of u, the sum over k, namely in $\tilde{g}_{\tau+2m,J-k}(u,v)$, encodes the contributions coming from operators with the same twist but different spins. For instance, consider a primary $\mathcal{O}^{\mu_1\cdots\mu_J}$ of twist $\tau = \Delta - J$. By acting either with P^2 or P_{μ_1} contracted with one of the indices of the primary, we obtain descendants of different spins but same twist, namely $\tau + 2$. It is the sum over k that translates exactly this degeneracy. In particular, for every twist, i.e. every m, there are $m+1$ descendants with different spins, such that the sum runs over $k \in \{0, \ldots, m\}$. Note that in here m does not denote the level as in the Euclidean OPE limit formula (4.26).

In this case, it is also convenient to separate the differential operator in two parts, one that keeps the degree in u fixed and another that raises it by one unit. It follows then, that the Casimir differential equation becomes:

$$[\mathcal{D}_0 + \mathcal{D}_1]\ G_{\mathcal{O}}(u,v) = C_{\Delta,J}\, G_{\mathcal{O}}(u,v) \ , \tag{4.33}$$

where

$$\begin{aligned}\mathcal{D}_0 =& \frac{1}{2}(1-v)\Delta_{12}\Delta_{34} + (2-\Delta_{12}+\Delta_{34})(1-v)^2\partial_v + 2(1-v)^2 v\,\partial_v \\ &+ u\left[2(1-d+v) + (1-v)(\Delta_{12}-\Delta_{34})\right]\partial_u - 4(1-v)\,u\,\partial_u\, v\,\partial_v + 2(1+v)\,u^2\partial_u^2 \ ,\end{aligned} \tag{4.34}$$

$$\begin{aligned}\mathcal{D}_1 =& u\left[\frac{1}{2}\,\Delta_{12}\Delta_{34} - (2-\Delta_{12}+\Delta_{34})\,(1+v) - 2\,v\,(1+v)\,\partial_v^2 - u\,(2-\Delta_{12}+\Delta_{34})\ \partial_u\right. \\ &\left. - 4\,u\,\partial_u\, v\,\partial_v - 2\,u^2\,\partial_u^2\right] \ .\end{aligned} \tag{4.35}$$

In similarity with the previous case, the functions $g_{\tau,J}(u,v)$ also satisfy an eigenvalue equation under the action of $\mathcal{D}_0$:

$$\mathcal{D}_0\, g_{T,j}(u,v) = C_{T,j}\, g_{T,j}(u,v)\ , \tag{4.36}$$

where the eigenvalue is simply the Casimir expressed in terms of the twist:

$$C_{T,j} = (j+T)(j+T-d) + j(d+j-2)\ . \tag{4.37}$$

What is more, eq.(4.36) coincides with the leading order of the Casimir differential operator, which admits the $m=0$ term as a solution. By imposing that $g_{T,j}(u,v) \sim u^{\frac{T}{2}}(1-v)^j$ in the limit $v \to 1$, we can unequivocally fix these functions. In particular, we find that:

$$g_{T,j}(u,v) = u^{\frac{T}{2}}\,(1-v)^j\,{}_2F_1\left(\frac{T+2j-\Delta_{12}}{2}, \frac{T+2j+\Delta_{34}}{2}, T+2j, 1-v\right)\ . \tag{4.38}$$

Analogously to the Euclidean case, we also have that $\mathcal{D}_1\, g_{T,j}(u,v)$ can be written in terms of these same functions with different T and j. This relation can be used to obtain recurrence relations for the coefficients $c_{m,k}$, by imposing they solve the Casimir differential equation order by order in u. After obtaining these recurrence relations, we choose the appropriate initial conditions such that the remaining coefficients become completely determined.

Lastly, note that whether we choose to consider the Euclidean limit or the Lorentzian limit depends on the analysis we wish to do, as each one of them has its own advantages. We will further discuss this later in subsection 4.2.5.

4.2.4 Differential operators method

In addition to the series expansion, we will now present an alternative procedure to obtain the conformal blocks, which makes use of a specific set of differential operators. We will also try to understand the advantages of this method in comparison with all the others.

To grasp the main point of this approach, start by recalling that conformal blocks can be directly computed with the OPE. In fact, this is relatively straightforward when the correlation function involves only scalar operators. However, as soon as we consider nonzero spin operators in the correlator, the required computations can become quite cumbersome. Nevertheless, what if instead of performing the OPE summations all over again, we could reuse the scalar result for the spinning case? Indeed, we will see that by applying some specific differential operators to the scalar conformal blocks, we come by the

desired spinning conformal blocks. This construction and associated differential operators were proposed in [47], in which this exposition is based upon.

4.2.4.1 General idea

We start by considering the OPE of two spinning operators. Although such a formula has not yet been introduced, a quick look at the Euclidean OPE equation (2.88) would lead us to propose:

$$\mathcal{O}_1^{\{\mu\}}(x_1)\,\mathcal{O}_2^{\{\nu\}}(x_2) = \sum_{\mathcal{O}} \lambda_{12\mathcal{O}}\, C\left(x_{12}, \partial_{x_2}\right)^{\{\mu,\nu,\alpha\}}\, \mathcal{O}_{\{\alpha\}}(x_2) \quad . \tag{4.39}$$

The above expression is very similar to the scalar formula, with the novelty that the coefficient functions must now encode the spinning indices of the external operators, $\{\mu\}$ and $\{\nu\}$.

By using this expression, we could define the conformal partial waves similarly to the scalar case, from which we could then extract the spinning conformal blocks. As it turns out, however, for external spinning operators each exchanged operator can have more than one conformal partial wave associated. In other words, the coefficient functions in (4.39) are actually a sum over different possible structures. As such, we first need to catalog all of these OPE structures.

In addition, we would later have to perform the sum over the indices like in (2.88). This would be a bothersome step, given that even in the simplest case of scalars this sum is not trivial. Fortunately for us, we can avoid this step by making use of the scalar result, whose computation was already done in [41]. The idea is to write the spinning coefficient functions in (4.39) as the action of differential operators on the scalar one:

$$C\left(x_{12}, \partial_{x_2}\right)^{\{\mu,\nu,\alpha\}} = D_{x_1,x_2}^{\{\mu,\nu\}}\, C\left(x_{12}, \partial_{x_2}\right)^{\{\alpha\}} \quad . \tag{4.40}$$

Since we will have several OPE structures, each of these differential operators are in a one-to-one correspondence with the different conformal partial waves.

It then follows from (4.40), that each of the spinning conformal partial waves can be expressed as the action of the D's on the scalar conformal partial wave:

$$W_{\mathcal{O}}^{\{\mu,\nu,\alpha,\beta\}}(x_1, x_2, x_3, x_4) = D_{x_1,x_2}^{\{\mu,\nu\}} D_{x_3,x_4}^{\{\alpha,\beta\}}\, W_{\mathcal{O}}(x_1, x_2, x_3, x_4) \ . \tag{4.41}$$

Before proceeding, however, an important comment is in order. In particular, because this method reuses the results from the scalar case, it can only give us the spinning conformal

blocks associated with the exchange of spinning operators in the symmetric and traceless representation. For any other case, such as the antisymmetric or mixed symmetry representations, another route must be taken. For a detailed discussion about this see [47].

4.2.4.2 Identifying OPE structures

The first step of this procedure is to identify the OPE structures that can appear in the OPE of two spinning operators. This is not as hard as it seems, given that the OPEs are in a one-to-one correspondence with three point functions. One such indication of this, is the fact that the OPE coefficients appearing in (2.89) are also the normalization constants of the corresponding three point functions. In fact, the OPE between two spinning operators can be written as a sum over the associated three point function structures [12]. As a result, our task is then that of identifying the structures of generic spin J_1 - spin J_2 - spin J three-point functions, so as to later express these in terms of the scalar-scalar-spin J three point functions:

$$\langle \mathcal{O}_1^{\{\mu\}}(x_1)\,\mathcal{O}_2^{\{\nu\}}(x_2)\,\mathcal{O}^{\{\alpha\}}(x_3)\rangle = D^{\{\mu,\nu\}}_{x_1,x_2}\langle \mathcal{O}_1(x_1)\,\mathcal{O}_2(x_2)\,\mathcal{O}^{\{\alpha\}}(x_3)\rangle\,. \tag{4.42}$$

These structures, however, were already introduced prior to this discussion. In the embedding space, they are nothing more than the numerator of each term of the sum (2.62), without the OPE coefficient. Meanwhile, in the physical space, they correspond to what we had previously denoted by $t^{\ell_1,\ell_2,\ell_3}(x,z_1,z_2,z_3)$, and are given by (2.68).

From now on we will denote these structures in the embedding space by:

$$\begin{bmatrix} \Delta_1 & \Delta_2 & \Delta_3 \\ J_1 & J_2 & J_3 \\ \ell_1 & \ell_2 & \ell_3 \end{bmatrix} \equiv \frac{V_{1,23}^{m_1} V_{2,31}^{m_2} V_{3,12}^{m_3} H_{12}^{\ell_3} H_{13}^{\ell_2} H_{23}^{\ell_1}}{(P_{12})^{\frac{1}{2}(\bar\tau_1+\bar\tau_2-\bar\tau_3)}(P_{13})^{\frac{1}{2}(\bar\tau_1+\bar\tau_3-\bar\tau_2)}(P_{23})^{\frac{1}{2}(\bar\tau_2+\bar\tau_3-\bar\tau_1)}}\,, \tag{4.43}$$

such that eq.(2.62) becomes

$$\tilde G(P_1,P_2,P_3;Z_1,Z_2,Z_3) = \sum_{\{\ell_i\}} \lambda^{\ell_1\ell_2\ell_3}_{J_1J_2J_3} \begin{bmatrix} \Delta_1 & \Delta_2 & \Delta_3 \\ J_1 & J_2 & J_3 \\ \ell_1 & \ell_2 & \ell_3 \end{bmatrix}\,. \tag{4.44}$$

4.2.4.3 Elementary Differential Operators

With the structures identified, we must now find the differential operators satisfying (4.42). In the embedding space and using the notation introduced above, this equality becomes:

$$\begin{bmatrix} \Delta_1 & \Delta_2 & \Delta \\ J_1 & J_2 & J \\ \ell_1 & \ell_2 & \ell \end{bmatrix} = \mathcal{D}\left(P_i, Z_i, \frac{\partial}{\partial P_i}, \frac{\partial}{\partial Z_i}\right) \begin{bmatrix} \Delta_1' & \Delta_2' & \Delta \\ 0 & 0 & J \\ 0 & 0 & 0 \end{bmatrix} \qquad (i = 1, 2)\,, \tag{4.45}$$

where we are implicitly dropping terms proportional to P_i^2, Z_i^2 and $P_i \cdot Z_i$. Note that, in general, $\Delta_{1,2}'$ will be different from $\Delta_{1,2}$ since these differential operators can raise or lower the conformal dimensions of the structures.

In order for the differential operators to be consistent with the embedding space and null polarization vectors formalisms, they must obey certain conditions. In particular:

- They must map terms of the type $O(P_i^2, Z_i^2, Z_i \cdot P_i)$ to the same kind, in order to keep the structures within the submanifold defined by

$$Z_i^2 = Z_i \cdot P_i = P_i^2 = 0 \quad (i = 1, 2)\ . \tag{4.46}$$

- They must be interior to the space of transverse functions.

Moreover, so as to satisfy (4.45), they must increase the degree on Z_1 and Z_2 from 0 to J_1 and J_2, respectively. In practice, we can think of these operators as composed of elementary differential operators which raise the degrees one unit at a time. Taking all of these considerations into account, one finds that the only independent operators which satisfy these conditions are the following first-order differential operators [47]:

$$\begin{aligned} D_{11} \equiv\ & (P_1 \cdot P_2)(Z_1 \cdot \frac{\partial}{\partial P_2}) - (Z_1 \cdot P_2)(P_1 \cdot \frac{\partial}{\partial P_2}) - (Z_1 \cdot Z_2)(P_1 \cdot \frac{\partial}{\partial Z_2}) \\ & + (P_1 \cdot Z_2)(Z_1 \cdot \frac{\partial}{\partial Z_2})\,, \\ D_{12} \equiv\ & (P_1 \cdot P_2)(Z_1 \cdot \frac{\partial}{\partial P_1}) - (Z_1 \cdot P_2)(P_1 \cdot \frac{\partial}{\partial P_1}) + (Z_1 \cdot P_2)(Z_1 \cdot \frac{\partial}{\partial Z_1})\,, \end{aligned} \tag{4.47}$$

and two more with $1 \leftrightarrow 2$, in addition to a zeroth order differential operator H_{12}, which is the building block defined back in (2.53). However, there is crucial difference between the operators D_{ij} and H_{12}. In particular, whereas the D_{ij} increase the spin at i by one unit and decrease the conformal dimension at position j by one unit, H_{12} increases the spin and decreases the conformal dimension by one unit at both points.

4.2.4.4 Differential Basis and Standard Basis

Once we have the elementary differential operators, we can compose them in order to raise the spins as much as we want. This translates into the following relation:

$$\left\{ \begin{array}{ccc} \Delta_1 & \Delta_2 & \Delta_3 \\ J_1 & J_2 & J_3 \\ \ell_1 & \ell_2 & \ell_3 \end{array} \right\} \equiv H_{12}^{\ell_3} D_{12}^{\ell_2} D_{21}^{\ell_1} D_{11}^{m_1} D_{22}^{m_2} \left[\begin{array}{ccc} \Delta_1 + m_1 + \ell_1 + \ell_3 & \Delta_2 + m_2 + \ell_2 + \ell_3 & \Delta_3 \\ 0 & 0 & J_3 \\ 0 & 0 & 0 \end{array} \right] . \tag{4.48}$$

Note that here, we have designated the LHS three point function structure with a different bracket. This happens because acting with the elemantary differential operators on a standard basis structure (4.43), does not produce a result which can be expressed in the same form. This new basis for spinning three point structures will be referred to as the differential basis, and denoted by curly brackets. Importantly, both basis can be related by inverting the matrix which relates them.

To understand the reasoning of this change of basis, consider an arbitrary spinning three point function with conformal dimensions Δ_i and spins J_i, where $i = 1, 2, 3$. Moreover, suppose there are N possible structures in the standard basis $[I]$ associated with this correlator, and necessarily, an identical number of analogous structures in the differential basis $\{I\}$ characterized by the same numbers ℓ_i. When acting with the differential operators according to (4.48), we obtain the differential basis elements $\{I\}$. However, each of these structures can be expressed as a linear combination of the standard basis elements, which is the same as saying it can be written in a different basis according to:

$$\{I\} = \sum_{J=1}^{N} a_{IJ} \, [J] \, . \tag{4.49}$$

However, the opposite is also true. If we invert the matrix with elements a_{IJ}, we are able express the standard basis structures as a linear combination of the previously obtained differential basis structures. Hence, we can freely go from one basis to the other.

Lastly, we stress out that not all of the differential operators commute among themselves. The order of operators in (4.48) is simply a matter of choice. In particular, the only non-vanishing commutation relations are:

$$[D_{11}, D_{22}] = \frac{1}{2} H_{12} \left(Z_1 \cdot \frac{\partial}{\partial Z_1} - Z_2 \cdot \frac{\partial}{\partial Z_2} + P_1 \cdot \frac{\partial}{\partial P_1} - P_2 \cdot \frac{\partial}{\partial P_2} \right) , \tag{4.50}$$

$$[D_{12}, D_{21}] = \frac{1}{2} H_{12} \left(Z_1 \cdot \frac{\partial}{\partial Z_1} - Z_2 \cdot \frac{\partial}{\partial Z_2} - P_1 \cdot \frac{\partial}{\partial P_1} + P_2 \cdot \frac{\partial}{\partial P_2} \right) . \tag{4.51}$$

4.2.4.5 Spinning Conformal Blocks

Now that we established the differential operators and how to go from one basis to the other, we may move on to the conformal blocks. In reality, the reasoning is going to be similar as for the three point structures. Namely, we will have to act with the differential operators in the scalar conformal partial wave, as represented in (4.41).

Given a spinning four point function, each conformal partial wave is characterized by the couplings of the exchanged field, which amount to the three point functions of this operator with the external ones. This relation is not difficult to understand, bearing in mind the correspondence between OPEs and three point functions, in addition to how conformal partial waves are defined. These three point functions, in turn, are associated with the following structures in the differential basis:

$$\left\{ \begin{array}{ccc} \Delta_1 & \Delta_2 & \Delta_0 \\ J_1 & J_2 & J_0 \\ \ell_1 & \ell_2 & \ell_0 \end{array} \right\} , \qquad \left\{ \begin{array}{ccc} \Delta_3 & \Delta_4 & \Delta_0 \\ J_3 & J_4 & J_0 \\ \ell_3 & \ell_4 & \ell_0 \end{array} \right\} , \tag{4.52}$$

where the label 0 denotes the exchanged field.

Each pair of these elements has an associated spinning conformal partial wave given by

$$\mathcal{D}_{\text{left}} \mathcal{D}_{\text{right}} W_{\mathcal{O}}(P_1, P_2, P_3, P_4) \,, \tag{4.53}$$

where

$$\mathcal{D}_{\text{left}} = H_{12}^{\ell_0} D_{12}^{\ell_2} D_{21}^{\ell_1} D_{11}^{m_1} D_{22}^{m_2} \, \Sigma^{m_1+\ell_1+\ell_0,\, m_2+\ell_2+\ell_0} \,, \tag{4.54}$$

and $\mathcal{D}_{\text{right}}$ is given by the same expression with $1 \to 3$ and $2 \to 4$. In the above expression, the operator $\Sigma^{a,b}$ amounts to the following shifts in the conformal dimensions:

$$\Delta_1 \to \Delta_1 + m_1 + \ell_0 + \ell_1 \,, \qquad \Delta_2 \to \Delta_2 + m_2 + \ell_0 + \ell_2 \,. \tag{4.55}$$

The shifts for $\Delta_{3,4}$ are similar but with the replacements $1 \to 3$ and $2 \to 4$. In addition, note that the scalar conformal partial wave written in the embedding space is given by (2.97), with $x_{ij}^2 \to P_{ij}$ as shown in (2.41).

After applying the differential operators on the scalar conformal block as in (4.53), we obtain the spinning partial waves in the differential basis. In order to obtain these functions in the standard basis, we must follow the same reasoning as for three point functions. In practice, we impose equality between the characteristic three point functions (couplings) as a sum over the standard basis elements, and a generic linear combination of the differential basis structures. This completely fixes the arbitrary coefficients of the linear combination

in terms of the OPE coefficients. This procedure will be seen further ahead in section (4.3.2.2), in particular in (4.102) and (4.103).

After taking all these actions, we obtain the spinning conformal partial waves in the embedding space, whose structure must be of the form:

$$\left(\frac{P_{24}}{P_{14}}\right)^{\frac{\bar{\tau}_1-\bar{\tau}_2}{2}}\left(\frac{P_{14}}{P_{13}}\right)^{\frac{\bar{\tau}_3-\bar{\tau}_4}{2}}\frac{\sum_k f_k(u,v)\,Q^{(k)}(\{P_i;Z_i\})}{(P_{12})^{\frac{\bar{\tau}_1+\bar{\tau}_2}{2}}(P_{34})^{\frac{\bar{\tau}_3+\bar{\tau}_4}{2}}}\,, \tag{4.56}$$

where the sum over k is simply here to label the different structures and associated cross ratios functions.

Here, $Q^{(k)}$ are transverse polynomials of P_i and Z_i, of degree J_i. They are constructed with the same basic building blocks ($V_{i,jk}$ and H_{ij}) that are used for three point functions.

In addition, the coefficient functions $f_k(u,v)$ consist of linear combinations of shifted scalar conformal blocks $G_{\mathcal{O}}(u,v)$ and respective derivatives with regard to the cross ratios u and v.

Similarly as we did for the scalar case, we can identify the spinning conformal blocks in (4.56) by the sum in k. Consequently, we see that with this definition, the spinning conformal blocks explicitly depend on the basic building blocks $V_{i,jk}$ and H_{ij}, since as previously mentioned, the polynomials $Q^{(k)}$ are generated with these.

4.2.5 Analytic continuation

Up until now, the methods we have presented concerned only correlators with all points spacelike separated. Thus, we must analytically continue them if we wish to analyze them in the Regge limit. This was already explained in section 4.1, where we introduced the Regge limit and the underlying ideas behind this analytic continuation. Here, we will revise some of those concepts and extend the discussion on the matter.

As always, the starting point of this subject are the correlators in the Euclidean region. Moreover, we assume we know the associated conformal blocks, which can be computed by any of the approaches given above. As already stated, we then need to analytically continue the correlators (which implies an analytic continuation of the blocks as well), by traversing a certain path in the cross ratios space, which depends on the initial and final configurations. We stress out that different paths lead in general to different analytic continuations, since some might find branch cuts, whereas others can avoid them altogether.

In the case of Regge kinematics, the path that must be followed was already presented in figure 4.3. We point out, however, that this figure only depicts the path for analytically

continuing the spacelike separated points to the configuration with the necessary causal relations. In practice, what we will do to consider the Regge limit ($z, \bar{z} \to 0$), is to start by taking $\bar{z}$ to be small, $\bar{z} \to 0$. Next, while keeping $\bar{z} > 0$ fixed, we take z counter-clockwise around 1 as previously mentioned. Finally, we take $z \to 0$, such that we find ourselves in the same region of the Regge limit: $z, \bar{z} \sim 0$. Note, however, that this will not correspond to the Regge limit, as we sent z and $\bar{z}$ to 0 in a certain order rather than simultaneously. Nonetheless, the result still provides us information about the behavior of the correlator or conformal blocks in the Regge limit, and can in fact be used as boundary conditions to obtain the blocks in this kinematical limit. In here, we have chosen to think about this procedure in terms of the u, v cross ratios. Equivalently, we start by sending $u \to 0$ and then take v counter-clockwise around 0, while holding $u > 0$ fixed. Finally, we send $v \to 1$, in order for the correlator to be in the same region of the Regge limit ($u \to 0$, $v \to 1$). This path is depicted in figure 4.5.

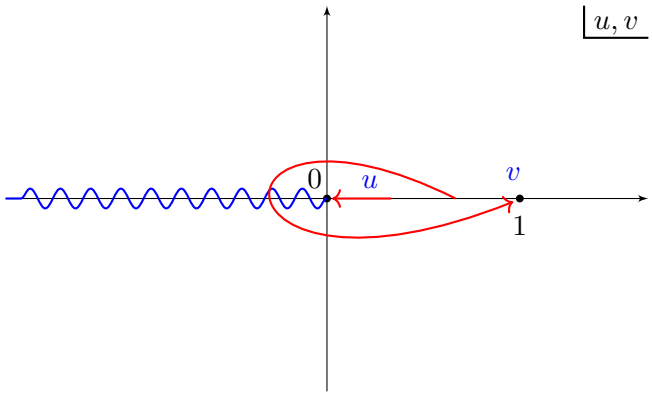

FIGURE 4.5: Schematic representation of the path in the u, v plane we must follow to analytically continue the conformal blocks.

It is important to be aware that we might pick discontinuities as we traverse the path, due to branch cuts of the correlator/conformal blocks. In particular, in the cases considered here, we will find the branch cut depicted in figure 4.5 by the wobbly blue line, which arises due to the hypergeometric functions through which the blocks are expressed. When this happens, we will generally find that the analytically continued conformal blocks will have an extra term, which is this discontinuity of the function across the cut:

$$G^{\circlearrowleft}_{\Delta,J}(u,v) = G_{\Delta,J}(u,v) + \text{Disc}\left[G_{\Delta,J}(u,v)\right] \ . \tag{4.57}$$

Recall that branch cuts arise in multi-valued functions, so as to impose we remain in a single sheet of the function, thus leading to the discontinuity. If instead we could move through

different sheets of it, the function would be continuous. Physically, these discontinuity terms arise when one of two spacelike separated points crosses the lightcone of the other, as mentioned in section 4.1.

To have a better understanding of this whole procedure, we have constructed figure 4.6. For simplicity, we have used conformal transformations to put the points in the same configuration of figure 2.1, with all points spacelike separated. Moreover, the blue lines represent the future and past lightcones of x_1 and x_3.

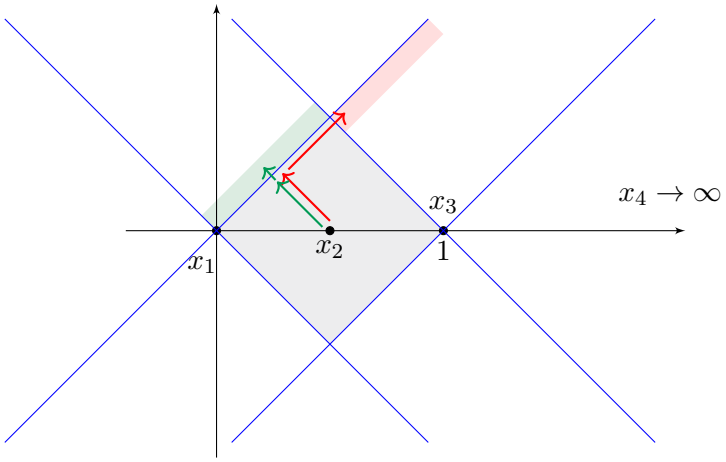

Figure 4.6: Schematic figure that depicts the analytic continuation of the conformal blocks.

The first thing we would like to point out, is the grey shaded region in which x_2 is spacelike separated from x_1 and x_3. Inside of it, the conformal blocks remain unchanged, independently to where the point x_2 is moved within this same region. The issue, however, is that we do not have an expression for the blocks in closed form for any dimension. Therefore, in order to overcome this problem, we must consider a specific kinematical limit, in which these objects become simpler. One possible choice is to consider the lightcone limit $x_{12}^2 \to 0$, where the usage of the Lorentzian lightcone OPE (2.94) provides us with an explicit expression of the blocks in this same limit. This is depicted by the red and green arrows coming out of x_2.

Next, we want to analytically continue the lightcone conformal blocks. In particular, if we wish to analyze the blocks in the Regge limit, x_2 has to cross the future lightcone of x_3. When the crossing takes place, x_2 and x_3 become lightlike ($x_{23}^2 = 0$) such that $v = 0$. Consequently, we must take v around 0 in the path of analytic continuation. This step is illustrated by the red arrow which crosses the future lightcone of x_3.

The obtained result, however, is only valid near the future lightcone of x_2 (red shaded region), since we have initially considered $x_{12}^2 \to 0$. In order to extend the result to the whole future lightcone of x_3, we would have to take a step further and analytically continue this function again.

Alternatively, we could have chosen to cross the future lightcone of x_1, although this would not correspond to the Regge kinematics. Such analytic continuation would involve taking u around 0, given that x_1 becomes lightlike from x_2 ($x_{12}^2 = 0$) throughout the path (small green arrow). By the same reasoning as before, the outcome of this procedure remains valid only near $x_{12}^2 = 0$ (green shaded region), but can be extended by analytic continuation.

It is important to remark that these two analytic continuations would yield different results, as the discontinuities of the correlator/conformal block across the branch cuts of the u plan are different from the ones in the v plan. This arises due to different dependencies on these cross ratios.

Figure 4.6 is also helpful to understand which one of the two limits, namely the Euclidean limit and the Lorentzian limit, is more useful depending on what we want to do. In particular, when one has to analytic continue the correlators to later take the Regge limit, x_2 must be taken to cross the future lightcone of x_3. If we considered the near coincidence limit, the result would only be valid around x_1, where $x_{12} \sim 0$, and x_1 could not be moved to cross this lightcone. Thus, we must take the lightcone limit, whose outcome is valid in the entire vicinity of the lightcone of x_1. Nevertheless, the near coincidence limit also has its uses. In fact, because it corresponds to the same limit in the u, v cross ratios as the Regge limit (u $\to 0$, $v \to 1$), one can compare the conformal blocks obtained from taking the Euclidean limit, with the same blocks in the Regge limit. Naturally, these will differ, as the latter resulted from an analytic continuation before taking this limit.

Now that we have presented all methods with which we can obtain the conformal blocks, and have extensively explained how to analytically continue these functions and take its Regge limit, we will begin by computing the blocks of the scalar correlator for the sake of clarity. We then proceed to compute the blocks of the two spinning four point functions mentioned at the beginning of this chapter.

4.3 Conformal Blocks in the Regge Limit

4.3.1 Scalar-Scalar-Scalar-Scalar

In this section, we compute the conformal blocks in the Regge limit of the scalar four-point function with operators of different dimensions $\langle\phi_1(x_1)\phi_2(x_2)\phi_3(x_3)\phi_4(x_4)\rangle$, by the different approaches we introduced so far. Throughout this analysis, we will compare the results obtained from the different methods to check whether or not they yield matching results, while also inferring about the advantages of each one.

4.3.1.1 With the Casimir differential equation

In order to obtain the scalar conformal blocks from the Casimir differential equation (4.33), we consider the lightcone limit. As we already argued before, in this limit the conformal blocks can be expanded in powers of u as in (4.32). Moreover, we know that the functions $g_{\tau,J}(u,v)$ satisfy an eigenvalue equation (4.36), which after choosing their asymptotic behavior fixes the solution. The missing pieces are then the expansion coefficients $c_{m,k}$.

We proceed as explained below (4.38). We start by acting with $\mathcal{D}_1$ in the functions $g_{\tau,J}(u,v)$, only to find that this can be written as a linear combination of the same kind of functions, but with a twist shifted by two units:

$$\begin{aligned}
&\mathcal{D}_1\, g_{\tau,J}(u,v) = b^{(-2)}_{\tau,J}\, g_{\tau+2,J-2}(u,v) + b^{(-1)}_{\tau,J}\, g_{\tau+2,J-1}(u,v) + b^{(0)}_{\tau,J}\, g_{\tau+2,J}(u,v)\ , \qquad (4.58)\\
&b^{(-2)}_{\tau,J} = -4\,J\,(J-1)\ ,\ b^{(-1)}_{\tau,J} = \frac{2\,J\,(\tau+J-1)\,\Delta_{12}\,\Delta_{34}}{(\tau+2J-2)(\tau+2\,J)}\ ,\\
&b^{(0)}_{\tau,J} = -\frac{\left(J^2+J(2\tau-1)+(\tau-1)\tau\right)\left((2J+\tau)^2-\Delta_{12}^2\right)\left((2J+\tau)^2-\Delta_{34}^2\right)}{4(\tau+2J-1)(\tau+2J)^2(\tau+2J+1)}\ .
\end{aligned}$$

It is important that the action of this operator involves functions of higher twist and not lower. Otherwise, the sum over m in (4.32) would have to run from $m=-\infty$ instead of starting at $m=0$.

Then, by using (4.58) in the Casimir differential equation, we can obtain the following recurrence relation for the coefficients $c_{m,k}$:

$$\begin{aligned}
&\left(C_{2m+\tau,J-k} - C_{\tau,J}\right)\, c_{m,k} + b^{(0)}_{\tau+2m-2,J-k}\, c_{m-1,k} + b^{(-1)}_{\tau+2m-2,J-k+1}\, c_{m-1,k-1} +\\
&+\ c_{m-1,k-2}\, b^{(-2)}_{\tau+2m-2,J-k+2} = 0 \qquad (4.59)
\end{aligned}$$

By choosing the initial conditions $c_{0,0}=1$ and $c_{m,k}=0$ for $m<k$, we completely determine all the coefficients $c_{m,k}$.

In the simplest case of external operators with equal conformal dimensions, the $b^{(i)}_{\tau,J}$ coefficients become simpler and the recurrence relation is given by:

$$\begin{aligned}&\left(C_{2m+\tau,J-k}-C_{\tau,J}\right)\, c_{m,k}-\tfrac{(J-k+2m+\tau-3)(J-k+2m+\tau-2)(2(J-k+m-1)+\tau)^2}{4(2J-2k+2m+\tau-3)(2J-2k+2m+\tau-1)}\, c_{m-1,k}\\&-\,4(1+J-k)(2+J-k)c_{m-1,k-2}=0\ .\end{aligned}\tag{4.60}$$

Since we know every quantity entering in (4.32), the next logical step would be to analytically continue this sum. Indeed, at each order in u, the conformal blocks are given by a finite sum of hypergeometric functions, whose discontinuity is easily computed. In spite of that, we will refrain from undertaking that procedure over here as it will be simpler to do this in the approach considered next.

4.3.1.2 With the Lorentzian lightcone OPE

The immediate use of the leading lightcone OPE (2.94) between $\phi_1\times\phi_2$ gives:

$$\begin{aligned}\langle\phi_1(x_1)\dots\phi_4(x_4)\rangle&\approx\sum_{\mathcal{O}}\frac{\lambda_{12\mathcal{O}}}{(x_{12}^2)^{\frac{\Delta_1+\Delta_2-\tau}{2}}}\int[dt]\,\langle\mathcal{O}(x_1+tx_{21},x_{12})\phi_3(x_3)\phi_4(x_4)\rangle\\&=\sum_{\mathcal{O}}\frac{\lambda_{12\mathcal{O}}\lambda_{34\mathcal{O}}}{(x_{12}^2)^{\frac{\Delta_1+\Delta_2-\tau}{2}}(x_{34}^2)^{\frac{\Delta_3+\Delta_4-\tau}{2}}}\int\frac{[dt]\,(x_{14}^2x_{23}^2-x_{13}^2x_{24}^2)^J}{(x_{23}^2t+(1-t)x_{13}^2)^{\frac{\bar\tau+\Delta_{34}}{2}}(x_{24}^2t+(1-t)x_{14}^2)^{\frac{\bar\tau-\Delta_{34}}{2}}}\ ,\end{aligned}\tag{4.61}$$

where we used the general expression for three point functions in the physical space (2.66).

To compute this integral, it is convenient to do the change of variables: $t\to t/(t+1)$ and $t\to t\,x_{14}^2/x_{24}^2$. This makes it easier to recognize the integral at hand as the integral representation of an hypergeometric function, whose arguments can be readily identified from the expression. In the end, the lightcone expansion of the scalar four point function is given by:

$$\langle\phi_1(x_1)\dots\phi_4(x_4)\rangle=\frac{\left(\frac{x_{24}^2}{x_{14}^2}\right)^{\frac{\Delta_{12}}{2}}\left(\frac{x_{14}^2}{x_{13}^2}\right)^{\frac{\Delta_{34}}{2}}}{\left(x_{12}^2\right)^{\frac{\Delta_1+\Delta_2}{2}}\left(x_{34}^2\right)^{\frac{\Delta_3+\Delta_4}{2}}}\sum_{\mathcal{O}}\lambda_{12\mathcal{O}}\lambda_{34\mathcal{O}}\left(G_{\mathcal{O}}(u,v)+\dots\right)\ ,\tag{4.62}$$

where

$$G_{\mathcal{O}}(u,v)=u^{\frac{\tau}{2}}\left(\frac{v-1}{2}\right)^J{}_2F_1\left(\frac{\bar\tau-\Delta_{12}}{2},\frac{\bar\tau+\Delta_{34}}{2},\bar\tau,1-v\right)\ ,\tag{4.63}$$

denotes the leading term of the lightcone blocks, and $\dots$ stand for the subleading terms of these same functions.

As a sanity check of the obtained result, we could compare it with the leading behavior of equation (28) in [33], in the limit $u\to 0$. Note that, although this expression is valid in the simultaneous limits of $u\to 0$ and $v\to 1$, expanding it for small u gives us its behavior

in the same kinematics we are considering, namely $u \to 0$ and fixed v. Indeed, by doing so, we find that the two expressions agree with each other.

The next step is to analytically continue the above result. As we mentioned previously, this involves passing through a branch cut. Hence, we must compute the discontinuity of (4.63). In particular, this was already done in [48]. To begin, we make use of the expansion of the hypergeometric function around 1, since as stated before, we wish to take v around zero. Thus, for $\frac{\Delta_{34}-\Delta_{12}}{2} \in \mathbb{Z}$ we may write:

$$
\begin{aligned}
&{}_2F_1\left(\frac{\bar{\tau}-\Delta_{12}}{2}, \frac{\bar{\tau}+\Delta_{34}}{2}, \bar{\tau}, 1-v\right) = \text{terms without branch cut} - \\
&-\frac{(-1)^{\frac{\Delta_{34}-\Delta_{12}}{2}}\Gamma(\bar{\tau})}{\Gamma\left(\frac{\bar{\tau}+\Delta_{12}}{2}\right)\Gamma\left(\frac{\bar{\tau}-\Delta_{34}}{2}\right)\Gamma\left(\frac{2+\Delta_{34}-\Delta_{12}}{2}\right)}\,{}_2F_1\left(\frac{\bar{\tau}-\Delta_{12}}{2}, \frac{\bar{\tau}+\Delta_{34}}{2}, \frac{2+\Delta_{34}-\Delta_{12}}{2}, v\right)\ln(v)\,.
\end{aligned}
\tag{4.64}
$$

When we go around $v = 0$ as in figure 4.5, the logarithm picks up a factor of $2\pi i$ and leads to a discontinuity given by:

$$
\begin{aligned}
&\text{Disc}\ \ G_{\mathcal{O}}(u,v) \sim \\
&-u^{\frac{\tau}{2}}\left(\frac{v-1}{2}\right)^{J}\frac{2\pi i(-1)^{\frac{\Delta_{34}-\Delta_{12}}{2}}\Gamma(\bar{\tau})}{\Gamma\left(\frac{\bar{\tau}+\Delta_{12}}{2}\right)\Gamma\left(\frac{\bar{\tau}-\Delta_{34}}{2}\right)\Gamma\left(\frac{2+\Delta_{34}-\Delta_{12}}{2}\right)}\,{}_2F_1\left(\frac{\bar{\tau}-\Delta_{12}}{2}, \frac{\bar{\tau}+\Delta_{34}}{2}, \frac{2-\Delta_{12}+\Delta_{34}}{2}, v\right)\,,
\end{aligned}
\tag{4.65}
$$

The leading behavior of this expression for $v \sim 1$ is:

$$
\text{Disc}\ \ G_{\mathcal{O}}(u,v) \sim -C_0\, u^{\frac{\tau}{2}}\left(\frac{v-1}{2}\right)^{1-\Delta}\,, \tag{4.66}
$$

where we have defined for simplicity:

$$
C_{k_{12}} = \frac{2\,i\,\pi\,(-1)^{\frac{\Delta_{34}-\Delta_{12}-k_{12}}{2}}\,\Gamma(\bar{\tau})\,\Gamma(\bar{\tau}-1)}{\Gamma\left(\frac{\bar{\tau}-\Delta_{12}-k_{12}}{2}\right)\Gamma\left(\frac{\bar{\tau}+\Delta_{12}+k_{12}}{2}\right)\Gamma\left(\frac{\bar{\tau}-\Delta_{34}}{2}\right)\Gamma\left(\frac{\bar{\tau}+\Delta_{34}}{2}\right)}\,. \tag{4.67}
$$

Here are anticipating the shifts ($k_{12} \equiv k_1 - k_2$) in the external dimensions, required by the differential operators, since this factor will reappear in that method as well.

Therefore, we find that the analytically continued lightcone block is given by:

$$
G^{\circlearrowleft}_{\mathcal{O}}(u,v) \approx u^{\frac{\tau}{2}}\left(\frac{v-1}{2}\right)^{J} - C_0\, u^{\frac{\tau}{2}}\left(\frac{v-1}{2}\right)^{1-\Delta}\,, \tag{4.68}
$$

where we have considered the leading behavior of (4.63) for $v \sim 1$. It will prove useful to express this result in terms of new cross ratios $\sigma^2 = z\bar{z}$, $t = \bar{z}/z$. Doing so we find:

$$
G^{\circlearrowleft}_{\mathcal{O}}(\sigma,t) \approx \left(-\tfrac{1}{2}\right)^{J}\left(t^{-\frac{J}{2}}\sigma^{\Delta} - C_0\, t^{\frac{\Delta-1}{2}}\sigma^{1-J}\right) \tag{4.69}
$$

In these new variables, the Regge limit corresponds to $\sigma \to 0$ and fixed t. As such, it

is immediate to see from the above expression that the second term dominates relatively to the first one when $J > 1$. However, the bootstrap equation imposes the necessity of exchanged fields with spin higher than 1, such that the whole sum on the LHS of (2.102) vanishes. Consequently, the discontinuity term will always dominate the conformal block in the Regge limit, such that we can ignore the other one.

Although (4.69) is valid in the region of $u \sim 0$ and $v \sim 1$, or equivalently $\sigma \sim 0$ and fixed t, it does not correspond to the Regge limit result because we have taken the limits in a certain order. Nevertheless, if we wish to obtain the conformal blocks in the Regge limit, we can use this result as boundary conditions for the Casimir differential equation near $\sigma \to 0$ and fixed t. In particular, the asymptotic behavior of the solution in the Regge limit must be $G^{\circlearrowleft}_{\mathcal{O}}(\sigma, t) \sim t^{\frac{\Delta-1}{2}}\, \sigma^{1-J}$. In general, the conformal block will be given by:

$$G^{\circlearrowleft}_{\mathcal{O}}(\sigma, t) \sim t^{\frac{\Delta-1}{2}} \sigma^{1-J}\, g(t)\,, \tag{4.70}$$

where the function $g(t)$ can be found by solving the Casimir equation. Near $\sigma \sim 0$ and fixed t, the Casimir operator expressed in terms of these cross ratios becomes:

$$\frac{2\,t\,(4 - d(1+t))}{1-t}\,\partial_t + 4\,t^2\,\partial_t^2 + \sigma\,\left((1-d)\,\partial_\sigma + \sigma\,\partial_\sigma^2\right)\,. \tag{4.71}$$

Inserting (4.70) in the Casimir differential equation and imposing the aforementioned boundary conditions, we find the solution:

$$G^{\circlearrowleft}_{\mathcal{O}}(\sigma, t) = -\left(-\tfrac{1}{2}\right)^J\, C_0\, t^{\frac{\Delta-1}{2}} \sigma^{1-J}\, {}_2F_1\left(\frac{d}{2} - 1, \Delta - 1, \Delta - \frac{d}{2} + 1, t\right)\,, \tag{4.72}$$

which corresponds precisely to the scalar conformal block in the Regge limit. The main aspect to notice about this expression is the σ^{1-J} behavior, which is characteristic of the Regge limit. Indeed, taking into account the relation between σ and the cross-ratios $z, \bar{z}$, one can see that this factor of σ^{1-J} was already present in (3.19), which makes sense, as this equation describes the four point function in the Regge limit in an integral representation. Therefore, we anticipate this dependence on σ for the upcoming results.

Now that we have demonstrated the different approaches to obtain the blocks in the case of the scalar four point function, we are ready to proceed to spinning correlators. In general, the analysis will not differ much from what was done here. However, for these cases the basic building blocks will make their appearance, in order to encode the spins of the external operators.

4.3.2 Spin J_1-Scalar-Scalar-Scalar

We begin by considering the case of a four point-function with one nonzero spin J_1 operator and three scalars. Although the discussion concerns the case of generic spin J_1, we we will mostly restrict to the case of $J_1 = 1$ to present the results.

In order to obtain the associated Casimir differential equation, it is essential to know the structure of the spinning correlator. Indeed, we are aware that correlation functions can generally be written as the product of a pre-factor, where the appropriate scaling weights are taken care of, and a linear combination of cross ratios functions. Moreover, given we are considering a spinning correlation function, we anticipate the basic building blocks (2.53) and (2.63) to appear. Accordingly, the conformal blocks will have a form like the sum over k in (4.56). Thus, this four point function ought to be given as [44]:

$$\langle \phi_1(P_1;Z_1)\phi_2(P_2)\phi_3(P_3)\phi_4(P_4)\rangle = \sum_{\mathcal{O}}\sum_{p} \lambda^{(p)}_{12\mathcal{O}}\lambda_{34\mathcal{O}}\, W^{(p)}_{\mathcal{O}}\left(P_i;Z_1\right) , \tag{4.73}$$

where the conformal partial waves are given by:

$$W^{(p)}_{\mathcal{O}}(P_i,Z_1) = \frac{\left(\frac{P_{24}}{P_{14}}\right)^{\frac{\Delta_{12}+J_1}{2}}\left(\frac{P_{14}}{P_{13}}\right)^{\frac{\Delta_{34}}{2}}}{(P_{12})^{\frac{\Delta_1+\Delta_2+J_1}{2}}(P_{34})^{\frac{\Delta_3+\Delta_4}{2}}}\sum_{s} G^{(p)}_{\mathcal{O},s}(u,v)\, Q^{(s)}(P_i;Z_1)\,. \tag{4.74}$$

Notice that we have two different labels in the above expressions. In particular, p labels the different structures of the three point function $\langle\phi_1(P_1;Z_1)\phi_2(P_2)\mathcal{O}(P;Z)\rangle$, where the exchanged operator must be in the symmetric and traceless representation of $SO(d)$, while s labels the independent tensor structures of the four point function.

For generic spin J_1, p can take $\min(J,J_1)+1$ values, whereas s can can be any of J_1+1 possibilities. In particular, each of these J_1+1 possible tensor structures for the four point function is given by:

$$Q^{(s)}\left(P_i;Z_1\right) = V^{J_1-s}_{1,23}\, V^{s}_{1,34}\,, \tag{4.75}$$

where $s\in\{0,\ldots,J_1\}$. Hence, the spinning conformal correlator can be written as:

$$\begin{aligned}&\langle \phi_1(P_1;Z_1)\phi_2(P_2)\phi_3(P_3)\phi_4(P_4)\rangle = \\ &\frac{\left(\frac{P_{24}}{P_{14}}\right)^{\frac{\Delta_{12}+J_1}{2}}\left(\frac{P_{14}}{P_{13}}\right)^{\frac{\Delta_{34}}{2}}}{(P_{12})^{\frac{\Delta_1+\Delta_2+J_1}{2}}(P_{34})^{\frac{\Delta_3+\Delta_4}{2}}}\sum_{\mathcal{O}}\sum_{p,s}\lambda^{(p)}_{12\mathcal{O}}\lambda_{34\mathcal{O}}\, V^{J_1-s}_{1,23}\, V^{s}_{1,34}\, G^{(p)}_{\mathcal{O},s}(u,v)\,.\end{aligned} \tag{4.76}$$

Let us now restrict to $J_1 = 1$. For this case, p can only be one of two values, $p = 1, 2$. This, however, is only if one assumes that the exchanged operator has spin $J \geq 1$. For $J = 0$, only one of these two structures of the associated three point function remains.

Moreover, the only independent four point function tensor structures are:

$$Q^{(1)}\left(P_i;Z_1\right)=V_{1,23}\ ,\qquad Q^{(2)}\left(P_i;Z_1\right)=V_{1,34}\ . \tag{4.77}$$

Thus, the previous expression for the spinning correlator (4.76) becomes:

$$\begin{aligned}&\langle\phi_1(P_1;Z_1)\phi_2(P_2)\phi_3(P_3)\phi_4(P_4)\rangle=\\&\frac{\left(\frac{P_{24}}{P_{14}}\right)^{\frac{\Delta_{12}+J_1}{2}}\left(\frac{P_{14}}{P_{13}}\right)^{\frac{\Delta_{34}}{2}}}{(P_{12})^{\frac{\Delta_1+\Delta_2+J_1}{2}}(P_{34})^{\frac{\Delta_3+\Delta_4}{2}}}\sum_{\mathcal{O}}\sum_{p=1}^{2}\lambda^{(p)}_{12\mathcal{O}}\lambda_{34\mathcal{O}}\left(V_{1,23}\,G^{(p)}_{\mathcal{O},1}(u,v)+V_{1,34}\,G^{(p)}_{\mathcal{O},2}(u,v)\right)\ .\end{aligned} \tag{4.78}$$

We can choose to organize the above expression differently, namely by the tensor structures of the four point function. By doing so, we get:

$$\langle\phi_1(P_1;Z_1)\dots\phi_4(P_4)\rangle=\frac{\left(\frac{P_{24}}{P_{14}}\right)^{\frac{\Delta_{12}+J_1}{2}}\left(\frac{P_{14}}{P_{13}}\right)^{\frac{\Delta_{34}}{2}}}{(P_{12})^{\frac{\Delta_1+\Delta_2+J_1}{2}}(P_{34})^{\frac{\Delta_3+\Delta_4}{2}}}\sum_{\mathcal{O}}\left(V_{1,23}\,f_1(u,v)+V_{1,34}\,f_2(u,v)\right)\ , \tag{4.79}$$

with

$$f_1(u,v)=\sum_{p=1}^{2}\lambda^{(p)}_{12\mathcal{O}}\,\lambda_{34\mathcal{O}}\,G^{(p)}_{\mathcal{O},1}(u,v)\ ,\qquad f_2(u,v)=\sum_{p=1}^{2}\lambda^{(p)}_{12\mathcal{O}}\,\lambda_{34\mathcal{O}}\,G^{(p)}_{\mathcal{O},2}(u,v)\ . \tag{4.80}$$

4.3.2.1 From the Casimir differential equation

We have previously defined the Casimir differential operator as $\mathcal{C}\equiv-\frac{1}{2}L^2$, where the $(d+2)-$dimensional rotations generator L^{AB} was given in (4.6). However, in this case where one of the operators has non zero spin, we must instead use [44]:

$$L_i^{AB}=P_i^A\partial_{P_i}^B-P_i^B\partial_{P_i}^A+Z_i^A\partial_{Z_i}^B-Z_i^B\partial_{Z_i}^A\,, \tag{4.81}$$

which accounts for the Z_i encoding the spin. In particular, we will only need this expression for the generator acting at position $i=1$.

Thus, acting with $-\frac{1}{2}\left(L_1^{AB}+L_2^{AB}\right)\left(L_{1,AB}+L_{2,AB}\right)$ (where L_1^{AB} is given by (4.81) and L_2^{AB} by (4.6)) on the four point function (4.76), we obtain the desired Casimir differential equation for the spinning conformal blocks. For $J_1=1$, acting with the Casimir operator in (4.79) and separating the $V_{1,23}$ and $V_{1,34}$ dependence of the Casimir equation, we obtain two coupled differential equations for f_1 and f_2. These are given in appendix C.1 by (C.1) and (C.2).

In order to solve these differential equations and obtain the conformal blocks, we need to provide boundary conditions. For this, we will take the OPE $\phi_1\times\phi_2$, by making use of

the leading order (in x_{12}) OPE between two spinning operators [12]:

$$\begin{aligned}&\phi_1(x_1,z_1)\phi_2(x_2,z_2)\approx\\&\approx\frac{1}{J!(h-1)_J}\frac{\mathcal{O}(x_2,D_z)}{(x_{12})^{\frac{\Delta_1+\Delta_2-\tau+J_1+J_2}{2}}}\sum_p\lambda^{(p)}_{12\mathcal{O}}\,t^{(p)}_J(-x_{12},z,I(x_{12})\cdot z_1,z_2)\,,\end{aligned}\tag{4.82}$$

where $t^{(p)}_J$ are the tensor structures of the associated three point function $\langle\phi_1(x_1;z_1)\phi_2(x_2;z_2)\mathcal{O}(x;z)\rangle$, which we defined in (2.68), and the superscript p labels each of these structures and associated OPE coefficients as before.

In our case, this expression is even simpler because ϕ_2 is a scalar and as such there is no dependence on z_2. Moreover, one can easily check that we only have two independent tensor structures:

$$t^{(1)}_J(x_{12},z,z_1)\equiv(x_{12}\cdot z)^J\,(x_{12}\cdot z_1)\,,\quad t^{(2)}_J(x_{12},z,z_1)\equiv(x_{12}\cdot z)^{J-1}\,(z\cdot z_1)\,x_{12}^2\,.\tag{4.83}$$

Notice that, as stated above, for $J=0$ only $t^{(1)}_J(x_{12},z,z_1)$ exists.

Therefore, taking the aforementioned OPE in the four point function and replacing (4.83) in (4.82) we find:

$$\begin{aligned}W_{\mathcal{O}}(x_1,x_2,x_3,x_4)\underset{x_4\to\infty}{\sim}&\frac{1}{J!\,(h-1)_J}\frac{\lambda_{34\mathcal{O}}\;(x_{23}\cdot D_z)}{\left(x_{12}^2\right)^{\frac{\Delta_1+\Delta_2-\tau+1}{2}}\left(x_{23}^2\right)^{\frac{\Delta_3-\Delta_4+\bar\tau}{2}}}\\&\times\left(\lambda^{(1)}_{12\mathcal{O}}\,(x_{12}\cdot z)^J\,(x_{12}\cdot z_1)+\lambda^{(2)}_{12\mathcal{O}}\,(x_{12}\cdot z)^{J-1}\,(z\cdot z_1)\,x_{12}^2\right),\end{aligned}\tag{4.84}$$

where for simplicity we have used conformal symmetry to send the point x_4 to infinity in the last step. In order to proceed, we need to know how to act with the contracted Todorov operator in the z polynomial inside the brackets. In fact, there are two crucial equations for this purpose, which can be found in [11, 47], respectively:

$$\begin{aligned}&\pi_{a_1\dots a_J,b_1\dots b_J}=\frac{1}{J!(h-1)_J}D_{a_1}\dots D_{a_J}\,z_{b_1}\dots z_{b_J}\,,\\&x^{a_1}\dots x^{a_J}\,\pi^{b_1\dots b_J}_{a_1\dots a_J}\,y_{b_1}\dots y_{b_J}=c_{d,J}\left(x^2y^2\right)^{\frac{J}{2}}\,C_J^{h-1}\,(\hat x\cdot\hat y)\,,\end{aligned}\tag{4.85}$$

where $c_{d,J}\equiv\frac{J!}{2^J\,(h-1)_J}$. Combining both equations of (4.85), it is then straightforward to compute the action of $(x_{23}\cdot D_z)$ on the first term inside the parenthesis in (4.84). The second one, though, requires a clever manipulation, namely:

$$(x_{23}\cdot D_z)\,(x_{12}\cdot z)^{J-1}\,(z\cdot z_1)=\frac{1}{J}\,\frac{d}{dw}\Big[\,(x_{23}\cdot D_z)\left(z\cdot(x_{12}+w\,z_1)\right)^J\Big]\Big|_{w=0}\,,\tag{4.86}$$

where w is a parameter we have introduced, but that must be taken to zero at the end.

The term inside the brackets on the last line of this expressions can be treated similarly as the first term, by applying (4.85). Then, we must take the derivative of the outcome with respect to w and evaluate it at zero. Naturally, the result will contain derivatives of Gegenbauer polynomials.

After performing the aforementioned computations, the outcome is given by:

$$W_{\mathcal{O}}(x_1,x_2,x_3,x_4) \sim \frac{\lambda_{34\mathcal{O}}\, c_{d,J}}{\left(x_{12}^2\right)^{\frac{\Delta_1+\Delta_2-\Delta+1}{2}} \left(x_{23}^2\right)^{\frac{\Delta_3-\Delta_4+\Delta}{2}}} \times$$
$$\Bigg[\lambda^{(1)}_{12\mathcal{O}}\ (x_{12}\cdot z_1)\, C_J^{h-1}(\zeta) + \frac{\lambda^{(2)}_{12\mathcal{O}}}{(x_{12}^2)^{1/2}(x_{23}^2)^{1/2}} \Big((x_{12}\cdot z_1)\,(x_{12}^2)^{1/2}(x_{23}^2)^{1/2} C_J^{h-1}(\zeta) \tag{4.87}$$
$$+ \Big((x_{12}\cdot x_{23})(x_{12}\cdot z_1) + (x_{23}\cdot z_1)x_{12}^2\Big)\, C_J^{h-1\,\prime}(\zeta)\Big)\Bigg]\,,$$

where

$$\zeta = \tfrac{x_{12}\cdot x_{23}}{(x_{12}^2)^{1/2}(x_{23}^2)^{1/2}}\,, \tag{4.88}$$

and the prime in the last term denotes the derivative of the Gegenbauer polynomial with respect to its argument. Note that if written in terms of cross ratios and the basic building blocks, we could identify from (4.87) the exact expression for the leading order of the conformal blocks.

In order to obtain a simpler expression out of (4.87), we will consider the lightcone limit ($x_{12}^2 \to 0$), which will allow us to retain only the dominant term of the Gegenbauer polynomials. Moreover, within this limit, we will also expand around $v \sim 1$. This expansion not only simplifies the expressions, but also focuses on the exchanged primary, associated with the leading term in $(1-v)$. This allows us to fix the normalization of the conformal blocks, such as to be consistent with the normalization of the associated three point functions. The outcome of this procedure, will act as boundary conditions and later help us fix the solution of the Casimir equations.

Performing the aforementioned expansions, keeping terms up to subleading order, and expressing the obtained result in terms of the cross ratios and the basic building blocks,

we obtain:

$$
\begin{aligned}
&W_{\mathcal{O}}(x_1,x_2,x_3,x_4) \sim \\
&\frac{u^{\frac{\tau}{2}}\,\lambda_{34\mathcal{O}}}{2^J\,\left(x_{12}^2\right)^{\frac{\Delta_1+\Delta_2+1}{2}}\left(x_{13}^2\right)^{\frac{\Delta_3-\Delta_4}{2}}}\left[V_{1,23}\left(\lambda_{12\mathcal{O}}^{(1)}\left[(v-1)^J-\tfrac{J(J-1)}{J+h-2}\,u\,(v-1)^{J-2}\right]\right.\right. \\
&\left.\left.-\lambda_{12\mathcal{O}}^{(2)}\tfrac{2\,(J-1)}{J+h-2}\,u\,(v-1)^{J-2}\right)+V_{1,34}\,\left(\lambda_{12\mathcal{O}}^{(1)}\,u\,(v-1)^J+2\lambda_{12\mathcal{O}}^{(2)}\,u\,(v-1)^{J-1}\right)\right]\,.
\end{aligned}
\tag{4.89}
$$

Comparing this expression with (4.79), projected to the physical space and in the conformal frame where $x_4 \to \infty$, yields the following identification of f_1 and f_2:

$$
\begin{aligned}
f_1(u,v) &\underset{\substack{u\to 0\\ v\to 1}}{\sim} \lambda_{12\mathcal{O}}^{(1)}\,\lambda_{34\mathcal{O}}\left(u^{\frac{\tau}{2}}(\tfrac{1}{2}(v-1))^J-\tfrac{J(J-1)}{4(J+h-2)}\,u^{\frac{\tau+2}{2}}\,(\tfrac{1}{2}(v-1))^{J-2}\right) \\
&\qquad -\lambda_{12\mathcal{O}}^{(2)}\lambda_{34\mathcal{O}}\,\tfrac{J-1}{2(J+h-2)}\,u^{\frac{\tau+2}{2}}\,(\tfrac{1}{2}(v-1))^{J-2}\,, \\
f_2(u,v) &\underset{\substack{u\to 0\\ v\to 1}}{\sim} \lambda_{12\mathcal{O}}^{(1)}\lambda_{34\mathcal{O}}\,u^{\frac{\tau+2}{2}}\,(\tfrac{1}{2}(v-1))^J+\lambda_{12\mathcal{O}}^{(2)}\lambda_{34\mathcal{O}}\,u^{\frac{\tau+2}{2}}\,(\tfrac{1}{2}(v-1))^{J-1}\,.
\end{aligned}
\tag{4.90}
$$

Although these results concern the spinning case, it is interesting to notice that the leading term of f_1, i.e. $f_1(u,v) \sim u^{\frac{\tau}{2}}(v-1)^J$, behaves exactly like the leading order term of the scalar conformal block for $u \to 0$ (4.63), near $v \sim 1$. The reason why it is f_1 that satisfies this and not f_2, is because f_2 is subleading in u comparatively to f_1. In due turn, this difference between the two functions stems from the different dependencies in u of the structures they are associated with ($V_{1,23}$ with f_1 and $V_{1,34}$ with f_2). Indeed, taking into account the definition of these building blocks (2.65), one immediately sees that $V_{1,34}$ does not depend explicitly on $x_{12}^2 \sim u$, which is not the case for $V_{1,23}$. In order to compensate for this difference, such that the two terms inside brackets in (4.79) are of the same order in u, $f_2(u,v)$ needs to be subleading in comparison with $f_1(u,v)$. The importance of these two equations lies in their role as boundary conditions.

Let us return to the differential equations in the appendix C.1. Bearing in mind the asymptotic behavior of the functions $f_i(u,v)$ in (4.90), it is reasonable to propose the following ansatz:

$$
f_1(u,v)=\sum_{m=0}^{\infty}u^{\frac{\Delta-J}{2}+m}\,g_{\mathcal{O},m}^{(1)}(v)\,,\quad f_2(u,v)=\sum_{m=0}^{\infty}u^{\frac{\Delta-J+2}{2}+m}\,g_{\mathcal{O},m}^{(2)}(v)\,. \tag{4.91}
$$

Plugging these into the coupled differential equations and expanding them for small u, we find that up to subleading order, the only contributions come from $g_{\mathcal{O},0}^{(1)}(v)$, $g_{\mathcal{O},0}^{(2)}(v)$ and their derivatives. Initially, however, we restrict the analysis to leading order, since interestingly, one of the differential equations decouples and becomes a differential equation solely for

$g^{(1)}_{\mathcal{O},0}(v)$, as can be seen in (C.3). This was to be expected given that f_2 is an order higher in u than f_1.

In order to proceed, we once again make use of the asymptotics to specify the v dependence of $g^{(1)}_{\mathcal{O},0}(v)$:

$$g^{(1)}_{\mathcal{O},0}(v) = \sum_{k=0}^{\infty} c^{(1)}_{\mathcal{O},0,k}\ (1-v)^{J+k}\ . \tag{4.92}$$

Earlier in section 4.2.3, we saw that the conformal blocks could be expanded in terms of hypergeometric functions of $(1-v)$. Given the definition of this function, this corresponds to a series in powers of $(1-v)$, which is precisely what we are proposing. We then expect the coefficients $c^{(1)}_{\mathcal{O},0,k}$ to be such that (4.92) corresponds to a sum of hypergeometric functions.

Inserting the above definition for $g^{(1)}_{\mathcal{O},0}(v)$ in (C.3), we obtain an equation relating different coefficients $c^{(1)}_{\mathcal{O},0,k}$, from which we can extract the following recurrence relation:

$$\begin{aligned} c^{(1)}_{\mathcal{O},0,k} = \frac{1}{4k(\Delta+J+k-1)} \Big[&(\Delta_{12}-\Delta-J-2k+5)\,(\Delta+\Delta_{34}+J+2k-6)\,c^{(1)}_{\mathcal{O},0,k-2} \\ &+ \Big(18-11J+J^2+\Delta(2J+8k-11)+8\,J\,k+8k^2-26k+\Delta_{34}(\Delta+J+2k-1) \\ &+\Delta^2-\Delta_{12}\,(\Delta+\Delta_{34}+J+2k-2)\Big)\,c^{(1)}_{\mathcal{O},0,k-1}\Big] \end{aligned} \tag{4.93}$$

with

$$c^{(1)}_{\mathcal{O},0,k} = 0\ \ (k<0)\ \ ,\ \ c^{(1)}_{\mathcal{O},0,0} = \left(-\frac{1}{2}\right)^{J}\ \lambda^{(1)}_{12\mathcal{O}}\lambda_{34\mathcal{O}}\,. \tag{4.94}$$

Note that, after choosing an initial condition, the rest of the coefficients become completely fixed.

Next, we take the expansion in u to subleading order. Doing so, results in the differential equation (C.4) for $g^{(2)}_{\mathcal{O},0}(v)$, which is coupled to $g^{(1)}_{\mathcal{O},0}(v)$. However, since we known the expansion coefficients of the latter, we may proceed analogously, such as to obtain a recurrence relation for the expansion coefficients of $g^{(2)}_{\mathcal{O},0}(v)$ in terms of the coefficients $c^{(1)}_{\mathcal{O},0,k}$. From (4.90), it seems plausible to propose:

$$g^{(2)}_{\mathcal{O},0}(v) = \sum_{k=0}^{\infty} c^{(2)}_{\mathcal{O},0,k}\ (1-v)^{J-1+k}\ . \tag{4.95}$$

Replacing this in the differential equation (C.4), gives us the following recurrence relation for $c^{(2)}_{\mathcal{O},0,k}$:

$$
\begin{aligned}
&c^{(2)}_{\mathcal{O},0,k} = \\
&\tfrac{1}{2\,k(\Delta+J-1+k)}\left[(\Delta-\Delta_{34}+J+2k-2)c^{(1)}_{\mathcal{O},0,k-1}-(\Delta-\Delta_{12}+J+2k-5)c^{(1)}_{\mathcal{O},0,k-2}\right]\\
&+\tfrac{1}{4k(\Delta+J-1+k)}\left[\Big(14+J(J+8k-9)-22k+8k^2+\Delta^2+\Delta(2J+8k-9)+\right.\\
&+\Delta_{34}(\Delta+J+2k-3)-\Delta_{12}\left(\Delta+\Delta_{34}+J+2k-2\right)\Big)\,c^{(2)}_{\mathcal{O},0,k-1}\\
&\left.-\left(\Delta-\Delta_{12}+J+2k-5\right)\left(\Delta+\Delta_{34}+J+2k-4\right)c^{(2)}_{\mathcal{O},0,k-2}\right]\,,
\end{aligned}
\tag{4.96}
$$

with initial conditions:

$$
c^{(2)}_{\mathcal{O},0,k}=0\ \ (k<0)\ \ ,\ \ c^{(2)}_{\mathcal{O},0,0}=\left(-\frac{1}{2}\right)^{J-1}\lambda^{(2)}_{12\mathcal{O}}\lambda_{34\mathcal{O}}\,. \tag{4.97}
$$

Therefore, we get that in the lightcone limit ($u\to 0$) the functions f_1 and f_2 can be expanded as:

$$
f_1(u,v)\underset{u\to 0}{\sim}u^{\frac{\tau}{2}}\sum_{k=0}^{\infty}c^{(1)}_{\mathcal{O},0,k}\,(1-v)^{J+k}\ ,\quad f_2(u,v)\underset{u\to 0}{\sim}u^{\frac{\tau+2}{2}}\sum_{k=0}^{\infty}c^{(2)}_{\mathcal{O},0,k}\,(1-v)^{J-1+k}\ , \tag{4.98}
$$

with the coefficients given by (4.93) and (4.96).

To proceed, we would have to analytically continue the above equations. This is not straightforward, as the discontinuity does not commute with the sum. Alternatively, we could write these in some other representation, which would make the analytic continuation easier. In particular, we have seen in the scalar case (4.32) that at each order in u, we have a finite sum of hypergeometric functions. Therefore, it is natural to expect that the two sums in (4.98) are equivalent to a linear combination of some hypergeometrics. Indeed, as we will see next, this turns out to be true. After knowing the specific coefficients of this linear combination, it would be easier to analytically continue f_1 and f_2, given that we know the discontinuity of the hypergeometric (see appendix B). Afterwards, we would take the limit $v\to 1$, so as to obtain the boundary conditions for the Casimir differential equations. If considered in the region $u\sim 0$ and $v\sim 1$, these equations combined with the aforementioned boundary conditions, would give us the conformal blocks in the Regge limit. Expressing these functions in the σ,t cross ratios and bearing in mind the scalar result (4.72), one would expect to observe the characteristic σ^{1-J} behavior of the Regge limit in the function f_1, which is the leading order function. As for f_2, it would be one order higher.

4.3.2.2 From the action of differential operators

We will now compute the same conformal blocks by means of the procedure from section 4.2.4. In particular, we will stick to the case of $J_1 = 1$, such that we may compare with the results from the previous section.

The starting point of this method, is to figure out all the possible differential operators we must act accordingly to (4.53), in order to obtain the desired conformal partial waves. In our case, we only have to act with $\mathcal{D}_{\text{left}}$, since $\mathcal{D}_{\text{right}}$ acts on positions x_3 and x_4, where we have scalars. It is not difficult to see that there are only two possibilities for $\mathcal{D}_{\text{left}}$ in this case:

$$\mathcal{D}_{11}\, W_{\mathcal{O}}^{1,0}\,, \qquad \mathcal{D}_{12}\, W_{\mathcal{O}}^{0,1}\,, \tag{4.99}$$

where $W_{\mathcal{O}}^{k_1,k_2}$ is the scalar conformal partial wave with the appropriate shifts in the external conformal dimensions Δ_1 and Δ_2.

The two quantities of (4.99) are simple to obtain, given that we have the definition of the D_{ij} operators in (4.47). Thus, acting with these operators and expressing the outcome in terms of cross ratios and the basic building blocks, and excluding the pre-factors, we get:

$$\begin{aligned}
F^{(1)}(u,v;V_{i,jk}) &= -\frac{v}{2}V_{1,23}\left((1+\Delta_{12})G_{\mathcal{O}}^{1,0}(u,v)+2(1-v)\partial_v G_{\mathcal{O}}^{1,0}(u,v)-2u\partial_u G_{\mathcal{O}}^{1,0}(u,v)\right)\\
&-\frac{1}{2}\,u\,V_{1,34}\left((1+\Delta_{12})\,G_{\mathcal{O}}^{1,0}(u,v)-2\,v\,\partial_v\,G_{\mathcal{O}}^{1,0}(u,v)-2\,u\,\partial_u\,G_{\mathcal{O}}^{1,0}(u,v)\right)\,,\\
F^{(2)}(u,v;V_{i,jk}) &= \frac{1}{2}\,v\,V_{1,23}\left((\Delta_{12}-1)\,G_{\mathcal{O}}^{0,1}(u,v)+2\,u\,\partial_u\,G_{\mathcal{O}}^{0,1}(u,v)\right)\\
&-\frac{1}{2}\,u\,V_{1,34}\left((1-\Delta_{12}+\Delta_{34})\,G_{\mathcal{O}}^{0,1}(u,v)-2\,v\,\partial_v\,G_{\mathcal{O}}^{0,1}(u,v)\right)\,,
\end{aligned} \tag{4.100}$$

where we have respectively designated $\mathcal{D}_{11}\, W_{\mathcal{O}}^{1,0}$ and $\mathcal{D}_{12}\, W_{\mathcal{O}}^{0,1}$, up to the pre-factor, by $F^{(1)}(u,v;V_{i,jk})$ and $F^{(2)}(u,v;V_{i,jk})$. Similarly to the notation used for the conformal partial waves, $G_{\mathcal{O}}^{k_1,k_2}(u,v)$ denotes the scalar conformal block with shifts in the external conformal dimensions, $\Delta_1 \to \Delta_1 + k_1$ and $\Delta_2 \to \Delta_2 + k_2$.

In order to identify the functions f_1 and f_2 of (4.79) from the two quantities in (4.100), we first have to express F_1 and F_2 in the standard basis. To do this, we first recognize that up to a pre-factor, the conformal partial wave in the standard basis is going to be given by a linear combination of F_1 and F_2:

$$a_1\, F^{(1)}(u,v;V_{i,jk}) + a_2\, F^{(2)}(u,v;V_{i,jk})\,, \tag{4.101}$$

given that standard basis elements can be expressed in the differential basis, according to the inverse relation of (4.49).

As already explained above (4.100), the coefficients a_1 and a_2 can be found from the relation between the three point function $\langle\phi_1(P_1;Z_1)\phi_2(P_2)\mathcal{O}(P)\rangle$ (which is one of the couplings characterizing the conformal partial wave) in the differential basis and the standard basis. In particular, these can be fixed by imposing the following equality:

$$\langle\phi_1(P_1;Z_1)\phi_2(P_2)\mathcal{O}(P_3)\rangle = a_1 D_{11}\begin{bmatrix}\Delta_1+1 & \Delta_2 & \Delta\\ 0 & 0 & J\\ 0 & 0 & 0\end{bmatrix} + a_2 D_{12}\begin{bmatrix}\Delta_1 & \Delta_2+1 & \Delta\\ 0 & 0 & J\\ 0 & 0 & 0\end{bmatrix} \Leftrightarrow \tag{4.102}$$
$$\lambda^{(1)}_{12\mathcal{O}}\begin{bmatrix}\Delta_1 & \Delta_2 & \Delta\\ 1 & 0 & J\\ 0 & 0 & 0\end{bmatrix} + \lambda^{(2)}_{12\mathcal{O}}\begin{bmatrix}\Delta_1 & \Delta_2 & \Delta\\ 1 & 0 & J\\ 0 & 1 & 0\end{bmatrix} = a_1\begin{Bmatrix}\Delta_1 & \Delta_2 & \Delta\\ 1 & 0 & J\\ 0 & 0 & 0\end{Bmatrix} + a_2\begin{Bmatrix}\Delta_1 & \Delta_2 & \Delta\\ 1 & 0 & J\\ 0 & 1 & 0\end{Bmatrix}.$$

Since we know how to write the standard basis elements from (4.43) and also how to act with the differential operators, we can easily write (4.102) in the embedding space, from which we find the coefficients to be given by:

$$a_1 = \frac{2\,J\,\lambda^{(1)}_{12\mathcal{O}} + \lambda^{(2)}_{12\mathcal{O}}\,(1-\Delta+J-\Delta_{12})}{2\,J(\Delta-1)}\,,\quad a_2 = \frac{2\,J\,\lambda^{(1)}_{12\mathcal{O}} - \lambda^{(2)}_{12\mathcal{O}}\,(1-\Delta-J+\Delta_{12})}{2\,J(\Delta-1)}\,. \tag{4.103}$$

Replacing these in (4.101) and comparing with (4.79), we identify the functions f_1 and f_2:

$$\begin{aligned} f_1(u,v) = \frac{v}{4J(\Delta-1)}\Big[&\Big(2J\lambda^{(1)}_{12\mathcal{O}} - (1-\Delta-J+\Delta_{12})\lambda^{(2)}_{12\mathcal{O}}\Big)\Big((\Delta_{12}-1)G^{0,1}_{\mathcal{O}} + 2u\,\partial_u G^{0,1}_{\mathcal{O}}\Big)\\ &-\Big(2J\lambda^{(1)}_{12\mathcal{O}} + (1-\Delta+J-\Delta_{12})\lambda^{(2)}_{12\mathcal{O}}\Big)\Big((1+\Delta_{12})\,G^{1,0}_{\mathcal{O}}(u,v) + 2(1-v)\,\partial_v G^{1,0}_{\mathcal{O}}\\ &-2u\,\partial_u G^{1,0}_{\mathcal{O}}\Big)\Big]\,, \end{aligned} \tag{4.104}$$

$$\begin{aligned} f_2(u,v) = \frac{u}{4J(\Delta-1)}\Big[&\Big(2J\lambda^{(1)}_{12\mathcal{O}} - (1-\Delta-J+\Delta_{12})\lambda^{(2)}_{12\mathcal{O}}\Big)\Big((\Delta_{12}-\Delta_{34}-1)G^{0,1}_{\mathcal{O}}\\ &-2v\partial_v G^{0,1}_{\mathcal{O}}\Big) - \Big(2J\lambda^{(1)}_{12\mathcal{O}} + (1-\Delta+J-\Delta_{12})\lambda^{(2)}_{12\mathcal{O}}\Big)\Big((1+\Delta_{12})\,G^{1,0}_{\mathcal{O}}\\ &-2v\,\partial_v G^{1,0}_{\mathcal{O}} - 2u\,\partial_u G^{1,0}_{\mathcal{O}}\Big)\Big]\,, \end{aligned} \tag{4.105}$$

where for simplicity, we have suppressed the dependency of the conformal blocks in the cross ratios.

We could now test whether or not (4.104) and (4.105) are consistent with the results we obtained from the Casimir equation in the previous section. For this, we consider the limit $u \to 0$, where the leading term of the scalar conformal block is given by (4.63).

First, we found by expanding (4.104) and (4.105) for small u, keeping only leading order terms, and considering these expressions near $v \sim 1$, that we obtain the same asymptotics

for $f_1(u,v)$ and $f_2(u,v)$ as the ones in (4.90).

Additionally, we have also replaced the scalar conformal block in (4.104) and (4.105) by (4.63), taking into account the dimension shifts, and expanded the expressions around $v \sim 1$. Doing so, we have confirmed that the coefficients of this expansion satisfied precisely the recurrence relations of (4.93) and (4.96), which we had found previously for the expansion in powers of $(1-v)$. Given that the scalar conformal block is given in terms of a hypergeometric function, this confirms our previous suspicion that the coefficients $c^{(i)}_{\mathcal{O},0,k}$ $(i=1,2)$, give a sum of hypergeometric functions of argument $(1-v)$ in (4.92) and (4.95).

Therefore, we are confident that we have obtained the same expansion of the conformal blocks in the limit $u \to 0$, as the one in (4.98). This demonstrates the coherence between both approaches.

Next, we will analytically continue the functions $f_i(u,v)$, to later analyze them in the Regge limit. We start by expressing (4.104) and (4.105) more compactly as:

$$f_i(u,v) = \mathcal{D}_i\, G_{\mathcal{O}}(u,v) \quad , \quad i=1,2 \ , \tag{4.106}$$

where $\mathcal{D}_i$ are differential operators, which also encode the necessary dimensions shifts in the scalar conformal blocks. Because the analytical continuation path we consider here, is the one represented in figure 4.5, we will most likely pick up a discontinuity. Consequently, when analytic continued, these functions gain an extra term:

$$f_i^{\circlearrowleft}(u,v) = \mathcal{D}_i\, G_{\mathcal{O}}(u,v) + \text{Disc}\left[\mathcal{D}_i G_{\mathcal{O}}(u,v)\right] \ . \tag{4.107}$$

Computing the above discontinuity could in practice be something non trivial. However, we have verified for a few cases, namely for hypergeometric functions, that the discontinuity commutes with derivatives. Therefore, because the scalar conformal block consists on a hypergeometric function and other terms without discontinuities, these two things commute:

$$\text{Disc}\left[\mathcal{D}_i G_{\mathcal{O}}(u,v)\right] = \mathcal{D}_i \left(\text{Disc}\left[G_{\mathcal{O}}(u,v)\right]\right) \ . \tag{4.108}$$

Moreover, it was seen before that the discontinuity term dominates in the Regge limit. Therefore, we can ignore the first term in the RHS of (4.107), such that the analytically continued $f_i(u,v)$'s are given by:

$$f_i^{\circlearrowleft}(u,v) = \mathcal{D}_i \left(\text{Disc}\ \left[G_{\mathcal{O}}(u,v)\right]\right) \ . \tag{4.109}$$

We could now think that, since we know the discontinuity of the scalar conformal block in the Regge limit, we could replace it in the above expression and obtain the $f_i(u,v)$ in the same limit. It turns out this is doable in our case, although the reason is not trivial. Note, however, that this is not valid in every case, such that caution is needed. Indeed, let us analyze the differential operators $\mathcal{D}_i$ expressed in the σ, t cross-ratios. Each of these can be separated according to:

$$\begin{aligned}\mathcal{D}_1 &= \mathcal{D}_1^{(0)} + \mathcal{D}_1^{(1)} \\ \mathcal{D}_2 &= \mathcal{D}_2^{(1)} + \mathcal{D}_2^{(2)} ,\end{aligned} \tag{4.110}$$

where the upper label in each $D_i^{(j)}$, denotes by how much the differential operator raises the degree in σ. In turn, these are given as

$$\mathcal{D}_1^{(0)} = \frac{1}{4J(\Delta-1)} \left\{ a\,(\Delta_{12}-1+\sigma\partial_\sigma+2t\partial_t)\,\Sigma^{0,1} - b\,(\Delta_{12}+1+\sigma\partial_\sigma-2t\partial_t)\,\Sigma^{1,0} \right\} , \tag{4.111}$$

$$\mathcal{D}_1^{(1)} = -\frac{\sigma}{\sqrt{t}}\,\mathcal{D}_1^{(0)} , \qquad \mathcal{D}_2^{(1)} = \frac{t^{\frac{3}{2}}\,\sigma}{J(\Delta-1)} \left\{ -a\,\partial_t\,\Sigma^{0,1} + b\,\partial_t\,\Sigma^{1,0} \right\} , \tag{4.112}$$

$$\mathcal{D}_2^{(2)} = \frac{\sigma^2}{4J(\Delta-1)} \left\{ a\,(\Delta_{12}-\Delta_{34}-1+4t\partial_t)\,\Sigma^{0,1} + b\,(\Delta_{12}+1-\sigma\partial_\sigma+2t\partial_t)\,\Sigma^{1,0} \right\} , \tag{4.113}$$

where we have made the following definitions for convenience:

$$a = 2\,J\,\lambda_{12\mathcal{O}}^{(1)} + (\bar{\tau}-\Delta_{12}-1)\,\lambda_{12\mathcal{O}}^{(2)} , \qquad b = 2\,J\,\lambda_{12\mathcal{O}}^{(1)} - (\tau+\Delta_{12}-1)\,\lambda_{12\mathcal{O}}^{(2)} , \tag{4.114}$$

and we recall that Σ^{k_1,k_2} denotes the shifts in the external dimensions $\Delta_{1,2}$.

Looking carefully at these expressions, we observe that the differential operators either keep or raise the degree in σ but never decrease it. Crucially, this trait of the operators is what makes it valid to replace Disc $G_{\mathcal{O}}$ by its Regge limit behavior (4.72). Indeed, taking into the account the leading behavior of the scalar conformal block in the Regge limit, it is reasonable to say that the functions $f_i^{\circlearrowleft}$ can be given as:

$$f_i^{\circlearrowleft}(\sigma,t) = \mathcal{D}_i \sum_{m=0}^{\infty} \sigma^{1-J+m}\, g_m(t) , \tag{4.115}$$

where $g_m(\xi)$ are some functions of the fixed cross-ratio t. In particular, $g_0(t)$ is found by changing the t dependence of (4.72) to t.

Now, as we have seen, the differential operators either keep or increase the degree in σ. Therefore, we have:

$$\begin{aligned} f_1^{\circlearrowleft}(\sigma,t) &= \left(\mathcal{D}_1^{(0)} + \mathcal{D}_1^{(1)}\right) \sigma^{1-J} \left(g_0(t) + \sigma\, g_1(t) + \dots\right) , \\ f_2^{\circlearrowleft}(\sigma,t) &= \left(\mathcal{D}_2^{(1)} + \mathcal{D}_2^{(2)}\right) \sigma^{1-J} \left(g_0(t) + \sigma\, g_1(t) + \dots\right) . \end{aligned} \tag{4.116}$$

In the Regge limit, where we take $\sigma \to 0$, the leading order terms in these functions are:

$$f_1^{\circlearrowleft}(\sigma,t) \underset{\sigma\to 0}{\sim} \mathcal{D}_1^{(0)}\,\sigma^{1-J} g_0(t)\ , \quad f_2^{\circlearrowleft}(\sigma,t) \underset{\sigma\to 0}{\sim} \mathcal{D}_2^{(1)}\,\sigma^{1-J} g_0(t)\ . \tag{4.117}$$

The term $\sigma^{1-J}\, g_0(t)$, however, is precisely the Regge behavior of Disc $G_{\mathcal{O}}(\sigma,t)$.

Thus, by making this replacement and keeping only the leading term of the differential operators $D_i^{(j)}$, we find the leading behavior of $f_i^{\circlearrowleft}(\sigma,t)$ in the Regge limit to be:

$$\begin{aligned} f_1^{\circlearrowleft}(\sigma,t) \approx \frac{\sigma^{1-J}\, t^{\frac{\Delta-1}{2}}}{2J} \Bigg\{ & t\,\frac{(d-2)(a\,\tilde{C}_{-1} - b\,\tilde{C}_1)}{2(\Delta+1)-d}\,{}_2F_1\left(\frac{d}{2},\Delta,\Delta-\frac{d}{2}+2,t\right) \\ & + \frac{a\,(\tau+\Delta_{12}-1)\,\tilde{C}_{-1} - b\,(\bar{\tau}+\Delta_{12}-1)\,\tilde{C}_1}{2(\Delta-1)}\,{}_2F_1\left(\frac{d}{2}-1,\Delta-1,\Delta-\frac{d}{2}+1,t\right)\Bigg\}\ , \end{aligned} \tag{4.118}$$

and

$$\begin{aligned} f_2^{\circlearrowleft}(\sigma,t) \approx \frac{\sigma^{2-J}\, t^{\frac{\Delta}{2}}}{2J}\,\left(b\,\tilde{C}_1 - a\,\tilde{C}_{-1}\right) \Bigg\{ & {}_2F_1\left(\frac{d}{2}-1,\Delta-1,\Delta-\frac{d}{2}+1,t\right) \\ & + t\,\frac{2(d-2)}{2(\Delta+1)-d}\,{}_2F_1\left(\frac{d}{2},\Delta,\Delta-\frac{d}{2}+2,t\right)\Bigg\}\ , \end{aligned} \tag{4.119}$$

where:

$$\tilde{C}_{k_{12}} = (-1)^{J+1} 2^{1-\tilde{\tau}}\, C_{k_{12}}\ , \tag{4.120}$$

with $C_{k_{12}}$ defined in (4.67).

Looking at the above equations for the f_i functions, we detect once again the characteristic leading order behavior of the Regge limit σ^{1-J}, and f_2 being subleading in σ (or equivalently u) with respect to f_1, by the same reasons we gave below (4.90). These two properties are also expected to be found in the results obtained in the last subsection, namely (4.98), since as previously mentioned, we checked that the expansion coefficients of (4.104) and (4.105) obeyed the recurrence relations (4.93) and (4.96).

4.3.2.3 From the lightcone expansion

We will now obtain the conformal blocks of the same spinning four point function, by taking the Lorentzian lightcone OPE (2.94). We will keep the discussion for generic spin J_1.

We start by performing the OPE $\phi_3 \times \phi_4$ between the two scalar operators. Similarly to the scalar correlator, the resulting integral defines a hypergeometric function whose arguments are easily identified. Moreover, given that a spinning three point function arises from the OPE, we will need to have a sum over the possible three-point structures. In

particular, we will only need one sum over ℓ, labeling these structures, as the correlator is of the type spin J_1 − scalar − spin J. After undergoing all of these steps, the four point function can be organized as:

$$\langle \phi_1(x_1,z_1)\,\phi_2(x_2)\,\phi_3(x_3)\,\phi_4(x_4)\rangle \approx \\ \frac{\left(\frac{x_{24}^2}{x_{14}^2}\right)^{\frac{\bar\tau_{12}}{2}}\left(\frac{x_{14}^2}{x_{13}^2}\right)^{\frac{\bar\tau_{34}}{2}}}{\left(x_{12}^2\right)^{\frac{\bar\tau_1+\bar\tau_2}{2}}\left(x_{34}^2\right)^{\frac{\bar\tau_3+\bar\tau_4}{2}}}\sum_{\mathcal{O}}\sum_{\ell=0}^{\min(J_1,J)}\lambda_{12\mathcal{O}}^{(\ell+1)}\,\lambda_{34\mathcal{O}}\,G_{\mathcal{O}}^{(\ell+1)}(u,v;V_{i,jk},H_{ij})\ . \tag{4.121}$$

Note that in contrast with expression (4.74), where we separated the cross ratios function $G_{\mathcal{O},s}(u,v)$ from the structures $Q^{(s)}(P_i;Z_i)$, here we denote everything by $G_{\mathcal{O}}^{(\ell)}(u,v;V_{i,jk},H_{ij})$. These functions, which include both the dependence on the cross ratios and the independent tensor structures of the four point function, are the conformal blocks, in accordance with what was said below (4.56). Moreover, notice the label of the OPE coefficients and the conformal blocks, which we chose to be $\ell+1$ rather than ℓ. This was done in order to maintain consistency with all of the above results, where we have labeled the three point structures with p and started at $p=1$ (see 4.73 for example).

By undertaking the aforementioned steps, we found that these conformal blocks are given by:

$$G_{\mathcal{O}}^{(\ell+1)}(u,v;V_{i,jk},H_{ij}) = \tag{4.122}$$
$$\sum_{m=0}^{J_1-\ell}\sum_{n=0}^{J_1-\ell-m}V_{1,23}^{J_1-\ell-n}\,V_{1,34}^{\ell+n}\,\frac{(-\frac{1}{2})^J\left(\frac{\bar\tau+\Delta_{34}}{2}\right)_m\left(\frac{\bar\tau-\Delta_{34}}{2}\right)_{J_1-\ell-m}}{(\bar\tau)_{J_1-\ell}}\binom{J_1-\ell}{m}\binom{J_1-\ell-m}{n}$$
$$\times\ u^{\frac{\tau}{2}+\ell+n}\,(1-v)^{J-\ell}\,v^{J_1-\ell-n}\,{}_2F_1\left(\tfrac{\bar\tau+J_1-\Delta_{12}}{2}-\ell,\tfrac{\bar\tau+\Delta_{34}}{2}+m,\bar\tau+J_1-\ell,1-v\right)\ .$$

There are a few things in the above expression worth being noted. The first is that the sums in m and n resulted from the binomial expansion of terms with $V_{1,23}$, $V_{1,34}$ and the cross ratios. Additionally, we observe that the combined exponents of both $V_{1,23}$ and $V_{1,34}$ is such that z_1 has degree J_1. This had to be the case in order for the result to be consistent with the formalism of the null polarization vectors.

As usual, we now analytically continue this result, by following the same reasoning of the scalar case. In particular, we first take v to go around 0 and then take $v\sim 1$, such that we find ourselves in the region of the Regge limit ($u\to 0$, $v\to 1$). Afterwards, we keep only the discontinuity term, which dominates in the Regge limit, and express the result in the

σ, t cross ratios. Doing so we find:

$$G_{\mathcal{O}}^{\circlearrowleft(\ell+1)}(\sigma,t;V_{i,jk},H_{ij}) = \sum_{m=0}^{J_1-\ell}\sum_{n=0}^{J_1-\ell-m} V_{1,23}^{J_1-\ell-n}\, V_{1,34}^{\ell+n}\, A_{m,n}^{(\ell)} \\ \times\, t^{\frac{\Delta+J_1-1}{2}}\,\sigma^{1-J-J_1+2\ell+2n}\sum_{k=0}^{k_{\max}} B_k^{(\ell)}\left(\frac{\sigma}{\sqrt{t}}\right)^k , \tag{4.123}$$

where

$$A_{m,n}^{(\ell)} = (-\tfrac{1}{2})^J\,\frac{\left(\frac{\bar\tau+\Delta_{34}}{2}\right)_m\left(\frac{\bar\tau-\Delta_{34}}{2}\right)_{J_1-\ell-m}}{(\bar\tau)_{J_1-\ell}}\binom{J_1-\ell}{m}\binom{J_1-\ell-m}{n} \\ \times\,\frac{2\pi i\,(-1)^{\frac{J_1+\Delta_{12}-\Delta_{34}}{2}-m-1}\,\Gamma(\bar\tau+J_1-\ell)\,\Gamma(\bar\tau+J_1-\ell-1)}{\Gamma\!\left(\frac{\bar\tau+J_1+\Delta_{12}}{2}\right)\Gamma\!\left(\frac{\bar\tau+J_1-\Delta_{12}}{2}-\ell\right)\Gamma\!\left(\frac{\bar\tau-\Delta_{34}}{2}+J1-\ell-m\right)\Gamma\!\left(\frac{\bar\tau+\Delta_{34}}{2}+m\right)} , \tag{4.124}$$

$$B_k^{(\ell)} = \frac{\left(\frac{\bar\tau+J_1+\Delta_{12}}{2}-1\right)_k\left(\frac{\bar\tau-\Delta_{34}}{2}+J_1-\ell-m-1\right)_k}{k!\,(\bar\tau+J_1-\ell-2)_k} , \quad k_{\max} = \frac{\Delta_{34}-\Delta_{12}-J_1+2m-2}{2} . \tag{4.125}$$

Notice, in the last line of (4.123), that we have kept several orders in σ. In due turn, these stemmed from the choice of also keeping several orders in the expansion around $v \sim 1$ of the hypergeometric emerging in the analytic continuation (see section 4.3.1.2). This is necessary because the sums over m and n of the first leading order terms vanish for some of the cross ratios functions multiplying the structures. In particular, the subleading order up to which we must take this expansion, such that we can obtain the leading behavior of all of these cross ratios functions, depends on J_1. In reality, because some of the terms in the above expression are actually zero when we take the sums, we should find a better formula that already accounts for this. Unfortunately, there was not enough time to do this, such that it remains a goal for the future.

To test this expression, we could set $J_1 = 1$ and see if it is consistent with the previous results. Indeed, this expression predicts $f_1(\sigma,t) \sim t^{\frac{\Delta-1}{2}}\sigma^{1-J}$ and $f_2(\sigma,t) \sim t^{\frac{\Delta}{2}}\,\sigma^{2-J}$, which is precisely the leading behavior obtained with the differential operators method (see (4.118) and (4.119)).

However, recall that the above result only serves as boundary conditions, which we could use to fix the solutions of the corresponding Casimir differential equations in the Regge limit. Here we will refrain from undertaking this procedure as the computations are too extensive. Nonetheless, by the same reasoning of (4.70), we expect each cross ratios function multiplying a structure, to have the same leading σ dependence we found here, combined with a function of the fixed cross ratio t.

4.3.3 Spin J_1-Spin J_2-Scalar-Scalar

The last case we will consider here, is the generic four-point function of two nonzero spin operators and two scalars, $\langle\phi_1(x_1;z_1)\phi_2(x_2;z_2)\phi_3(x_3)\phi_4(x_4)\rangle$. We will only compute the spinning conformal blocks by applying the Lorentzian lightcone OPE (2.94), as the necessary computations for generic spins are simpler than the ones for the Casimir equation procedure. Moreover, we do not consider the differential operators method as it would require us to specify the spins of the external operators.

4.3.3.1 With the Lorentzian lightcone OPE

The procedure is equivalent to what was done in the case of one external spinning operator. The only difference is that the spinning three point function resulting from the OPE $\phi_3\times\phi_4$ is of the type spin J_1 − spin J_2 − spin J, such that we will have a sum over three indices, ℓ_0,ℓ_1,ℓ_2, instead of just one.

By undertaking the same kind of steps, we find that this correlator can be written as:

$$\langle\phi_1(x_1,z_1)\,\phi_2(x_2,z_2)\,\phi_3(x_3)\,\phi_4(x_4)\rangle \approx \frac{\left(\frac{x_{24}^2}{x_{14}^2}\right)^{\frac{\bar\tau_{12}}{2}}\left(\frac{x_{14}^2}{x_{13}^2}\right)^{\frac{\bar\tau_{34}}{2}}}{\left(x_{12}^2\right)^{\frac{\bar\tau_1+\bar\tau_2}{2}}\left(x_{34}^2\right)^{\frac{\bar\tau_3+\bar\tau_4}{2}}}\times$$
$$\sum_{\mathcal{O}}\sum_{\ell_0=0}^{\min(J_1,J_2)}\sum_{\ell_1=0}^{\min(J,J_2)}\sum_{\ell_2=0}^{\min(J,J_1)}\lambda_{12\mathcal{O}}^{(\tilde\ell_0,\tilde\ell_1,\tilde\ell_2)}\,\lambda_{34\mathcal{O}}\,G_{\mathcal{O}}^{(\tilde\ell_0,\tilde\ell_1,\tilde\ell_2)}(u,v;V_{i,jk},H_{ij})\ , \tag{4.126}$$

where $\tilde\ell_i=\ell_i+1$ and the conformal blocks are given by:

$$\begin{aligned}
&G_{\mathcal{O}}^{(\tilde\ell_0,\tilde\ell_1,\tilde\ell_2)}(u,v;V_{i,jk},H_{ij}) = \qquad (4.127)\\
&\sum_{m=0}^{J_1-\ell_0-\ell_2}\sum_{n=0}^{J_1-\ell_0-\ell_2-m}\sum_{p=0}^{J_2-\ell_0-\ell_1}\sum_{q=0}^{\ell_1} H_{12}^{\ell_0}\,V_{1,23}^{J_1-\ell_0-\ell_2-n}\,V_{1,34}^{l_2+n}\,V_{2,13}^{p+q}\,V_{2,14}^{J_2-\ell_0-p-q}\\
&\times\binom{J_1-\ell_0-\ell_2}{m}\binom{J_1-\ell_0-\ell_2-m}{n}\binom{J_2-\ell_0-\ell_1}{p}\binom{\ell_1}{q}\\
&\times(-1)^{\ell_0+\ell_1-J_2-q}(-\tfrac{1}{2})^{J}\,\frac{\left(\frac{\bar\tau-\Delta_{34}}{2}\right)_{J_1+J_2-2\ell_0-\ell_1-\ell_2-m-p}\left(\frac{\bar\tau+\Delta_{34}}{2}\right)_{m+p}}{(\bar\tau)_{J_1+J_2-2\ell_0-\ell_1-\ell_2}}\\
&\times v^{J_1-\ell_0+\ell_1-\ell_2-n-q}\,u^{\frac{\tau}{2}+\ell_2+n}\,(1-v)^{J-\ell_1-\ell_2}\\
&\times{}_2F_1\left(\tfrac{\bar\tau-\Delta_{12}+J_1+J_2}{2}-\ell_0-\ell_2,\tfrac{\bar\tau+\Delta_{34}}{2}+m+p,\bar\tau+J_1+J_2-2\ell_0-\ell_1-\ell_2,1-v\right)\ .
\end{aligned}$$

Once again, we now analytically continue this expression and keep only the discontinuity terms. Expanding around $v \sim 1$ and expressing the result in the cross ratios σ, t, we find:

$$\begin{aligned} &G_{\mathcal{O}}^{\circlearrowleft(\tilde{\ell}_0,\tilde{\ell}_1,\tilde{\ell}_2)}(u,v;V_{i,jk},H_{ij}) = \\ &\sum_{m=0}^{J_1-\ell_0-\ell_2}\sum_{n=0}^{J_1-\ell_0-\ell_2-m}\sum_{p=0}^{J_2-\ell_0-\ell_1}\sum_{q=0}^{\ell_1} H_{12}^{\ell_0}\, V_{1,23}^{J_1-\ell_0-\ell_2-n}\, V_{1,34}^{\ell_2+n}\, V_{2,13}^{p+q}\, V_{2,34}^{J_2-\ell_0-p-q} \\ &\times\ \tilde{A}^{(\ell_0,\ell_1,\ell_2)}_{m,n,p,q}\, t^{\frac{\Delta+J_1+J_2-2\ell_0-1}{2}}\sigma^{1-J-J_1-J_2+2\ell_0+2\ell_2+2n}\sum_{k=0}^{k_{\max}}\tilde{B}_k^{(\ell_0,\ell_1,\ell_2)}\left(\frac{\sigma}{\sqrt{t}}\right)^k , \end{aligned} \tag{4.128}$$

where

$$\begin{aligned} \tilde{A}^{(\ell_0,\ell_1,\ell_2)}_{m,n,p,q} &= (-\tfrac{1}{2})^J \binom{J_1-\ell_0-\ell_2}{m}\binom{J_1-\ell_0-\ell_2-m}{n}\binom{J_2-\ell_0-\ell_1}{p}\binom{\ell_1}{q} \\ &\times \frac{(-1)^{\frac{J_1-J_2+\Delta_{12}-\Delta_{34}}{2}+m+p-q+1}\left(\frac{\bar{\tau}-\Delta_{34}}{2}\right)_{J_1+J_2-2\ell_0-\ell_1-\ell_2-m-p}\left(\frac{\bar{\tau}+\Delta_{34}}{2}\right)_{m+p}}{(\bar{\tau})_{J_1+J_2-2\ell_0-\ell_1-\ell_2}\,\Gamma\left(\frac{\bar{\tau}+\Delta_{34}}{2}+m+p\right)} \\ &\times \frac{2\pi i\,\Gamma(\bar{\tau}+J_1+J_2-2\ell_0-\ell_1-\ell_2)\Gamma(\bar{\tau}+J_1+J_2-2\ell_0-\ell_1-\ell_2-1)}{\Gamma\left(\frac{\bar{\tau}+J_1+J_2+\Delta_{12}}{2}-\ell_0-\ell_1\right)\Gamma\left(\frac{\bar{\tau}+J_1+J_2-\Delta_{12}}{2}-\ell_0-\ell_2\right)\Gamma\left(\frac{\bar{\tau}-\Delta_{34}}{2}+J_1+J_2-2\ell_0-\ell_1-\ell_2-m-p\right)} , \end{aligned} \tag{4.129}$$

$$\tilde{B}_k^{(\ell_0,\ell_1,\ell_2)} = \frac{\left(\frac{\bar{\tau}+J_1+J_2+\Delta_{12}-2\ell_0-2\ell_1-2}{2}\right)_k\left(\frac{\bar{\tau}-\Delta_{34}}{2}+J_1+J_2-2\ell_0-\ell_2-\ell_2-m-p-1\right)_k}{k!\,(\bar{\tau}+J_1+J_2-2\ell_0-\ell_1-\ell-2)_k} , \tag{4.130}$$

$$k_{\max} = \frac{\Delta_{34}-\Delta_{12}-J_1-J_2+2\ell_0+\ell_1+2m+2r-2}{2} . \tag{4.131}$$

Similarly to the one spinning operator case, we keep several orders of the expansion of the hypergeometric near $v \sim 1$, as the sums of the first orders can cancel for certain values of ℓ_i. This is why we find the sum over several orders in σ in the last line. To obtain the leading behavior of each of the cross ratios function multiplying a given structure, the order of the hypergeometric to which we must take the expansion depends on the external spins. One test we did do check this result, was to send $J_2 \to 0$, $\ell_0, \ell_1 \to 0$ and $p, q \to 0$. By doing so, we recovered the result of the one spinning operator case.

It is also relevant to stress that the above formula is the main result of this thesis. Although it does not give us the blocks in the Regge limit, it provides us information about them, such as its leading σ behavior. Later, we could also use them as boundary conditions to find the explicit blocks in the Regge limit, by means of the Casimir equations. Moreover, because correlators with the stress tensor are objects of interest in our context, we could replace $J_1 = J_2 = 2$ in the above formula to see how the corresponding blocks would behave in the Regge limit.

Chapter 5

Conclusions and future work

To finish off this thesis, we will go over the main results and ideas presented here, as well as point out the future directions of this work.

We started by introducing the basics of Conformal Field Theories in chapter 2, where we became aware of the importance of conformal blocks.

We then proceeded to the main topic of this thesis, which is that of locality of the bulk theory. We kicked off chapter 3 by introducing a quite well known and generally accepted conjecture, which asserts the necessary conditions a CFT must obey, in order for its bulk dual to be local at sub-AdS scales. Subsequently, we briefly presented the key concepts behind the functioning of the holographic cameras, whose signals allow for a quick inference regarding the locality of the bulk theory. In particular, when considering the vacuum state, we explained why the the active camera correlator was equivalent to the Regge limit correlator, such that we could use the results from Conformal Regge theory to compute the camera's signal. This was done in [1] for a couple of cases, where the aforementioned conjecture was seen to hold. However, as this paper only considered scalar correlators, we believed that a natural extension of this work was to perform the same kind of analysis, for correlation functions with external spinning operators.

In order to do this, one first needs to compute the conformal blocks of these spinning four point functions in the Regge limit, such as to later be able to write the correlators in an integral representation. The first of these two steps was exactly the main focus of chapter 4. We began by presenting three distinct approaches to obtain the conformal blocks: by solving the Casimir differential equation, by applying the specific differential operators of [47] and by performing the OPE (either Euclidean or Lorentzian, although we only used the second). We have also minutely described the procedure to analytically continue the

blocks, having emphasized the required care due to branch cuts and associated discontinuities. After this initial presentation and exemplification for scalar four point functions, we proceeded to compute the conformal blocks of spin J_1-scalar-scalar-scalar correlators in the Regge limit, by means of the three methods. Given that in this case, the exchanged operator can only be in the symmetric and traceless representation, we were able to compute all possible conformal blocks. We then moved on to spin J_1-spin J_2-scalar-scalar correlators, having computed the blocks purely with the Lorentzian OPE, since the necessary computations were simpler for generic spins J_i $(i = 1, 2)$ in comparison with the other two approaches. However, contrarily to the previous case, these correlators admit the exchange of operators in the antisymmetric or mixed symmetry representations. To compute the respective conformal blocks one could either solve the Casimir differential equation or use the construction of [49]. Here, however, the computed conformal blocks concern only exchanged operators in the symmetric and traceless representation. We inferred that the different methods are consistent with each other, as they provided matching results for the same functions. Additionally, we observed the characteristic leading behavior σ^{1-J} of the conformal blocks in the Regge limit.

Although it was not done here, the next step would be to write these correlation functions in terms of the corresponding Regge limit blocks, analogously to (3.19). Afterwards, one could choose the $\mathcal{N} = 4$ SYM theory to plot the signal of the camera and compare the results with those of [1]. It would be interesting to see if this would lead us to find peaks with a different shape and/or sharpness, which could give us a better understanding.

In the future, it would also be compelling to perform a similar analysis with the correlators $\langle \mathcal{J}\mathcal{J}\mathcal{J}\mathcal{J} \rangle$ and $\langle TTTT \rangle$, where $\mathcal{J}$ is a vector operator and T the stress-tensor. In particular, the latter has a special relevance because the stress tensor is present in every CFT and also because the bulk dual is a gravitational theory. Naturally, computing the conformal blocks in the Regge limit of these functions would be far from as easy task. In addition to an increase of the computations difficulty, we would also have to consider the exchange of operators in the antisymmetric and mixed symmetry representations besides the symmetric one. Nevertheless, it would be interesting to see whether or not these correlators provided us with new information. Moreover, in the context of [48], knowledge of these correlators' conformal blocks could also allow us to obtain a bound on the associated OPE coefficients, such as λ_{TTT}.

Furthermore, it would also be interesting to compare the construction of the holographic

cameras with more recent methods [50, 51], which also aim at a better understanding of the bulk locality in AdS/CFT.

To finish, we would like to comment on something partly related. Although outside the context of this thesis, one of the things we are usually interested in computing while studying a CFT are its OPE coefficients. Because the conformal bootstrap for scalar four point functions is the best examined case, the majority of the known OPE coefficients involve two scalars and one spinning operator. On the other hand, OPE coefficients with more spinning operators remain less studied. To compute these constants we would have to consider four point functions with spinning external operators. However, as it became clear in this work, the conformal blocks computations increase significantly in complexity as we consider more external operators with nonzero spin. Alternatively, we can consider higher point functions with scalar operators, and impose consistency conditions with which we could compute the OPE coefficients. Although the conformal blocks for higher point functions are generally not known in an explicit form, the case of five points functions has already been studied. In particular, the five point block for a scalar exchange was obtained in [52] and there have also been some proposals to obtain the spinning five point blocks [38, 39, 53]. In spite of this, the existing methods for the latter are still unsatisfactory, as they involve too many sums that lead to larger computational times. However, it was recently noticed in [14], that a different choice of cross ratios leads to a factorized form of the conformal blocks. As such, we are presently applying some of the concepts presented here for four point functions, namely the series expansion associated with the Casimir differential equation, to compute the conformal blocks of scalar five points functions, with this choice of cross ratios.

Appendix A

Holographic camera integral (3.19) by saddle-point approximation

Here we will present the computation of the holographic camera integral (3.19), by means of the saddle point approximation. We will closely follow what was done in [48], since we are dealing with a similar kind of integral.

We will start by rewriting the integral in a more practical way. For simplicity, we will drop the "bulk" label in the two quantities of (3.21), which from now on are denoted by s and b, and we will set $R = 1$. Furthermore, we demonstrate in A.1 that the integrand term $\rho(\nu)\mathcal{P}_{\frac{2-d}{2}+i\nu}(b)$, is essentially the harmonic function $\Omega_{i\nu}(b)$ on H_{d-1} of [48, 54]. Therefore, we may rewrite (3.19) as:

$$G|_{\text{CRT}} - 1 \approx -2i \int_0^\infty d\nu\, \tilde{\alpha}(\nu)\, s^{J(\nu)-1}\, \Omega_{i\nu}(b)\, e^{-\frac{\nu^2}{2}\sigma_o^2} \ . \tag{A.1}$$

Next, we use the fact that $\Omega_{i\nu}$ can be written in terms of the scalar propagators in hyperbolic space H_{d-1}, which are defined as [54]:

$$\Pi_{i\nu+\frac{d}{2}-1}(\rho) = \frac{\Gamma(i\nu+\frac{d}{2}-1)}{2\pi^{\frac{d}{2}-1}\Gamma(i\nu+1)}\, e^{-\rho(i\nu+d/2-1)}\, {}_2F_1\left(i\nu+\frac{d}{2}-1, \frac{d}{2}-1, i\nu+1, e^{-2\rho}\right) \ . \tag{A.2}$$

In particular, we have:

$$\Omega_{i\nu}(\rho) = \frac{i\nu}{2\pi}\left(\Pi_{i\nu}(\rho) - \Pi_{-i\nu}(\rho)\right) \ . \tag{A.3}$$

What is more, $\tilde{\alpha}(\nu)$ and $J(\nu)$ are both even functions of ν, such that the integral domain can be expanded to $-\infty$. Hence, the correlator becomes:

$$G|_{\text{CRT}} - 1 \approx \frac{1}{\pi}\int_{-\infty}^{\infty} d\nu\, \nu\, e^{\left[J(\nu)-1\right]\ln(s)}\, \tilde{\alpha}(\nu)\, \Pi_{i\nu}(b)\, e^{-\frac{\nu^2}{2}\sigma_o^2} \ . \tag{A.4}$$

Before we start discussing the saddle-point approximation let us take one more extra step, which is that of multiplying by $e^{ib\nu}\, e^{-ib\nu}$. There is no problem in doing so, since this amounts to multiplying by one. In addition, we shall assume that $\tilde{\alpha}(\nu)$ might have an exponential dependency on ν, such that:

$$\tilde{\alpha}(\nu) = e^{\tilde{\alpha}_e(\nu)} h(\nu) \ , \tag{A.5}$$

where $\tilde{\alpha}_e(\nu)$ is a function which characterizes the exponential dependency on ν of $\tilde{\alpha}(\nu)$, and $h(\nu)$ is a function that represents the remaining behavior of the coefficient functions.

Taking all of these considerations into account, we are able to rewrite (3.19) as:

$$\begin{aligned} G|_{\text{CRT}} - 1 &\approx \frac{1}{\pi} \int_{-\infty}^{\infty} d\nu \, e^{\left[J(\nu)-1\right] \ln(s) - \frac{\nu^2}{2}\sigma_o^2 + \tilde{\alpha}_e(\nu) - ib\nu} \, \left[\nu \, e^{ib\nu} \, h(\nu) \, \Pi_{i\nu}(b)\right] \\ &\approx \frac{1}{\pi} \int_{-\infty}^{\infty} d\nu \, e^{\ln(s)\left(J(\nu)-1-\frac{\sigma_o^2}{2\ln(s)}\nu^2 + \frac{\tilde{\alpha}_e(\nu)}{\ln(s)} - i\frac{b}{\ln(s)}\nu\right)} \, \left[\nu \, e^{ib\nu} \, h(\nu) \, \Pi_{i\nu}(b)\right] \ . \end{aligned} \tag{A.6}$$

The structure of this integral is exactly the same of equation (4.3) in [48], with the exception of an additional Gaussian factor, which accounts for the optical resolution of the camera. Importantly, this integral is of the form:

$$F(\lambda) = \int_{\mathcal{C}} d\nu \, g(\nu) e^{\lambda \, f(\nu)} \quad , \quad \mathcal{C} = \text{integration contour} \ , \tag{A.7}$$

which is exactly the general structure of the integrals, in which the saddle-point approximation can be performed to evaluate the asymptotic behavior of $F(\lambda)$ at large λ. In particular, in order for this approximation to be valid, certain conditions must be met:

- $g(\nu)$ and $f(\nu)$ must be analytic functions of ν;
- The integration contour $\mathcal{C}$ is, or can be deformed, such that in the large λ limit the dominant contribution to the integral comes from the neighborhood of the saddle point ν_0, where $|f(\nu_0)|$ is maximum on the path;
- The integration path traverses ν_0 with an orientation that leads to a rapid decrease of $|f(\nu)|$ as we move away from ν_0, in any direction of the path;
- In the large λ limit, the integral's contribution coming from the vicinity of ν_0, asymptotically approaches the exact value of $F(\lambda)$;
- $g(\nu)$ is a slowly-varying function near the saddle point and does not depend on λ.

When the only significant contribution to the integral comes from the vicinity of a single saddle point ν_0 and the above conditions are satisfied, the result from the saddle-point

approximation is [55]:

$$\begin{aligned} F(\lambda) &\approx \frac{\sqrt{2\pi}\, g(\nu_0)\, e^{\lambda f(\nu_0)}\, e^{i\theta}}{|\lambda f''(\nu_0)|^{\frac{1}{2}}} \\ &\approx \sqrt{\frac{2\pi}{-f''(\nu_0)\lambda}}\, g(\nu_0)\, e^{\lambda f(\nu_0)} \quad , \end{aligned} \tag{A.8}$$

where $\theta = \frac{\pi}{2} - \frac{1}{2}\arg(f''(\nu_0))$, specifies the direction with which the integral contour must cross the saddle-point. In other words, this angle specifies the path of steepest descent.

Fortunately, in our case, the aforementioned requirements can be fulfilled, such that the saddle approximation can be used to evaluate (A.6). In particular, we may identify the term inside brackets in (A.6), as the slowly varying function $g(\nu)$ of (A.7):

$$g(\nu) = \nu\, e^{ib\nu}\, h(\nu)\, \Pi_{i\nu}(b) \ . \tag{A.9}$$

This stems from the fact that this term does not have any exponential dependency on ν. Indeed, one easily sees that $e^{iB\nu}\, \Pi_{i\nu}(B)$ has no exponential behavior, due to the definition of the scalar propagator (A.2). Moreover, $f(\nu)$ can be identified with:

$$f(\nu) = J(\nu) - 1 - \frac{\sigma_o^2}{2\ln(s)}\nu^2 + \frac{\tilde{\alpha}_e(\nu)}{\ln(s)} - i\,\frac{b}{\ln(s)}\nu \ , \tag{A.10}$$

whereas $\ln(S)$, which is real and positive, is recognized as the parameter λ, which will be taken to be large. Furthermore, the saddle-point of (A.6) is defined by:

$$J'(\nu_0)\, \ln(s) - \sigma_o^2\, \nu_0 + \tilde{\alpha}_e'(\nu_0) - ib = 0 \ . \tag{A.11}$$

We stress out that the saddle point is itself a function of b, such that a change in b implies a variation of the saddle point position.

Before writing the final expression, there is a relevant observation to be made. In particular, when we expand the integrand of (A.6) around the saddle point, we find:

$$G|_{\mathrm{CRT}} - 1 \approx \frac{e^{\ln(S) f(\nu_0) + i\theta}}{\pi} \int_{-\infty}^{\infty} d\nu\, g(\nu)\, e^{-\ln(S)|f''(\nu_0)|\frac{(\nu-\nu_0)^2}{2} + \ldots} \ , \tag{A.12}$$

where we are keeping with the notation of $f(\nu)$ and $g(\nu)$ for simplicity. It is intuitive to infer that $\ln(s)\,|f''(\nu_0)|$ is essentially the rate at which the integrand decreases, as we move away from ν_0. Therefore, in order to meet the third necessary condition for the viability of the saddle-point approximation, this rate must be large:

$$|\ln(s)\, J''(\nu_0) - \sigma_o^2 + \tilde{\alpha}_e''(\nu_0)| \gg 1 \ . \tag{A.13}$$

This condition can always be achieved by making $\ln(s)$ large enough, even if the remaining quantities are small.

Finally, making use of (A.8) and the aforementioned identifications, we get that the saddle point approximation of the holographic camera signal (3.19) is given by:

$$\begin{aligned} &G\left(0,p,L;e,p',L'\right)\Big|_{\text{CRT}} - 1 \approx \\ &\approx \frac{s^{J(\nu_0)-1}}{\pi}\,\nu_0\,h(\nu_0)\,\Pi_{i\nu_0}(b)\,\sqrt{\frac{2\pi}{\sigma_o^2 - \ln(s)\,J''(\nu_0) - \tilde{\alpha}_e''(\nu_0)}}\,e^{-\frac{\sigma_o^2}{2}\nu_0^2+\tilde{\alpha}_e(\nu_0)} \quad . \end{aligned} \tag{A.14}$$

In the limit we are interested ($b \ll \ln s$), the saddle point equation (A.11) demands that $\text{Im}(J'(\nu_0)) \ll 1$ and $\text{Im}(\alpha_e'(\nu_0)) \ll 1$. Accordingly, we can expand this equation around the symmetric point $\nu = 0$, where $J'(0) = 0$, and obtain an explicit expression for the saddle point. If we replace this in the above expression, while also making use of the definition of $\Pi_{i\nu}(\rho)$ (see (A.2)), we find that the maximum value of (A.14), which corresponds to the peak, occurs for $b = 0$, in accordance with what was said in the main text.

A.1 Equivalence between $\rho(\nu)\,\mathcal{P}_{\frac{2-d}{2}+i\nu}(\eta)$ and $\Omega_{i\nu}(\eta)$

Here, we will show that $\rho(\nu)\,\mathcal{P}_{\frac{2-d}{2}+i\nu}(\eta)$ and $\Omega_{i\nu}(\eta)$ are equivalent. In particular, they differ from a choice to absorb or not the measure $\rho(\nu)$ in the definition of the harmonic functions, combined with a decision of expressing the Gamma functions differently. The exact relation between these two quantities which we will prove is:

$$\frac{1}{4\pi}\,\rho(\nu)\,\mathcal{P}_{\frac{2-d}{2}+i\nu}(\eta) = \Omega_{i\nu}(\eta)\ . \tag{A.15}$$

To begin, it will be useful to have the explicit expression for $\Omega_{i\nu}(\eta)$. Using (A.3) together with the transverse scalar propagators definition (A.2), we find:

$$\Omega_{i\nu}(\eta) = \frac{\nu\,\sinh(\pi\nu)\,\Gamma\left(\frac{d-2}{2}-i\nu\right)\Gamma\left(\frac{d-2}{2}+i\nu\right)}{2^{d-1}\pi^{\frac{d+1}{2}}\Gamma\left(\frac{d-1}{2}\right)}\,{}_2F_1\left(\frac{d-2}{2}-i\nu,\frac{d-2}{2}+i\nu,\frac{d-1}{2},\frac{1-\eta}{2}\right)\ . \tag{A.16}$$

This is exactly what appears in [54] if we take into account the change of variable:

$$\eta = 1 + 2\sinh^2\left(\frac{r}{2}\right) = \cosh r\ , \tag{A.17}$$

where the r represents the same as our b, i.e, it is the bulk impact parameter. Now that we know the expression for $\Omega_{i\nu}(\nu)$, we can rewrite (A.15) as:

$$\begin{aligned}&\frac{1}{4\pi}\frac{2^{d-2}\,\Gamma\left(\frac{d-1}{2}\right)}{2\pi^{\frac{d-1}{2}}}\frac{\Gamma\left(\frac{d-2}{2}-i\nu\right)\Gamma\left(\frac{d-2}{2}+i\nu\right)\Gamma\left(\frac{d-2}{2}\right)^2}{\Gamma(i\nu)\,\Gamma(-i\nu)\Gamma\left(\frac{d-2}{2}\right)^2}\,{}_2F_1\left(\tfrac{d-2}{2}-i\nu,\tfrac{d-2}{2}+i\nu,\tfrac{d-1}{2},\tfrac{1-\eta}{2}\right)=\\&=\frac{\nu\,\sinh(\pi\nu)\,\Gamma\left(\frac{d-2}{2}-i\nu\right)\Gamma\left(\frac{d-2}{2}+i\nu\right)}{2^{d-1}\pi^{\frac{d+1}{2}}\Gamma\left(\frac{d-1}{2}\right)}\,{}_2F_1\left(\tfrac{d-2}{2}-i\nu,\tfrac{d-2}{2}+i\nu,\tfrac{d-1}{2},\tfrac{1-\eta}{2}\right)\ .\end{aligned}\tag{A.18}$$

Using the following property of the Gamma functions:

$$\Gamma(i\nu)\,\Gamma(-i\nu)=\frac{\pi}{\nu\,\sinh(\pi\nu)}\quad,\quad\text{with}\ \ \nu\in\mathbb{R}\ ,\tag{A.19}$$

it is easy to see that among others, the $\sinh(\pi\nu)$ terms cancel out and we are left with:

$$\left(\frac{\Gamma\left(\frac{d}{2}-1\right)}{\Gamma\left(d-2\right)}\right)^2=\frac{\pi}{2^{2d-6}\,\Gamma\left(\frac{d-1}{2}\right)^2}.\tag{A.20}$$

Next, we use another property of the Gamma functions, namely:

$$\Gamma\left(z-\frac{1}{2}\right)\,\Gamma\left(z\right)=e^{2-2z}\sqrt{\pi}\ .\tag{A.21}$$

In our case, $z=d/2$, such that:

$$\Gamma\left(\frac{d}{2}-\frac{1}{2}\right)=2^{2-d}\,\sqrt{\pi}\,\frac{\Gamma(d-1)}{\Gamma\left(\frac{d}{2}\right)}\quad.\tag{A.22}$$

Using this equality, (A.20) becomes:

$$\frac{1}{4}\left(\frac{\Gamma\left(\frac{d}{2}-1\right)}{\Gamma\left(\frac{d}{2}\right)}\,\frac{\Gamma(d-1)}{\Gamma(d-2)}\right)^2=1\ ,\tag{A.23}$$

which can be verified to hold by applying the defining property of the Gamma function:

$$\Gamma(z+1)=z\,\Gamma(z)\ ,\ \ z\in\mathbb{Z}\ .\tag{A.24}$$

This concludes our demonstration that, in fact, $\rho(\nu)\,\mathcal{P}_{\frac{2-d}{2}+i\nu}(\eta)$ and $\Omega_{i\nu}(\eta)$ denote the same function.

Appendix B

Hypergeometric function discontinuity

The hypergeometric functions ${}_2F_1(a,b;c;z)$ are defined as solutions of the so-called hypergeometric differential equation:

$$z(1-z)\,y''(z) + [c-(a+b+1)z]\,y'(z) - a\,b\,y(z) = 0\ , \tag{B.1}$$

which has singularities at $z = 0, 1, \infty$. Relatedly, these functions can be expressed in terms of a power series, which converges absolutely in $|z| < 1$:

$${}_2F_1(a,b;c;z) = \sum_{n=0}^{\infty} \frac{(a)_n (b)_n}{(c)_n} \frac{z^n}{n!}\ . \tag{B.2}$$

Moreover, the function as defined above is analytic in this same region, provided that c is neither zero or a negative integer. We can also analytically continue the function to outside of the unit disk. This can be done so, by using one of the possible integral representations of the hypergeometric:

$$\begin{gathered} {}_2F_1(a,b;c;z) = \frac{\Gamma(c)}{\Gamma(a)\Gamma(c-a)} \int_0^1 t^{a-1}(1-t)^{c-a-1}(1-zt)^{-b}dt \\ (\mathrm{Re}(c) > \mathrm{Re}(a) > 0;\ |arg(1-z)| \leq \pi - \epsilon\ \ (0 < \epsilon < \pi)) \end{gathered} \tag{B.3}$$

or equivalently:

$$\begin{gathered} {}_2F_1(a,b;c;z) = \frac{\Gamma(c)}{\Gamma(b)\Gamma(c-b)} \int_0^1 t^{b-1}(1-t)^{c-b-1}(1-zt)^{-a}dt \\ (\mathrm{Re}(c) > \mathrm{Re}(b) > 0;\ |arg(1-z)| \leq \pi - \epsilon\ \ (0 < \epsilon < \pi))\,. \end{gathered} \tag{B.4}$$

Note that when we consider z to satisfy $z \in \mathbb{Z}$ and $|z| > 1$, the term $(1 - zt)$ inside the integral will certainly vanish at some point along the integration interval, causing the integral to diverge. We thus say that the integral is ill-defined. For this reason, the analytic continuation of the hypergeometric function is defined for the whole complex plane except for the cut in the real axis going from $z = 1$ to $z = \infty$ (branch cut). We will keep denoting this analytic continuation by ${}_2F_1(a, b; c; z)$.

As the hypergeometric function is multi-valued, it happens to have a discontinuity as we cross the aforementioned branch cut. In due turn, this discontinuity is defined as:

$$\text{Disc } {}_2F_1(a, b; c; z) = {}_2F_1(a, b; c; z + i0) - {}_2F_1(a, b; c; z - i0) \tag{B.5}$$

To compute it, we are going to use the integral representation of the hypergeometric function. Moreover, it will prove useful to split this integral over two regions:

$$\begin{aligned} {}_2F_1(a, b; c; z) =& \frac{\Gamma(c)}{\Gamma(b)\Gamma(c-b)} \int_0^{1/z} t^{b-1}(1-t)^{c-b-1}(1-zt)^{-a} dt \\ &+ \frac{\Gamma(c)}{\Gamma(b)\Gamma(c-b)} \int_{1/z}^{1} t^{b-1}(1-t)^{c-b-1}(1-zt)^{-a} dt \,. \end{aligned} \tag{B.6}$$

The first integral is associated with the region $0 < |z| < 1$ over the real axis, where there is no branch cut. Thus, the difference of these terms in (B.5) vanishes. On the other hand, because the second integral is defined over $|z| \geq 1$, the discontinuity must arise from it. Lastly, we have that right above the cut $\theta = 0$, whereas below it $\theta = 2\pi$. As such, we must take $z \to z$ and $z \to ze^{2\pi i}$, respectively, in the above integrals. Doing so, we obtain:

$$\begin{aligned} &{}_2F_1(a, b; c; z + i0) - {}_2F_1(a, b; c; z - i0) = \\ &= \frac{\Gamma(c)}{\Gamma(b)\Gamma(c-b)} \Big[\int_{1/z}^{1} t^{b-1}(1-t)^{c-b-1}(1-zt)^{-a} dt - e^{-2\pi a i} \int_{1/z}^{1} t^{b-1}(1-t)^{c-b-1}(1-zt)^{-a} dt \Big] \\ &= \frac{\Gamma(c)}{\Gamma(b)\Gamma(c-b)} (1 - e^{-2\pi a i}) \int_{1/z}^{1} t^{b-1}(1-t)^{c-b-1}(1-zt)^{-a} dt \,. \end{aligned} \tag{B.7}$$

Changing variables according to:

$$t = (1 - \frac{1}{z})\,\tau + \frac{1}{z} \,, \tag{B.8}$$

the former expression becomes:

$$\frac{\Gamma(c)}{\Gamma(b)\Gamma(c-b)} (1 - e^{-2\pi a i}) z^{1-c} (1-z)^{-a} (z-1)^{c-b} \int_0^1 \tau^{-a} (1-\tau)^{c-b-1} (1-(1-z)\tau)^{b-1} d\tau \,. \tag{B.9}$$

But this integral is simply the integral representation of the hypergeometric function, up

to some constants, and where the argument is $(1-z)$ rather than z. Hence, we can rewrite the former expression as:

$$\frac{\Gamma(c)\Gamma(1-a)}{\Gamma(b)\Gamma(c-a-b+1)}(1-e^{-2\pi a i})z^{1-c}(1-z)^{-a}(z-1)^{c-b}{}_2F_1(1-a,1-b;c-a-b+1;1-z)\,. \tag{B.10}$$

Lastly, we make use of the following Gamma functions property:

$$\Gamma(a)\,\Gamma(1-a)=\frac{\pi}{\sin\pi a}\quad,\quad a\notin\mathbb{Z}\,, \tag{B.11}$$

with which we finally obtain the discontinuity:

$$\begin{aligned}&\text{Disc }{}_2F_1(a,b;c;z)=\\&=\frac{2\pi i\Gamma(c)}{\Gamma(a)\Gamma(b)\Gamma(c-a-b+1)}z^{1-c}(z-1)^{c-a-b}\,{}_2F_1\left(1-a,1-b;c-a-b+1;1-z\right)\,.\end{aligned} \tag{B.12}$$

It is curious to see that the discontinuity of the hypergeometric function along its branch cut is another hypergeometric function with different arguments.

Appendix C

Casimir differential equations

C.1 Spin 1-Scalar-Scalar-Scalar

By acting with the correct differential operator one obtains the Casimir differential equation. From this, it is possible to obtain the two following coupled differential equations by separating the $V_{1,23}$ and $V_{1,34}$ dependence:

$$\frac{1}{2v}\Big[(C_{\Delta,J}+2)v+u-v^2-1+\Delta_{34}\left(v^2-u(v+2)-3v+2\right)-\Delta_{12}\left(2\,\Delta_{34}\,v\,(u-v+1)\right.$$
$$\left.-2u+2(v-1)^2\right)\Big]\,f_1(u,v)+v\,f_2(u,v)+\Big(-\Delta_{12}\left(u(v+1)-(v-1)^2\right)+\Delta_{34}\left(u(v+1)\right.$$
$$\left.-(v-1)^2\right)+(v-1)(u+v-1)\Big)\,\partial_v f_1(u,v)-2v(1+v)\partial_v f_2(u,v)-2v\Big[(v-1)^2$$
$$-u(v+1)\Big]\,\partial_v^2 f_1(u,v)-u\left[-2d+\Delta_{12}(u-v+1)+\Delta_{34}(-u+v-1)-u-v+5\right]\partial_u f_1(u,v)$$
$$-2u\,v\,\partial_u f_2(u,v)+4\,u\,v(u-v+1)\,\partial_u\,\partial_v f_1(u,v)+2u^2\,(u-v-1)\,\partial_u^2 f_1(u,v)=0\ , \qquad \text{(C.1)}$$

$$-\frac{u f_1(u,v)\left(\Delta_{34}+\Delta_{12}(v-1)+v-1\right)}{v}+\Big[C_{\Delta,J}-\frac{1}{2}\Delta_{34}(u-v+1)-2d+u$$
$$-\frac{1}{2}\Delta_{12}\left(\Delta_{34}(u-v+1)-2u\right)\Big]\,f_2(u,v)+2u(v-1)\partial_v f_1(u,v)-\Big\{\Delta_{12}\left[u(v+1)-(v-1)^2\right]$$
$$-\Delta_{34}\left[u(v+1)-(v-1)^2\right]+(v-1)(u+v-1)\Big\}\partial_v f_2(u,v)-2v\left[(v-1)^2-u(v+1)\right]\partial_v^2 f_2(u,v)$$
$$+2u^2\partial_u f_1(u,v)-u\left(-2\,d+\Delta_{12}(u-v+1)+\Delta_{34}(-u+v-1)+u+v-1\right)\partial_u f_2(u,v)$$
$$+4\,u\,v\,(u-v+1)\,\partial_u\partial_v f_2(u,v)+2\,u^2\,(u-v-1)\,\partial_u^2 f_2(u,v)=0\ , \qquad \text{(C.2)}$$

where $C_{\Delta,J}$ is given by (4.11).

After finding the boundary conditions for the above differential equations, plugging in the ansatz (4.91) and expanding until leading order in u we obtain a differential equation which concerns only one of the cross ratio functions. This is given by:

$$
\begin{aligned}
&-\frac{1}{2v}\Big(2+v^2(J+1-\Delta)(J+2-\Delta)-v\Big(4+J^2+\Delta(\Delta-3)+(2\Delta-1)J\Big)\\
&-\Delta_{34}(v-1)(v(J+1-\Delta)-2)+\Delta_{12}(v-1)\left(v\,(J+2-\Delta)-\Delta_{34}\,v-2\right)\Big)\,g^{(1)}_{\mathcal{O},0}(v)\\
&+(v-1)\left(2\,v\,(J-\Delta)+\Delta_{12}(v-1)-\Delta_{34}(v-1)+v-1\right)\,\partial_v\,g^{(1)}_{\mathcal{O},0}(v)\\
&-2(v-1)^2\,v\,\partial_v^2\,g^{(1)}_{\mathcal{O},0}(v)=0\,.
\end{aligned}
\tag{C.3}
$$

The above equation enables us to obtain recurrence relations for $c^{(1)}_{\mathcal{O},0,k}$ (see (4.93)). In order to obtain the same kind of recurrence relations for the coefficients of $g^{(2)}_{\mathcal{O},0,k}$ we need to consider the subleading terms of the coupled differential equations (C.1) and (C.2) in the u expansion. By doing this, we obtain the following differential equation:

$$
\begin{aligned}
&-\frac{1}{v}\left(\Delta_{34}+Jv-\Delta v+\Delta_{12}(v-1)+v-1\right)\,g^{(1)}_{\mathcal{O},0}(v)+2u(v-1)\,\partial_v g^{(1)}_{\mathcal{O},0}(v)\\
&+\frac{1}{2}\Big(\Delta-2\Delta J(v+1)+\Delta_{12}(v-1)\,(-\Delta-\Delta_{34}+J-2)-\Delta_{34}(v-1)(-\Delta+J-1)\\
&+(J-2)(J-1)(v-1)+\Delta^2(v-1)+3\Delta v\Big)\,g^{(2)}_{\mathcal{O},0}(v)+(v-1)\left(1+v(-2\Delta+2J-5)\right.\\
&\left.+\Delta_{12}+(v-1)-\Delta_{34}(v-1)\right)\,\partial_v g^{(2)}_{\mathcal{O},0}(v)-2(v-1)^2 v\,\partial_v^2 g^{(2)}_{\mathcal{O}}(v)=0\,.
\end{aligned}
\tag{C.4}
$$

Similarly to before, we write $g^{(2)}_{\mathcal{O},0}$ as in (4.95) and obtain the recurrence relations for $c^{(2)}_{\mathcal{O},0,k}$ (see (4.96)).

Bibliography

[1] S. Caron-Huot, "Holographic cameras: an eye for the bulk," *JHEP* **03** (2023) 047, arXiv:2211.11791 [hep-th].

[2] J. M. Maldacena, "The Large N limit of superconformal field theories and supergravity," *Adv. Theor. Math. Phys.* **2** (1998) 231–252, arXiv:hep-th/9711200.

[3] M. E. Peskin and D. V. Schroeder, *An Introduction to Quantum Field Theory*. Westview Press, 1995.

[4] D. Tong, "David Tong: Lectures on General Relativity," 2019.

[5] S. El-Showk, Y. Nakayama, and S. Rychkov, "What Maxwell Theory in D<>4 teaches us about scale and conformal invariance," *Nucl. Phys. B* **848** (2011) 578–593, arXiv:1101.5385 [hep-th].

[6] S. Rychkov, *EPFL Lectures on Conformal Field Theory in D>= 3 Dimensions*. SpringerBriefs in Physics. 1, 2016. arXiv:1601.05000 [hep-th].

[7] V. Riva and J. L. Cardy, "Scale and conformal invariance in field theory: A Physical counterexample," *Phys. Lett. B* **622** (2005) 339–342, arXiv:hep-th/0504197.

[8] D. Simmons-Duffin, "The Conformal Bootstrap," in *Theoretical Advanced Study Institute in Elementary Particle Physics: New Frontiers in Fields and Strings*. 2017. arXiv:1602.07982 [hep-th].

[9] S. Ferrara, P. Gatto, and A. F. Grilla, "Conformal algebra in space-time and operator product expansion," *Springer Tracts Mod. Phys.* **67** (1973) 1–64.

[10] S. Weinberg, "Six-dimensional Methods for Four-dimensional Conformal Field Theories," *Phys. Rev. D* **82** (2010) 045031, arXiv:1006.3480 [hep-th].

[11] M. S. Costa, J. Penedones, D. Poland, and S. Rychkov, "Spinning Conformal Correlators," *JHEP* **11** (2011) 071, arXiv:1107.3554 [hep-th].

[12] J. Penedones, E. Trevisani, and M. Yamazaki, "Recursion Relations for Conformal Blocks," *JHEP* **09** (2016) 070, arXiv:1509.00428 [hep-th].

[13] A. Antunes, M. S. Costa, V. Goncalves, and J. V. Boas, "Lightcone bootstrap at higher points," *JHEP* **03** (2022) 139, arXiv:2111.05453 [hep-th].

[14] M. S. Costa, V. Goncalves, A. Salgarkar, and J. Vilas Boas, "Conformal multi-Regge theory," arXiv:2305.10394 [hep-th].

[15] A. L. Fitzpatrick, J. Kaplan, D. Poland, and D. Simmons-Duffin, "The Analytic Bootstrap and AdS Superhorizon Locality," *JHEP* **12** (2013) 004, arXiv:1212.3616 [hep-th].

[16] Z. Komargodski and A. Zhiboedov, "Convexity and Liberation at Large Spin," *JHEP* **11** (2013) 140, arXiv:1212.4103 [hep-th].

[17] J. Penedones, "TASI lectures on AdS/CFT," in *Theoretical Advanced Study Institute in Elementary Particle Physics: New Frontiers in Fields and Strings*, pp. 75–136. 2017. arXiv:1608.04948 [hep-th].

[18] J. Kaplan, "Lectures on AdS/CFT from the Bottom Up,".

[19] M. Gary, S. B. Giddings, and J. Penedones, "Local bulk S-matrix elements and CFT singularities," *Phys. Rev. D* **80** (2009) 085005, arXiv:0903.4437 [hep-th].

[20] J. Maldacena, D. Simmons-Duffin, and A. Zhiboedov, "Looking for a bulk point," *JHEP* **01** (2017) 013, arXiv:1509.03612 [hep-th].

[21] I. Heemskerk, J. Penedones, J. Polchinski, and J. Sully, "Holography from Conformal Field Theory," *JHEP* **10** (2009) 079, arXiv:0907.0151 [hep-th].

[22] L. F. Alday, A. Bissi, and E. Perlmutter, "Holographic Reconstruction of AdS Exchanges from Crossing Symmetry," *JHEP* **08** (2017) 147, arXiv:1705.02318 [hep-th].

[23] N. Kajuri, "Lectures on Bulk Reconstruction," *SciPost Phys. Lect. Notes* **22** (2021) 1, arXiv:2003.00587 [hep-th].

[24] A. Hamilton, D. N. Kabat, G. Lifschytz, and D. A. Lowe, "Holographic representation of local bulk operators," *Phys. Rev. D* **74** (2006) 066009, arXiv:hep-th/0606141.

[25] V. E. Hubeny, "Extremal surfaces as bulk probes in AdS/CFT," *JHEP* **07** (2012) 093, arXiv:1203.1044 [hep-th].

[26] P. Arnold and D. Vaman, "Jet quenching in hot strongly coupled gauge theories simplified," *JHEP* **04** (2011) 027, arXiv:1101.2689 [hep-th].

[27] A. Kamenev, "Introduction to the keldysh formalism," 2009.

[28] A. K. Das, "Topics in finite temperature field theory," arXiv:hep-ph/0004125.

[29] Y. BenTov, "Schwinger-Keldysh path integral for the quantum harmonic oscillator," arXiv:2102.05029 [hep-th].

[30] D. M. Hofman and J. Maldacena, "Conformal collider physics: Energy and charge correlations," *JHEP* **05** (2008) 012, arXiv:0803.1467 [hep-th].

[31] L. Cornalba, M. S. Costa, J. Penedones, and R. Schiappa, "Eikonal Approximation in AdS/CFT: Conformal Partial Waves and Finite N Four-Point Functions," *Nucl. Phys. B* **767** (2007) 327–351, arXiv:hep-th/0611123.

[32] L. Cornalba, M. S. Costa, J. Penedones, and R. Schiappa, "Eikonal Approximation in AdS/CFT: From Shock Waves to Four-Point Functions," *JHEP* **08** (2007) 019, arXiv:hep-th/0611122.

[33] M. S. Costa, V. Goncalves, and J. Penedones, "Conformal Regge theory," *JHEP* **12** (2012) 091, arXiv:1209.4355 [hep-th].

[34] S. Caron-Huot, "Analyticity in Spin in Conformal Theories," *JHEP* **09** (2017) 078, arXiv:1703.00278 [hep-th].

[35] J. Maldacena, S. H. Shenker, and D. Stanford, "A bound on chaos," *JHEP* **08** (2016) 106, arXiv:1503.01409 [hep-th].

[36] S. H. Shenker and D. Stanford, "Stringy effects in scrambling," *JHEP* **05** (2015) 132, arXiv:1412.6087 [hep-th].

[37] R. C. Brower, J. Polchinski, M. J. Strassler, and C.-I. Tan, "The Pomeron and gauge/string duality," *JHEP* **12** (2007) 005, arXiv:hep-th/0603115.

[38] V. Gonçalves, R. Pereira, and X. Zhou, "20′ Five-Point Function from $AdS_5 \times S^5$ Supergravity," *JHEP* **10** (2019) 247, arXiv:1906.05305 [hep-th].

[39] D. Poland, V. Prilepina, and P. Tadić, "The five-point bootstrap," arXiv:2305.08914 [hep-th].

[40] D. Simmons-Duffin, "TASI Lectures on Conformal Field Theory in Lorentzian Signature," 2019.

[41] F. A. Dolan and H. Osborn, "Conformal four point functions and the operator product expansion," *Nucl. Phys. B* **599** (2001) 459–496, arXiv:hep-th/0011040.

[42] F. A. Dolan and H. Osborn, "Conformal partial waves and the operator product expansion," *Nucl. Phys. B* **678** (2004) 491–507, arXiv:hep-th/0309180.

[43] M. Hogervorst and S. Rychkov, "Radial Coordinates for Conformal Blocks," *Phys. Rev. D* **87** (2013) 106004, arXiv:1303.1111 [hep-th].

[44] M. S. Costa, T. Hansen, J. Penedones, and E. Trevisani, "Radial expansion for spinning conformal blocks," *JHEP* **07** (2016) 057, arXiv:1603.05552 [hep-th].

[45] D. Simmons-Duffin, D. Stanford, and E. Witten, "A spacetime derivation of the Lorentzian OPE inversion formula," *JHEP* **07** (2018) 085, arXiv:1711.03816 [hep-th].

[46] M. Billò, V. Gonçalves, E. Lauria, and M. Meineri, "Defects in conformal field theory," *JHEP* **04** (2016) 091, arXiv:1601.02883 [hep-th].

[47] M. S. Costa, J. Penedones, D. Poland, and S. Rychkov, "Spinning Conformal Blocks," *JHEP* **11** (2011) 154, arXiv:1109.6321 [hep-th].

[48] M. S. Costa, T. Hansen, and J. Penedones, "Bounds for OPE coefficients on the Regge trajectory," *JHEP* **10** (2017) 197, arXiv:1707.07689 [hep-th].

[49] M. S. Costa and T. Hansen, "Conformal correlators of mixed-symmetry tensors," *JHEP* **02** (2015) 151, arXiv:1411.7351 [hep-th].

[50] N. Levine and M. F. Paulos, "Bootstrapping bulk locality. Part I: Sum rules for AdS form factors," arXiv:2305.07078 [hep-th].

[51] M. Meineri, J. Penedones, and T. Spirig, "Renormalization group flows in AdS and the bootstrap program," arXiv:2305.11209 [hep-th].

[52] V. Rosenhaus, "Multipoint Conformal Blocks in the Comb Channel," *JHEP* **02** (2019) 142, arXiv:1810.03244 [hep-th].

[53] D. Poland and V. Prilepina, "Recursion relations for 5-point conformal blocks," *JHEP* **10** (2021) 160, arXiv:2103.12092 [hep-th].

[54] J. Penedones, "High Energy Scattering in the AdS/CFT Correspondence," arXiv:0712.0802 [hep-th].

[55] G. B. Arfken, H.-J. Weber, and F. E. Harris, *Mathematical Methods for Physicists*. Academic, Oxford, 2012.